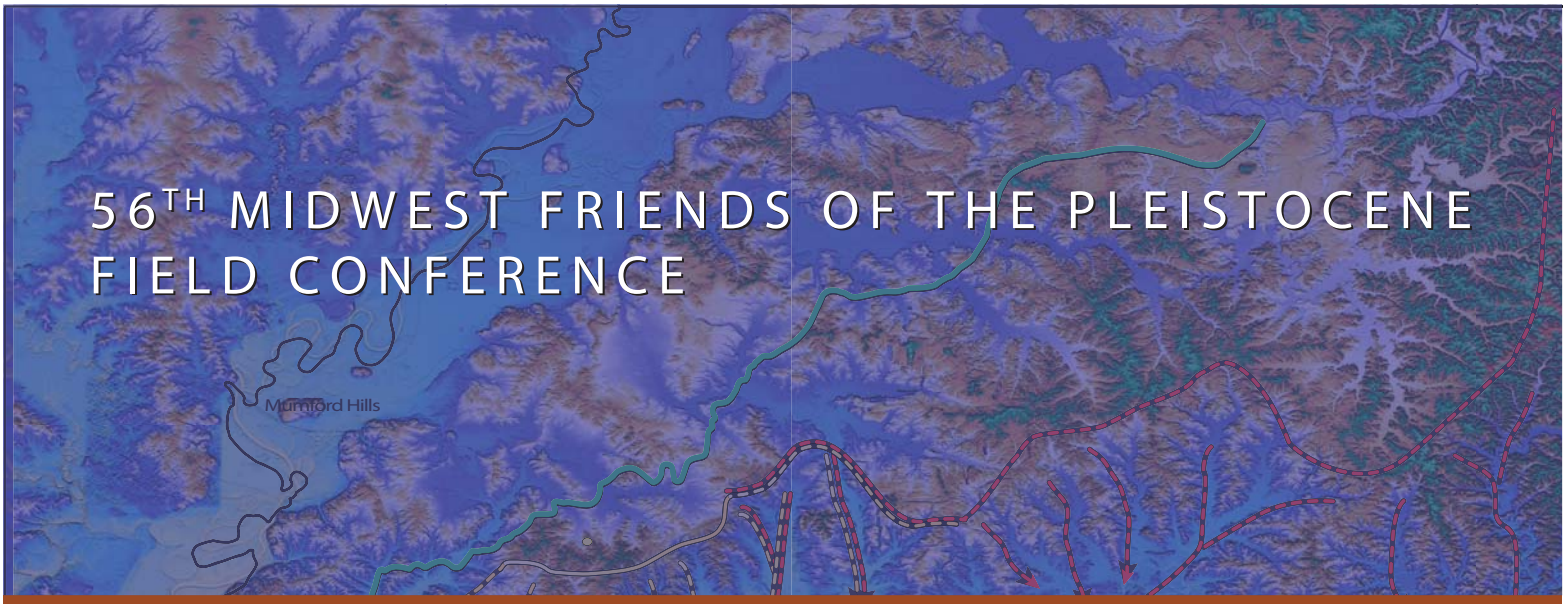

Quaternary Geology and Geoarchaeology of the Lower Ohio River Valley, Southwestern Indiana

Midwest Friends of the Pleistocene
2014
56th Field Conference, Evansville, Indiana

Angel Mounds
Evansville, Indiana
May 30–June 1, 2014

Ronald Counts (USGS)
G. William Monaghan (IGS/IU)
Edward Herrmann (IU)


Midwest Friends of the Pleistocene
56th Field Conference, Evansville, Indiana 2014

-acknowledgements-

When I first considered doing an FOP trip in the lower Ohio valley 7 years ago, I envisioned doing it completely from the water. There are spectacular exposures of alluvium visible from the water, unlike from the terrace surfaces where you are lucky to get a handful of 2 inch cores to characterize landforms that can span tens of miles. The water is the way to see the architecture of the aluvium; but alas, the Army Corps of Engineers had no boats to loan for such a venture, and the bargemen were too busy hauling coal and sand and gravel to worry about the safety of a group of meddling scientists. I actually checked into renting a half dozen house boats, and financially it could fly, but I've always said I didn't have time to run a trip and that I would do it the next year. After several years I learned that waiting until I had time to run an FOP trip was like someone waiting until they could afford kids before having any: in both examples it likely won't happen! Planning this trip has been a lot of work (last minute of course), but it has also been a lot of fun. Too many people have contributed to the contents of this guidebook, so we won't even try to acknowledge them here, but a few have made this field conference possible and we'd like to acknowledge them. We thank the Indiana Geological Survey and the University of Indiana for support with logistics, registration, and the eventual publication of this guidebook. We also thank Tom Mumford and the Mumford family for allowing us to access their property. And lastly we thank Mike Linderman from Angel Mounds and the Indiana State Museums for allowing us to use Angel Mounds for the meeting headquarters.

Meetings of the Midwest Friends of the Pleistocene*

1	1950 Eastern Wisconsin	Sheldon Judson
2	1951 Southeastern Minnesota	H.E. Wright Jr., R.V. Ruhe, and L. Gould
3	1952 Western Illinois and eastern Iowa	P.R. Shaffer and W.H. Scholtes
4	1953 Northeastern Wisconsin	F.T. Thwaites
5	1954 Central Minnesota	H.E. Wright, Jr., and A.F. Schneider
6	1955 Southwestern Iowa	R.V. Ruhe
7	1956 Northwestern lower Michigan	J.H. Zumberge and W.N. Melhorn
8	1957 South-central Indiana	W.D. Thornbury and W.J. Wayne
9	1958 Eastern North Dakota	W.M. Laird and others
10	1959 Western Wisconsin	R.F. Black
11	1960 Eastern South Dakota	A.G. Agnew and others
12	1961 Eastern Alberta	C.P. Gravenor and others
13	1962 Eastern Ohio	R.P. Goldthwait
14	1963 Western Illinois	J.C. Frye and H.B. Willman
15	1964 Eastern Minnesota	H.E. Wright, Jr. and E.J. Cushing
16	1965 Northeastern Iowa	R.V. Ruhe and others
17	1966 Eastern Nebraska	E.C. Reed and others
18	1967 South-central North Dakota	L. Clayton and T.F. Freers
19	1969 Cyprus Hills, Saskatchewan and Alberta	W.O. Kupsch
20	1971 Kansas and Missouri Border	C.K. Bayne and others
21	1972 East-central Illinois	W.H. Johnson, L.R. Follmer and others
22	1973 West-central Michigan/ east-central Wisconsin	E.B. Evenson and others
23	1975 Western Missouri	W.H. Allen and others
24	1976 Meade County, Kansas	C.K. Bayne and others
25	1978 Southwestern Indiana	R.V. Ruhe and C.G. Olson
26	1979 Central Illinois	L.R. Follmer, E.D. McKay III and others
27	1980 Yarmouth, Iowa	G.R. Hallberg and others
28	1981 Northeastern lower Michigan	W.A. Burgis and D.F. Eschman
29	1982 Driftless Area, Wisconsin	J.C. Knox and others
30	1983 Wabash Valley, Indiana	N.K. Bleuer and others
31	1984 West-central Wisconsin	R.W. Baker
32	1985 North-central Illinois	R.C. Berg and others
33	1986 Northeastern Kansas	W.C. Johnson and others
34	1987 North-central Ohio	S.M. Totten and J.P. Szabo
35	1988 Southwestern Michigan	G.J. Larson and G.W. Monaghan
36	1989 Northeastern South Dakota	J.P. Gilbertson
37	1990 Southwestern Iowa	E.A. Bettis III and others
38	1991 Mississippi Valley, Missouri and Illinois	E.R. Hajic, W.H. Johnson and others
39	1992 Northeastern Minnesota	J.D. Lehr and H.C. Hobbs
40	1993 Door Peninsula, Wisconsin	A.F. Schneider and others
41	1994 Eastern Ohio and western Indiana	T.V. Lowell and C.S. Brockman
42	1995 Southern Illinois and SE Missouri	S.P. Esling and M.D. Blum
43	1996 Eastern North Dakota & NW Minnesota	K.I. Harris and others
44	1998 North-central Wisconsin	J.W. Attig and others
45	1999 North-central Indiana & south-central Michigan	S.E. Brown, T.G. Fisher and others
46	2000 Southeast Nebraska and NE Kansas	R.D. Mandel and E.A. Bettis III
47	2001 NW Ontario and NE Minnesota	B.A.M. Phillips and others
48	2002 East-central Upper Michigan	W.L. Loope and J.B. Anderton
49	2003 Southwestern Michigan	B.D. Stone, K.A. Kincare and others
50	2004 Central Minnesota	A.R. Knaeble, G.N. Meyer and others
51	2005 North-central Illinois	E.D. McKay III, R.C. Berg and others
52	2006 Northwest-central North Dakota	L.A. Manz
53	2007 East-central Wisconsin	T S. Hooyer
54	2008 Northeastern Illinois	B.B. Curry
55	2011 Southwestern Illinois	D.A. Grimley and A.C. Phillips
55	2014 Southwestern Indiana	R,C.Counts, G.W. Monaghan, and E.Herrmann

* Field conferences were not held in 1968, 1970, 1974, 1977, 1997, 2009, 2010, 2012, or 2013.

-preface-

Welcome to Evansville, Indiana, and the 56th Midwest Friends of the Pleistocene meeting! We are looking forward to some insightful discussion about the late Wisconsinan and Holocene terraces of the Ohio River, Illinois glaciation, and the geoarchaeology of Angel Mounds. The weather looks perfect and we anticipate that a good time will be had by all. We have planned a full day trip for Saturday and a half day trip on Sunday. The Saturday trip will begin at Angel Mounds and go west to near the Wabash River, ending up back at Angel Mounds by (cross your fingers)5:30 pm. We will focus on loess and terrace sequences and chronology of the lower Ohio River, Illinoian (or earlier) glaciation near the confluence of the Ohio and Wabash River, and neotectonics in the region. We will also discuss how human settlement fits into the landscape. Sunday we will visit Angel Mounds for a morning discussion of the geoarchaeology of the site. Will focus on the work that we done over the past decade on mound construction and site chronology and what these results tell us about late prehistoric settlement of the lower Ohio valley.

Here is a summary of what we will say about the lower Ohio River valley:

- Ohio River tributary valleys are composite landscapes that owe much of their current morphologies to inheritance of pre-MIS 2 glacial landscapes (Fig 3.1).
- In northwestern Vanderburgh County, the MIS 6 ice margin lies at least 5 km farther south than it is mapped (Fig 3.1).
- The Ohio River responded rapidly to changes in Quaternary and Holocene climate by aggrading and forming terraces during cool intervals and incising during transitions to warm intervals (Fig 6.1.5).
- Responses of the Mississippi and Ohio Rivers to changing Quaternary climate were largely in phase with one another (Fig 3.9).
- There is a significant phase of aggradation in the Ohio valley during MIS 4 or MIS 3; this record is preserved in both the mainstem river and in the Pigeon Creek tributary valley (Fig 3.7,Fig. 6.2.2).
- There is a pre-Loveland silt in the Ohio River valley (Fig. 3.3, Fig 3.5).
- In thick Ohio River Peoria loess, total carbonate with depth correlates very well with the GISP 2 ice core record and seems to be a good proxy for temperature (Fig 6.1.5).
- The Ohio River is susceptible to neotectonic activity in the Wabash Valley seismic zone.
- There may be pre-MIS 6 diamict under the Mumford Hills.
- Much more work needs to be done regarding MIS 6 and older glaciations in southwestern Indiana.

Quaternary geology and geoarchaeology of the lower Ohio River Valley, southwestern Indiana

Ronald C. Counts[1], G. William Monaghan[2], and Edward Herrmann[3]

(United States Geological Survey[1], Indiana Geological Survey, Indiana University[2], and Department of Geological Sciences, Indiana University[3]**)**

1. Introduction and Background

The advance and retreat of Pleistocene continental ice sheets profoundly affected the Ohio River, transforming it from a bedrock stream that emerged from a relatively small watershed into a major drainage of the northeastern United States. The 56th Midwest Friends of the Pleistocene (FOP) field conference will focus on the Quaternary evolution of the Ohio River in southwestern Indiana. To avoid differences in nomenclature used for continental glaciations (e.g., Wisconsin Episode, Wisconsinan, pre-Illinois Episode) we will reference glaciations and interglacial periods according to the marine oxygen-isotope record (MIS 2, MIS 4, etc.). We will visit recently discovered exposures of diamicton older than MIS 2 and discuss how glaciation affected the development of the landscape. We will also discuss the chronology of MIS 2 outwash terraces, Holocene terraces, and how the Ohio River responded to the changing Quaternary and Holocene climate, and will discuss human landscape modifications to those terraces. Lastly, we will discuss regional neotectonic events that have left seismic signatures in Holocene sediments (primarily) that form these natural and human landscapes. Much of the data related to the chronology and character of the terraces was collected and synthesized by Ron Counts in his dissertation (Counts, 2013), but some of the exposures we will visit are recently discovered and have barely been described or examined. This guidebook includes new and unpublished data as well as data that was previously reported elsewhere; these publications are referenced within the text. The geoarchaeology research related to human landscape modifications has been reported by Bill Monaghan and colleagues (Monaghan and Peebles, 2010; Monaghan et al., 2013) and was collected from 2005, related to Indiana University field school excavations and to our ongoing National Science Foundation Research Experience for Undergraduate (NSF-REU) grant.

The 2014 FOP starts with the concept that rivers are dynamic and continuously adjust to changes in environmental conditions, including crustal deformation, changes in base level, and climate (e.g., Leopold et al., 1964; Schumm, 1977, 1987; Bull, 1991, Maddy et al., 2000, 2001). Consequently, fluvial deposits and landforms provide an important record of Quaternary paleoenvironmental change and landscape development. However, few studies of fluvial systems in the midwestern United States use modern methods, particularly numerical dating. An exception to this is Rittenour et al. (2003, 2005, 2007). They used optically stimulated luminescence (OSL) to develop detailed and robust chronologies for terrace formation on the lower Mississippi valley, and their results provide detail to the timing and nature of environmental change that rivers in the central continental U.S. responded to during the Quaternary. Similarly, we have developed a chronology of fluvial and alluvial landforms for the lower Ohio River valley, but have done so over a smaller geographic area, producing a detailed, high-resolution chronostratigraphic framework for the Ohio River valley.

The area covered by the trip includes the lower Ohio River and Wabash River valleys in southwestern Indiana, between Evansville, Ind., and the confluence of the Ohio and Wabash Rivers and the Illinois state line. However, we will also include and discuss data from adjacent western Kentucky and southwestern Illinois. During the field trip on Saturday we will visit five locales (Fig. 1.1) that are associated with MIS 2

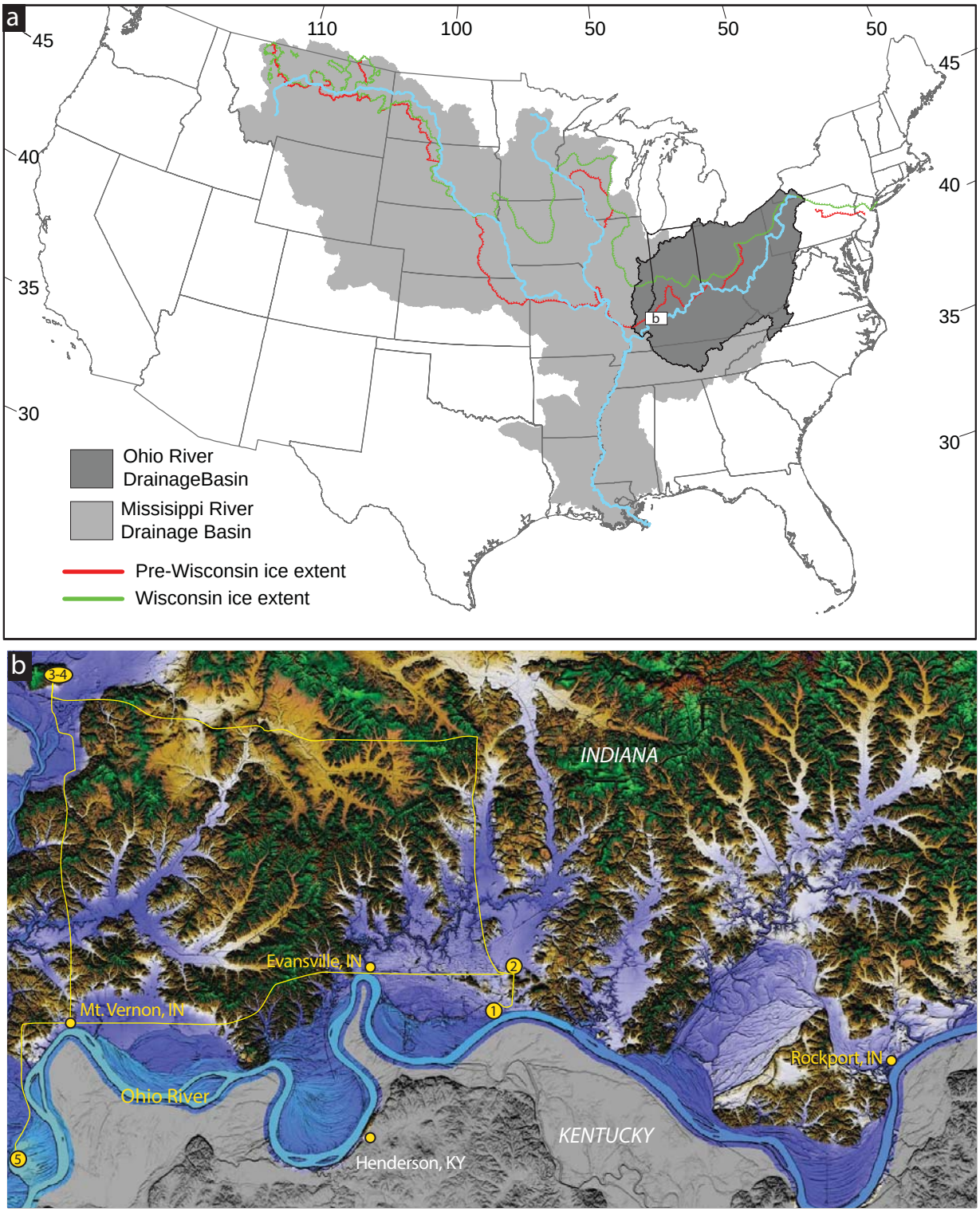

Figure 1.1. (a) Map showing the extent of the Ohio River drainage basin in the northeastern United States. (b) LiDAR DEM of the study area from Rockport, Indiana, to the confluence of the Wabash River showing route and field trip stops.

outwash terraces and alluvium of the Ohio valley and sediments associated with MIS 6 ice in the Wabash valley. The first and second stops are related mainly to the chronology of MIS 2 terraces in the Ohio River. We will discuss the formation and ages of the terraces and the environmental history implied. The third and fourth locales (where we will have a lunch stop) are devoted to evidence of the MIS 6 ice or older glaciofluvial or lacustrine events in southwestern Indiana. The final Saturday stop is devoted to discussions of evidence for seismic events in the region and on late Holocene paleoenvironmental data that we are collecting in the lower Ohio valley. On Sunday we will visit three locations at Angel Mound. Each is related to the geoarchaeology of Mound construction or to evidence of late Holocene seismic events in the region.

The Ohio River is the largest river in the eastern U.S., traversing much of the glaciated northeastern U.S. through the physiographic provinces of the Appalachian highlands of Pennsylvania, the glaciated Central Lowlands of Ohio, the Interior Low Plateaus of Kentucky and (Fig. 1.1). The morphology of the upper Ohio River valley is very different from the lower. The upper Ohio River is characterized by a narrow constricted bedrock valley. River terraces and alluvium in the upper Ohio River are typically discontinuous and are either the remnants of glacial outwash or narrow bands of Holocene floodplain deposits (e.g., Swadley, 1969, 1976, 1978; Luft, 1971; Gibbons, 1972), though a few reaches of the constricted valley widen and contain more extensive alluvium (e.g., Crittenden and Hose, 1965; Kepferle, 1974). In contrast, where the lower Ohio River flows through the physiographic province of the Illinois Basin (from Tell City, Ind., to the Wabash-Ohio River confluence), the river meanders across a broad valley and has thick and continuous alluvial fill successions with multiple river terrace levels (Ray, 1965; Moore et al., 2007, 2009).

The river terraces and fluvial deposits along the lower Ohio River are particularly important. They provide useful geomorphic proxies that record late Quaternary hydrologic and paleoenvironmental change and were greatly influenced by advance and retreat of the Laurentide ice sheet in the eastern U.S. Yet, little modern research has been undertaken on the Quaternary fluvial record of the Ohio River. During the trip we will discuss alluvium and terraces in the lower Ohio River valley, and how OSL and radiocarbon dating was used to develop a chronostratigraphic framework for the lower Ohio River (Fig. 2.1), which can be used to relate deposition and incision to Quaternary paleoenvironmental change.

2. Previous Research

The first research on Quaternary sediments in the lower Ohio River valley, which included interpreting the loess deposits as water-lain in origin, was undertaken by David Dale Owen (1859). His work was followed much later by that of Fuller and Ashley (1902) and Fuller and Clapp (1904), who produced two U.S. Geological Survey (USGS) folios for the region immediately northeast of the Ohio-Wabash River confluence. These publications included the recognition of pre-Wisconsinan glacial deposits and detailed 1:125,000-scale surficial geologic maps. Theis (1922) recognized multiple bedrock and alluvial terraces in Henderson County, Kentucky, and used gastropod assemblages to conclude that loess was an eolian deposit. Other research in the lower Ohio valley in the 1960s and 1970s included geologic mapping at a 7.5-minute quadrangle scale by the USGS. However, this mapping was based on the early 20th century paradigm of four continental glaciations in North America (e.g., Walker, 1957; Ray, 1965, 1974) and the fluvial deposits were primarily mapped as a single undifferentiated unit (e.g., Johnson, 1972, 1973, 1974; Norris, 1974). Alexander and Prior (1971) and Alexander and Nunnally (1972) used radiocarbon dating to study the timing of floodplain formation and determined that three intervals of changing vertical aggradation rates occurred during the Holocene.

Straw et al. (1977) described the environmental geology of the Evansville area, which included descriptions of landforms and deposits, their engineering properties, environmental hazards, and a geologic map.

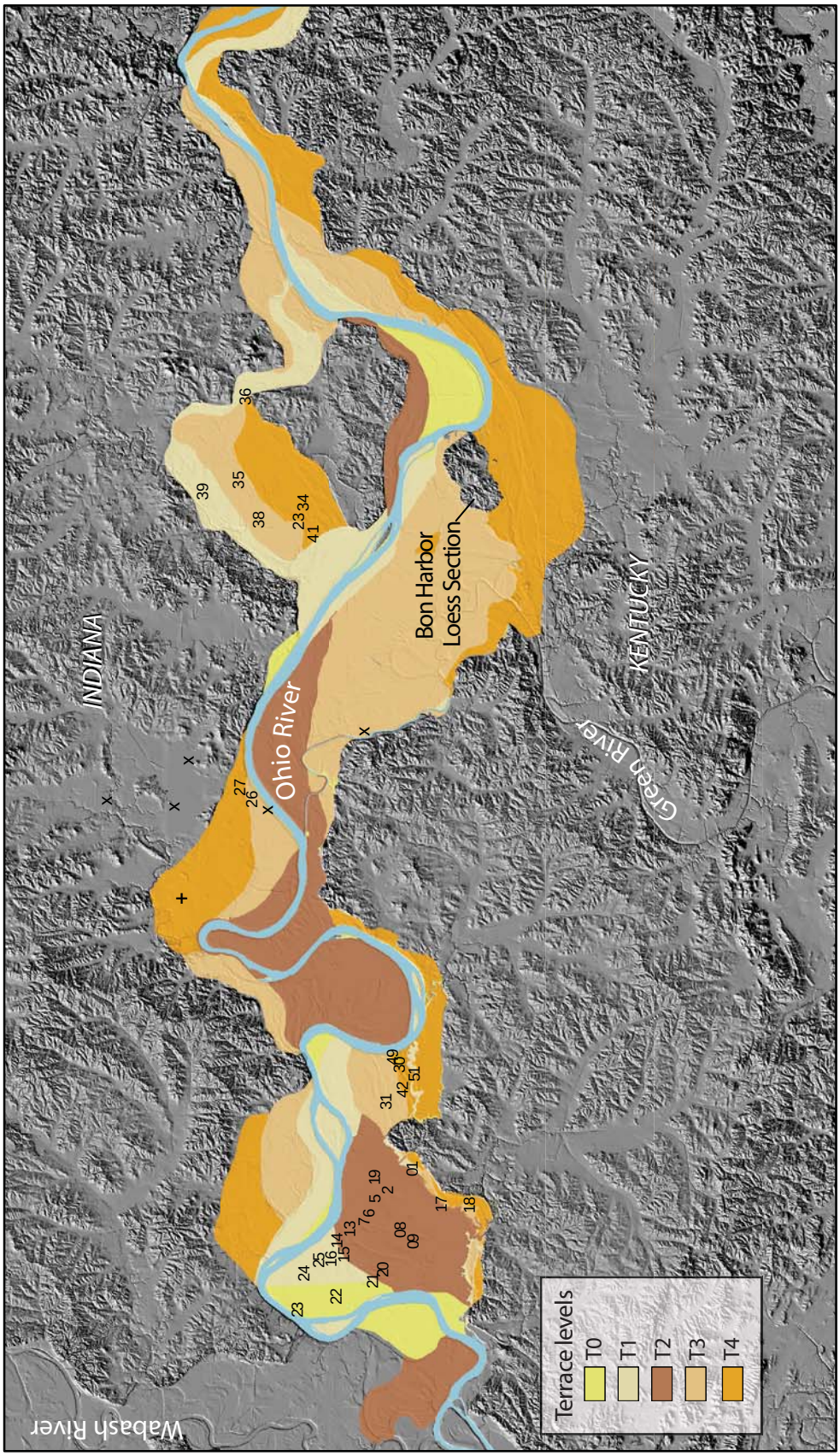

Figure 2.1. Map showing Wisconsinan and Holocene terraces, geochronology sample locations, and geomorphic relationships between terraces in the lower Ohio valley. Terrace numbers are from youngest (T0) to oldest (T4). Numbered locations are OSL ages from Counts (2013). Locations marked with an X are unpublished OSL and radiocarbon ages. Location marked with a (+) is from Woodfield (1998).

Fraser (1986) drilled cores and concluded the mid-channel islands in the Ohio River were not depositional landforms of the modern flow regime but relict braid bars that were obstructions to the modern flow regime. Fraser and Fishbaugh (1986) drilled a core transect across part of the lower Ohio valley and identified Holocene, Wisconsinan, and pre-Wisconsinan alluvium. Later, Woodfield (1998) used auger cuttings, gamma logs, and several radiocarbon ages to propose that megafloods down the Wabash River were responsible for much of the tributary valley fill in the Little Pigeon basin in Vanderburgh County, Ind. Most recently, the USGS (Moore et al., 2007, 2009) completed a 1:24,000-scale surficial geologic map, with supporting geochronology, for seven contiguous quadrangles that include parts of Vanderburgh and Warrick Counties in Indiana and Henderson County, Kentucky.

Though there are many site-specific, local investigations in the lower Ohio valley, no one has yet critically evaluated the high-level terraces on the Ohio River. This lack of study partially reflects the fact that high-energy fluvial environments like the braided late Pleistocene Ohio River typically lack sufficient organic material for reliable radiocarbon dating. Dateable organic material (wood, charcoal) is commonly destroyed in such high-energy settings, and where organic material is preserved it is impossible to know if it is contemporaneous with the time of deposition or whether it was reworked from older deposits. Therefore, multiple samples from the same deposit are required to establish a reliable age for any particular unit, a difficult task given the scarcity of organic material and the associated expense of dating, particularly from cores. Fluvial sediments such as those found in the Ohio River, however, are well suited for OSL dating (Duller, 1996; Stokes, 1999; Wallinga, 2002; Rittenour, 2003; Wintle, 2008), which provides the basis for our chronostratigraphic sequences.

3. Quaternary deposits, paleoclimate, and paleoenvironments

3.1. Flora and Fauna

Boreal forest with spruce and pine dominated the forest vegetation from ~23 ka to ~20 ka during the global last glacial maximum (LGM) (Wilkins et al., 1991; Jackson et al., 1997, 2000). During the Late Glacial (~15 ka to ~12 ka), boreal forest transitioned into taiga-boreal woodland dominated by pine and sedge (Jackson et al., 1997, 2000), and during the Pleistocene-Holocene transition (~12 ka to ~9 ka), deciduous woodlands replaced the taiga-boreal woodland (Jackson et al., 1997; Williams, 2003). Megafauna fossils are common within the Pleistocene deposits in the study area. The type specimen for the dire wolf (*Canis dirus*) was discovered on the banks of the Ohio River in 1854 near Evansville, Indiana (Leidy, 1856). Giant ground sloth (*Megalonyx jeffersonii*) bones were discovered in an exposure of a tributary paleochannel being eroded by the Ohio River near Henderson, Kentucky (Owen, 1861), and wood taken from the same strata from the clay beds was 9,400 ± 160 yrs BP (Rubin and Alexander, 1958). The *Mammut americanum* skull (Masotodon) on display at Big Bone Lick was discovered in 1953 along Canoe Creek in Henderson County, Kentucky. A cursory examination of a clay smear slide, taken from a core recently drilled at the 1953 discovery site, revealed abundant and very well preserved spruce and pine pollen. Sedge pollen was also present but not as abundant, and there was virtually no pollen from deciduous species (Eric Grimm, personal communication). There have also been *Castoroides* (giant beaver) and *Dicotyles* and *Tapirus* (peccary) found in Gibson and Vanderburgh Counties (14th report Indiana geology), and there are at least six sites with Mastodon remains in Gibson and Posey Counties (references), in Indiana.

Currently, the lower Ohio River valley in southwestern Indiana has a humid continental climate with large seasonal temperature fluctuations of hot and humid summers and cold to very cold winters (Kottek et al., 2006). Prevailing winds are from the south to southwest, and precipitation is evenly distributed throughout the year. Topography is characterized by flat-lying fluvial terraces and floodplains and includes oxbow lakes and sloughs. Streams in the area are low-gradient with sand and silt bedloads. Rolling hills that range

from 125 to 165 m above sea level (asl) lie to the north and south of the fluvial landscapes. Native vegetation (pre-European settlement) of the flat bottomlands included mixed hardwood forests dominated by oak and hickory, marshes populated with cord grass and bulrush, and bald cypress swamps. Discontinuous prairies, forest openings, and beech-maple-oak-hickory forests were native to the upland hills (Woods et al., 1998). Today, much of the forested areas on flat-topped upland hills and flat bottomlands have been cleared for agriculture, and most forested areas exist in small patches on flatlands and on steeper upland slopes. The late prehistoric landscape was probably similar, and during specific intervals, particularly during the Mississippian period, was likely also at least partly cleared of forest.

3.2. Glacial deposits

Diamicton deposited by MIS 6 ice occurs in the northern reaches of the study area in the 1:125,000-scale mapping of Fuller and Ashley (1902) and Fuller and Clapp (1904). We are aware of no studies in the past 100 years to re-examine the MIS 6 glaciation in southwestern Indiana, other than a couple of site-specific studies done by geomorphology students at the University of Southern Indiana. The diamicton, presumed to be MIS 6 till, is relatively thin in the few places it is exposed and is covered by younger sediments or is eroded, all of which makes it extremely difficult to map. The two class projects that drilled cores in the region found diamicton in a core drilled approximately 5 km south of the mapped glacial limit, but no diamicton was present in a core drilled immediately north of the limit, illustrating some of the challenges involved in mapping the southern glacial boundary.

Though the presence of diamicton is the most conclusive evidence of glaciation, it is not the only evidence for ice advances older than MIS 2. The effects of these older glaciations are imprinted on the landscape of southwestern Indiana. Smoothed topography and landforms revealed by the new Indiana LiDAR data suggest the southern ice limit is farther south than was previously mapped (Fig. 3.1). Using the LiDAR data and the location of the core that penetrated diamicton, the MIS 6 ice limit can be shifted south ~5 km with some confidence from the Wabash River to about 25 km north of Angel Mounds (Fig. 3.1). East of this position, however, in the absence of additional field work, it is difficult to determine whether the MIS 6 limit continues north or parallels an apparent glacial ice margin to the east. The presence of a glacial boundary to the east is inferred because it readily explains the many southward-flowing, severely underfit streams that occur north of the Ohio River (Fig. 3.1). This boundary deviates significantly from the mapped MIS 6 ice margin, so it is hypothesized to be an unrecognized pre-MIS 6 glacial margin or, possibly, the true MIS 6 ice limit.

3.3. Tributary valley fill

The presence of glacial ice in the northern part of the Ohio River drainage basin caused rapid aggradation in the main valley (e.g., Leverett, 1902; Wayne, 1952; Ray, 1965, 1974; Straw, 1968; Fraser, 1994). Ohio River tributaries had much smaller sediment loads and did not aggrade in phase with the main valley, and outwash blocked the mouths of the tributaries, creating an extensive network of lakes (Shaw, 1911, 1915; Frye et al., 1972; Fraser, 1994). Sediments deposited in tributary valleys are primarily composed of fine silt and clay from the main Ohio River valley, with coarser outwash prograding up the tributaries as fluvial-deltaic successions during large flood events (Fraser, 1994; Kvale and Archer, 2007).

3.4. Loess

Loess associated with glacial advances accumulated on upland hills of the study area. The Peoria, Roxana, and Loveland loess units are typically found throughout the Midwest and are all present and common in the study area (Fig. 3.2). Loess thickness varies in the valley, but is typically thicker on the southern and

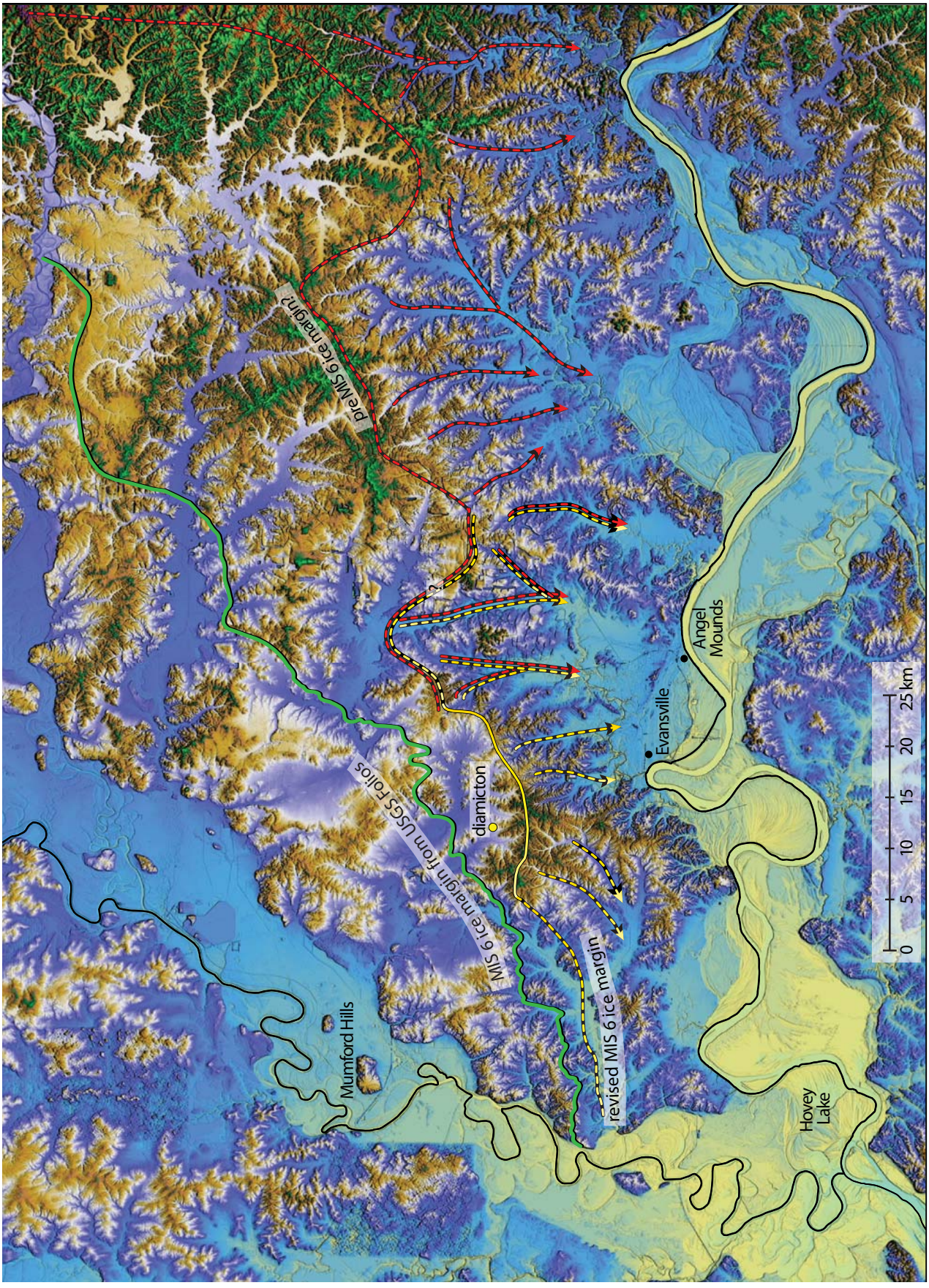

Figure 3.1. Diamicton, inferred to be MIS 6 till, was present in a core drilled ~5 km south of the mapped glacial limit. In many places the landscape south of the glacial limit is smoothed or subdued as if it was overridden by ice, also suggesting ice traveled further south than previously mapped. Likewise, many of the drainages flowing south to the Ohio River are underfit stream valleys, suggesting pre-MIS 6 or MIS 6 meltwater contributed to the larger hydrologic flow regimes that shaped them.

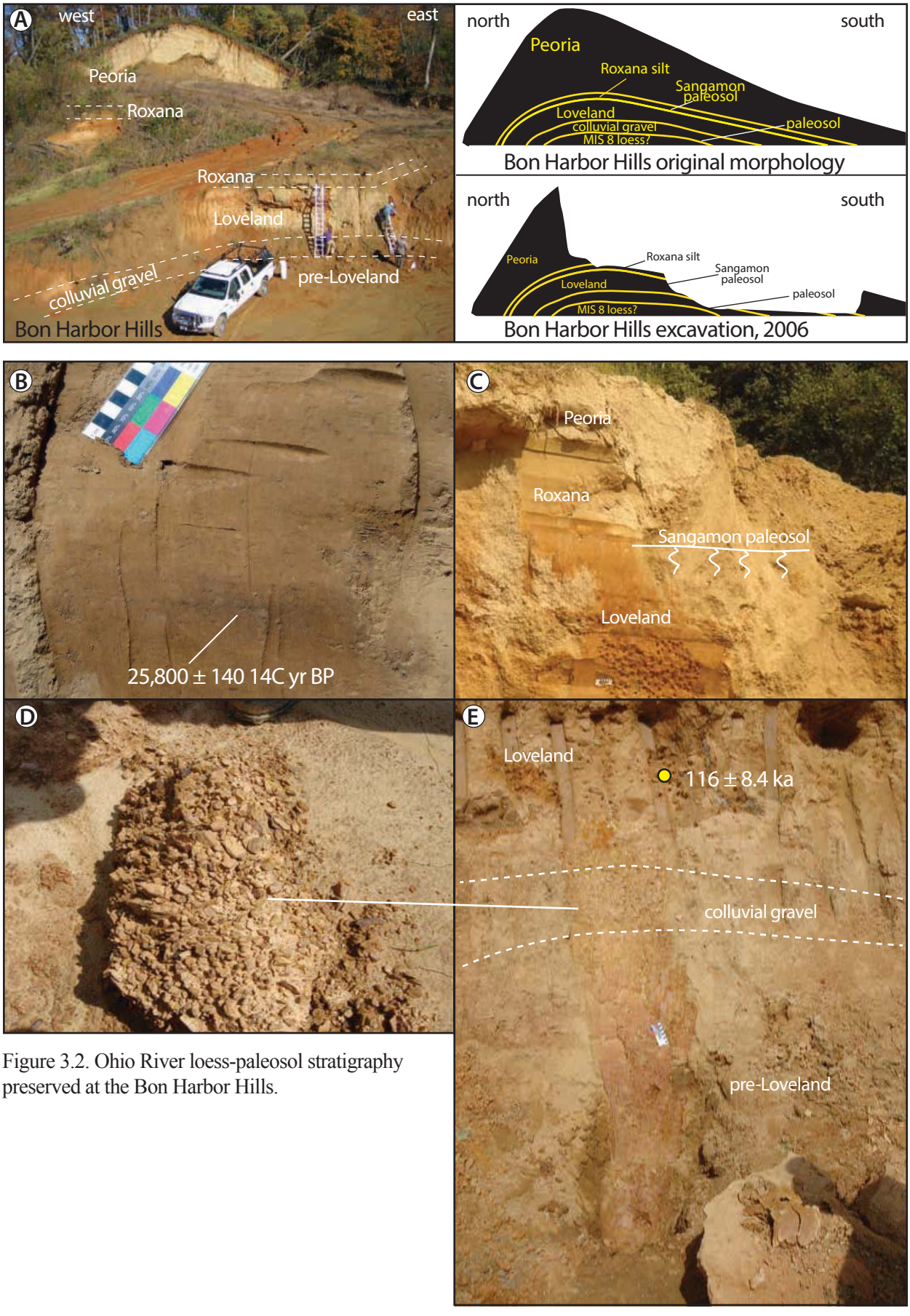

Figure 3.2. Ohio River loess-paleosol stratigraphy preserved at the Bon Harbor Hills.

eastern sides of the Ohio and Wabash Rivers, respectively. This is especially true for the Peoria loess, which can be more than 10 m thick (Fig. 3.2). The thick Peoria loess contains alternating, faint bands of light and dark layers that represent multiple incipient soil (A) horizons; it also contains several discernible weakly developed soils (Counts et al., 2008). Similar banding and paleosols are present in thick Peoria loess in Illinois (Wang et al., 2003, 2009). The Peoria loess is very calcareous, has large prismatic carbonate concretions, and is rich in terrestrial gastropod fossils.

The chronostratigraphy from OSL ages and radiocarbon ages of material from paleosols differ from that of radiocarbon ages of gastropods (Fig. 3.3). If we discount the gastropod ages, deposition of the Peoria began soon after 30 ka, with 8 m of accumulation by 11.5 ± 0.7 ka (Counts et al., 2008), or approximately 0.5 m/ka. After ~11.5 ka, there were an additional 2 m of loess deposited, likely into the early Holocene, but unfortunately this section could not be dated because of pedogenic alteration. If we discount the OSL and radiocarbon ages from paleosols and use gastropod ages, Peoria loess deposition began before ~26.5 ka and had aggraded 7.5 m by ~20 ka, or a rate of 1 m/ka. After ~20 ka, accumulation was much slower, with 2.5 m of loess accumulation in 20 ka, or 0.1 m/ka. OSL dating is known to work exceptionally well on eolian deposits, and likewise, recent research has shown that late Pleistocene gastropods can be used to reliably date loess deposits (Pigati et al., 2010, 2013). The discrepancies between the OSL and gastropod ages are something we still need to investigate by doing additional dating of Peoria loess in the lower Ohio River valley.

The mid-Wisconsinan Roxana silt underlies the Peoria throughout the valley and is typically 0.3 to ~1.0 m thick (Johnson, 1965; Ray, 1957, 1960, 1963, 1965; Ruhe and Olson, 1978, 1980). The Farmdale paleosol, which developed on the Roxana silt, is present locally but commonly is missing or weakly developed and can be difficult to recognize. At the Bon Harbor Hills site (location noted on Fig. 2.1), the Roxana silt appears to be welded onto the A horizon of the Sangamon paleosol (Fig. 3.2c), which is developed on the Loveland loess. The Loveland loess is generally 1 to 2 m thick in the study area and is easily recognized by its landscape position, which is typically overlying bedrock residuum, and the presence of the Sangamon paleosol on the surface of the Loveland (where it is not eroded). The Loveland had a feldspar thermoluminescence age of 116 ± 8.35 ka at the Bon Harbor Hills, which is younger than other reported ages for the Loveland, but at this site there was no material that was not pedogenically modified, so this age likely reflects bioturbation during the development of the Sangamon paleosol. At the Bon Harbor Hills site, the Loveland loess overlies weakly cemented colluvial gravel (Fig 3.2, Fig. 3.4). Beneath the colluvial gravel is a pre-Loveland silt that is at least 1 m thick (Fig. 3.4). Though it is pedogenically altered, the degree of soil development in this silt is less than in the Sangamon paleosol. Whether the silt was deposited during MIS 8 or earlier has not been established. The presence of a pre-Loveland silt has only been reported at one other location in the Ohio River valley (Ray, 1957).

3.5. Quaternary outwash and Holocene alluvium

The lower Ohio River valley is a terraced fluvial landscape that has been profoundly influenced by changes in hydrological flow regimes associated with late Pleistocene and Holocene climate changes. River terraces and terrace deposits, T0 (youngest) to T7 (oldest), were mapped along ~70 km of the lower Ohio River near Evansville. OSL dating combined with allostratigraphy were used to develop a detailed chronology of aggradation, terrace formation, and incision over the past ~160 ka, providing new insights into the evolution of the lower Ohio River valley.

A chronology was created using more than 50 geochronology samples (Table 1). The examination of cores combined with OSL and radiocarbon dating identifies four major phases of aggradation and incision over the past ~130 ka (Fig. 3.5). Deposits and landforms from the LGM and younger are abundant in the lower Ohio valley, and most ages are for these deposits. Older deposits (T7–T5) have been extensively

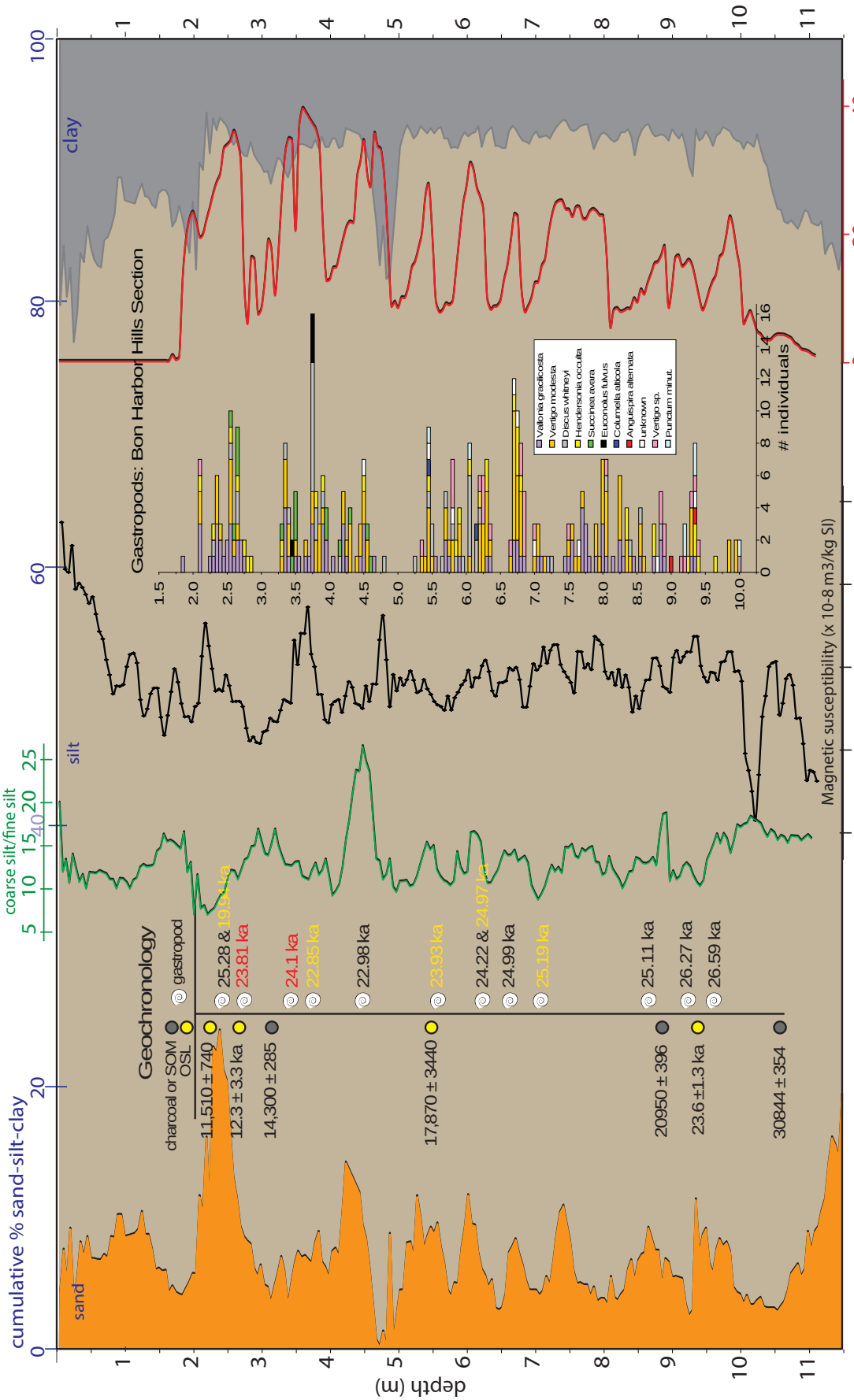

Figure 3.3. Cumulative particle-size data, coarse silt/fine silt ratio, magnetic susceptibility, OSL and radiocarbon geochronology, gastropod paleoecology, and total carbonate data collected every 5 cm from the Peoria loess at the Bon Harbor hills. Different colors for gastropod radiocarbon ages represent different species. Magnetic susceptibility and gastropod species identification provided by Dave Grimley (ISGS). Soil organic matter ^{14}C ages and total carbonate provided by Hong Wang (ISGS). Gastropod ^{14}C ages provided by Jason Rech (Miami) and Jeff Pigati (USGS).

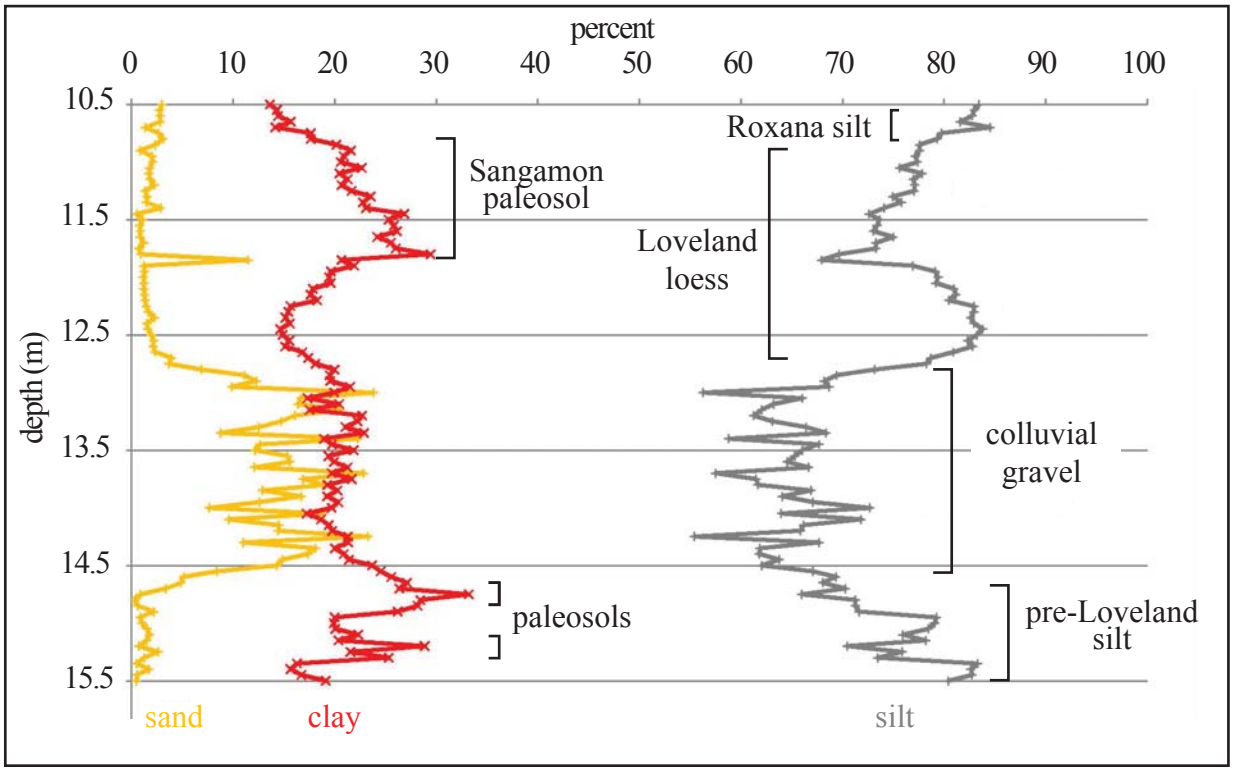

Figure 3.4. Particle size distribution of material below the Peoria loess at the Bon Harbor Hills. Samples were collected every 5 cm.

eroded or are deeply buried, making them difficult to sample for OSL dating, with only ~10% of our samples representing these deposits. (Table 2 provides a summary of the distinguishing characteristics for each fluvial unit.)

Pre-T7 history

Coring data from this study and from online databases at the Indiana and Kentucky Geological Surveys show that the study area has a flat bedrock floor with broad strath terraces at 90 and 75 m asl that are overlain by up to 50 m of alluvium (Fig. 3.5a). The bedrock valley was deeply incised after the Ohio River captured the much larger Teays River (Fowke, 1925; Melhorn and Kempton, 1991). This stream capture occurred ~1.4 Ma (Grainger et al., 2001) when early Pleistocene continental ice sheets blocked the Teays River valley and forced water into the headwaters of the Ohio River (Melhorn and Kempton, 1991). Cosmogenic burial ages of sediments deposited in Mammoth Cave in Kentucky indicate that the Green River, a tributary of the Ohio River, deeply incised into bedrock ~1.24 Ma and experienced major aggradation between ~0.8 and 0.7 Ma in response to Ohio River base level changes caused by continental glaciations (Grainger et al., 2001).

T7 alluvium

Several properties of T7 alluvium indicate it is a MIS 6 (Illinoian) or older deposit. T7 alluvium was the lowest unconsolidated unit in the fluvial landscape, directly overlying bedrock. The MIS 6 Loveland loess overlies residuum and bedrock in the upland regions of the study area, which is a similar landscape position (Ray, 1957, 1965; Ruhe et al., 1974; Ruhe and Olson, 1978, 1980; Counts et al., 2008). T7 alluvium includes much larger clasts than the younger overlying alluvium, suggesting that its source area was closer, which is

Table 1. Equivalent dose and dates estimated using single aliquot regenerative (SAR) method. Each date was calculated using Grun (1991).

Sample	Landform/ Deposit	Discs (n)	Elev (m)	Depth (cm)	Lat. (N)/ Lon (E)	Wt_mean	Mean	Dose rate (Gy/ka)	Mean age (ka)	Wt mean age (ka)
LORV-23	T0 terrace	24(24)	107.59	502.9	37.8966/ -87.9176	1.84 ±0.01	1.88 ±0.18	2.49 ±0.13	0.8 ±0.1	0.7 ±0.1
LORV-22	T0 terrace	22(24)	106.68	198.1	37.8675/ -87.9108	1.69 ±0.01	1.72 ±0.17	1.85 ±0.10	0.9 ±0.1	0.9 ±0.1
LORV-25	T0 terrace	23(24)	107.9	502.9	37.8829/ -87.8726	8.16 ±0.03	8.14 ±0.98	2.92 ±0.15	2.9 ±0.2	2.8 ±0.2
LORV-24	T0 terrace	19(24)	108.2	228.6	37.8933/ -87.8842	3.91 ±0.04	4.21 ±0.71	1.23 ±0.06	3.5 ±0.6	3.2 ±0.2
LORV-13	T0 terrace	21(24)	109.42	411.5	37.8571/ -87.8420	7.00 ±0.02	7.12 ±0.51	1.74 ±0.11	4.1 ±0.4	4 ±0.02
LORV-15	T0 terrace	21(24)	109.73	289.6	37.8702/ -87.8683	6.45 ±0.03	6.67 ±0.71	1.51 ±0.09	4.4 ±0.5	4.3 ±0.02
STL400	T0 terrace	21(24)	102	400	37.85943/ -879423	7.1 ±0.03	7.4 ±1	1.52 ± 0.01	4.86 ±.7	4.7 ±0.2
LORV-21A	T1 terrace	24(24)	109.73	259.1	37.8461/ -87.8903	9.12 ±0.02	9.8 ±1.24	1.83 ±0.09	5.4 ±0.7	5 ±0.3
LORV-21B	T1 terrace	20(24)	109.73	259.3	37.8461/ -87.8903	7.99 ±0.02	8.24 ±0.84	1.40 ±0.07	5.9 ±0.7	5.7 ±0.3
LORV-14	T1 terrace	23(24)	109.12	320.0	37.8727/ -87.8540	7.51 ±0.02	7.77 ±0.97	1.30 ±0.08	6.0 ±0.8	5.8 ±0.4
LORV-10	T2 terrace	24(24)	110.34	228.6	37.8420/ -87.8577	10.56 ±0.03	11.72 ±1.93	1.71 ±0.09	6.6 ±1.2	6.2 ±0.3
LORV-09	T2 terrace	24(24)	108.81	472.4	37.8199/ -87.8516	9.77 ±0.03	10.08 ±1.01	1.39 ±0.16	7.3 ±1.1	7 ±0.8
LORV-20	T2 terrace	23(24)	110.03	426.7	37.8472/ -87.8806	7.64 ±0.04	8.08 ±1.32	1.02 ±0.06	7.9 ±1.3	7.5 ±0.4
LORV-19	T2 terrace	24(24)	109.73	198.1	37.8471/ -87.7970	9.62 ±0.03	12.94 ±3.03	1.21 ±0.07	10.7 ±2.6	8 ±0.5
LORV-05	T2 terrace	23(24)	109.73	228.6	37.8461/ -87.8236	11.05 ±0.06	11.72 ±1.72	1.35 ±0.08	8.7 ±1.3	8.2 ±0.5
LORV-12	T2 terrace	24(24)	109.73	198.1	37.8458/ -87.7350	14.05± 0.03	14.72 ±1.74	1.58 ±0.10	9.3 ±1.3	8.9 ±0.6
LORV-41	T2 terrace	17(24)	117.35	195	37.9016/ -87.2241	26.17 ±0.23	26.69 ±4.1	2.82 ±0.14	9.46 ±1.53	9.3 ±0.5
LORV-06	T2 terrace	22(24)	109.12	381	37.8472/ -87.8275	12.68 ±0.05	13.35 ±1.62	1.35 ±0.08	9.9 ±1.3	9.4 ±0.5
LORV-03	T2 terrace	24(24)	109.73	137.2	37.8389/ -87.8065	12.03 ±0.02	14.62 ±3.24	1.25 ±0.08	11.7 ±2.7	9.6 ±0.6
LORV-08	T2 terrace	24(24)	107.29	228.6	37.8266/ -87.8447	16.32 ±0.03	17.03 ±2.98	1.66 ±0.10	10.3 ±1.9	9.8 ±0.6
LORV-07	T2 terrace	24(24)	109.42	228.6	37.8525/ -87.8385	9.15 ±0.03	9.95 ±1.70	0.87 ±0.05	11.9 ±2.1	11.5 ±0.6
LORV-42	T3L terrace	20(24)	119.18	785	37.8268/ -87.7180	26.17 ±0.21	29.83 ±5.18	2.06 ±0.1	14.46 ±2.61	12.7 ±0.6
LORV-36	T3L terrace	20(24)	118.5	119.5	37.9487/ -87.1082	27.66 ±0.27	29.04 ±6.01	2.07 ±0.104	30.70 ±6.58	13.4 ±0.7
LORV-18	T3L terrace	23(24)	114.6	381	37.7792/ -87.8189	15.63 ±0.05	16.4 ±2.30	1.16 ±0.06	14.2 ±2.1	13.5 ±0.7
LORV-16	T3 alluvium	20(24)	109.73	167.6	37.8753/ -87.8693	21.67±0.12	21.78±3.10	1.61±0.08	13.5±2.1	13.5 ±0.8
LORV-32	T3L terrace	22(24)	119.18	465	37.8268/ -87.7180	31.15±0.23	33.99±7.54	2.14±0.106	15.86±3.60	14.5 ±0.7
LORV-31	T3L terrace	24(24)	112.77	315	37.8402/ -87.7322	23.32±0.14	26.99±5.59	1.58±0.078	17.08±3.64	14.8 ±0.7
LORV-11	T3 alluvium	23(24)	110.03	228.6	37.8366/ -87.8726	19.90±0.08	20.04±2.74	1.33±0.07	15.0±2.2	14.9 ±0.8
LORV-39	T3U terrace	23(24)	117.65	165	37.9767/ -87.1955	25.2±0.2	27.21±6.13	1.66±0.088	16.39±3.79	15.2 ±2.8
LORV-35	T3U terrace	20(24)	117.65	165	37.9517/ -87.1825	31.84±0.25	33.65±5.44	2.07±0.103	16.26±2.75	15.4 ±0.8
LORV-01	T3U terrace	24(24)	113.39	259.1	37.8177/ -87.7879	20.44±0.05	19.11±3.14	1.28±0.07	14.9±2.6	15.9 ±0.8
LORV-17	T3U terrace	24(24)	110.64	381	37.7984/ -87.8192	36.52±0.17	36.83±4.55	2.19±0.13	16.8±2.3	16.7 ±1
LORV-38	T4 terrace	17(24)	117.65	145	37.9361/ -87.2149	25.86±0.27	27.34±4.42	1.47±0.074	18.58±3.15	17.6 ±0.9
LORV-26	T4 alluvium	22(24)	117.04	435	37.9450/ -87.4511	32.49±0.24	32.96±5.66	1.82±0.09	18.1±3.2	17.8 ±0.9
LORV-28	T4 terrace	21(24)	118.87	187	37.9085/ -87.2155	30.84±0.18	35.14±6.66	1.65±0.082	21.25±4.2	18.6 ± 0.9
LORV-34	T4 Dune	21(24)	119.79	180	37.9094/ -87.2000	31.47±0.27	32.47±5.39	1.70±0.081	19.16±3.31	18.6 ±0.9
LORV-47	T4 alluvium	10(20)	112.47	1372	37.8550/ -87.6979	15.1 ± 1.77	16.2 ± 1.78	0.94 ± 0.06	20.3 ± 2.57	18.9 ± 2.53
LORV-29	T4 Dune	23(24)	128.32	250	37.8359/ -87.6918	32.29±0.26	33.3±4.68	1.71±0.083	19.50±2.90	18.9 ±0.9
LORV-37	T4 alluvium	23(24)	117.65	465	37.9361/ -87.2149	31.26±0.18	32.86±4.96	1.65±0.084	19.90±3.17	18.9 ±1
LORV-33	T4 terrace	20(24)	119.79	370	37.9094/ -87.2000	27.72±0.27	30.94±6.32	1.39±0.033	22.31±4.69	20 ±1
LORV-27	T4 terrace	19(22)	122.8	445	37.9483/ -87.4494	31.69±0.25	32.68±5.72	1.50±0.068	21.8±4.0	21.2 ±1
LORV-30	T4 Dune	17(24)	127.1	530	37.8358/ -87.6919	32.43±0.26	33.19±6.64	1.51±0.072	21.92±4.51	21.4 ±1
LORV-48	T4 alluvium	21(22)	112.47	2408	37.8550/ -87.6979	22.0 ± 1.28	26.3 ± 1.26	0.89 ± 0.06	35.5 ± 3.02	29.9 ± 2.7
LORV-50	T5 alluvium	18(20)	123.75	2652	37.8207/ -87.7074	96.0 ± 6.92	111.3 ± 22.2	2.50 ± 0.11	44.5 ± 3.11	38.4 ± 5.92
LORV-49	T5 alluvium	15(30)	128.32	2408	37.8317/ -87.6969	42.6 ± 1.45	45.2 ± 1.45	1.29 ± 0.07	41.1 ± 2.55	38.8 ± 2.44
LORV-51	T6 alluvium	21(24)	123.74	3673	37.8207/ -87.7074	334 ± 23.4	344 ± 34.1	2.93 ± 0.12	117 ± 10.8	114 ± 11.5

***The number outside parenthesis is number of aliquots used for age caclulations.**

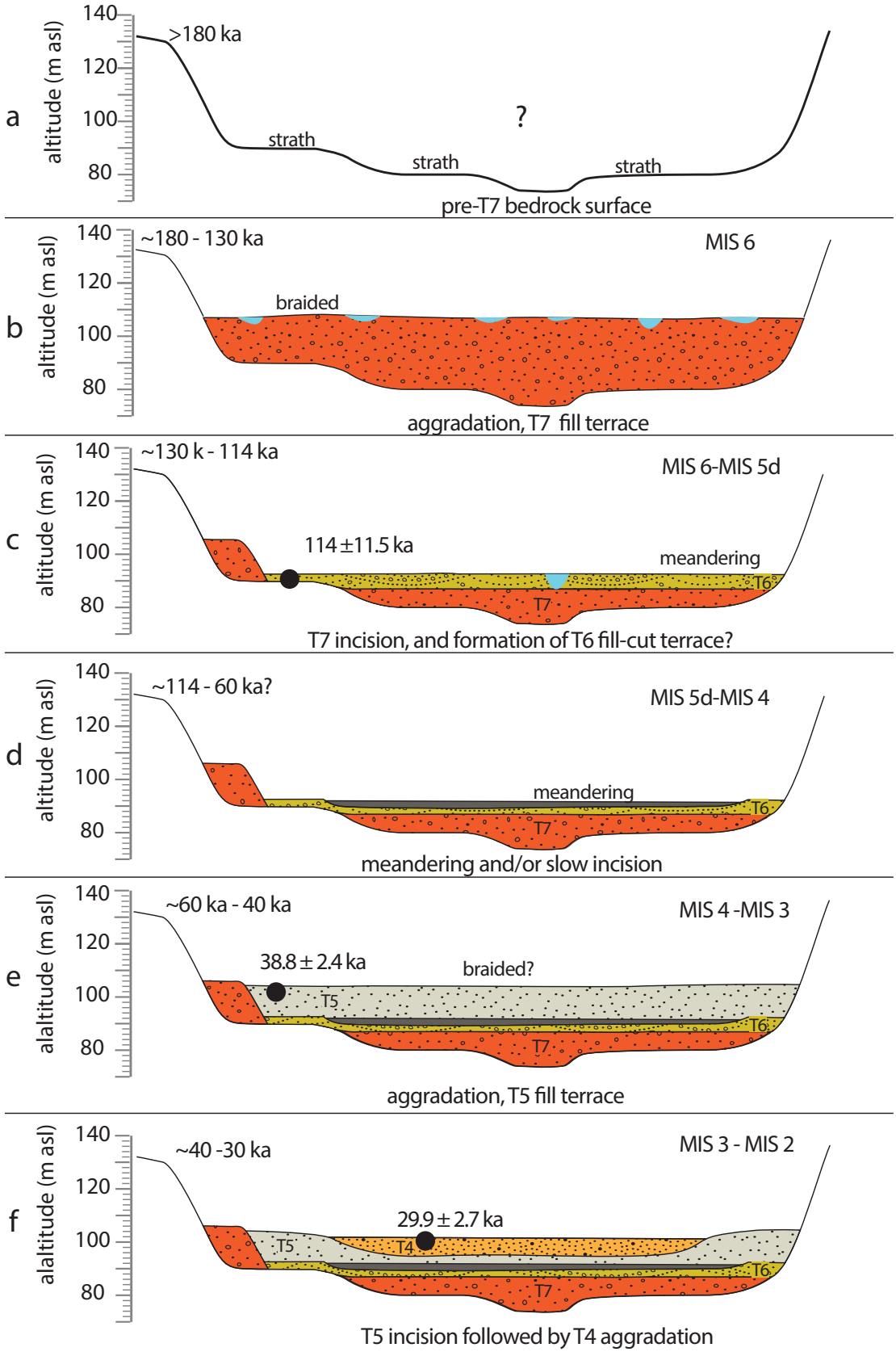

Figure 3.5. Fluvial evolution of the Ohio River over the past 160 ka. .

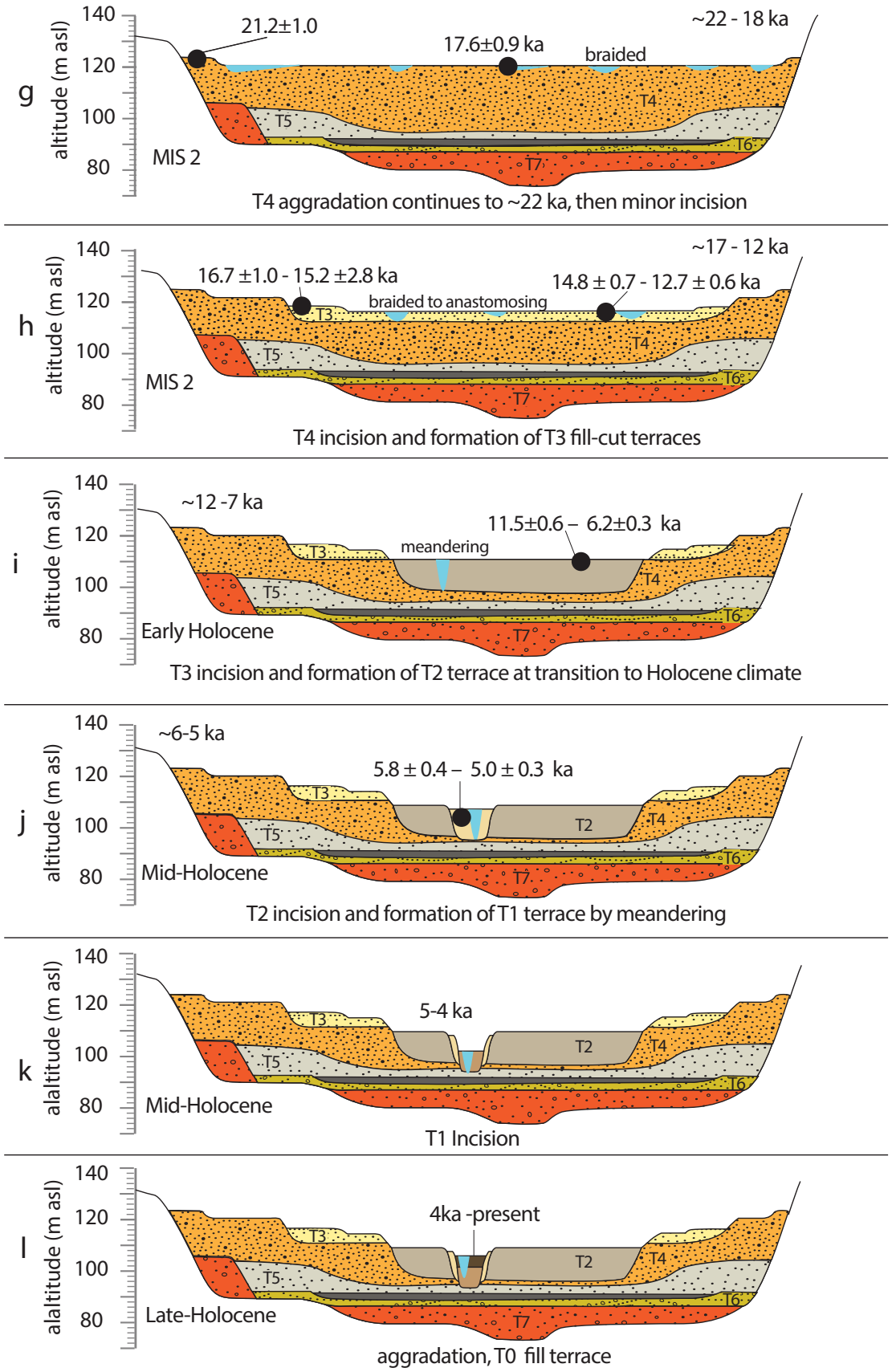

Figure 3.5 (cont). Fluvial evolution of the Ohio River over the past 160 ka. .

Table 2. Summary of alluvial deposits and landforms in the lower Ohio River valley

Deposit	Description	Munsell	Thickness (m)	Landscape Position*	Geomorphic Characteristics	Diagnostic Features	Interpretation
T7 alluvium	coarse gravel and sandy gravel, composed of chert, siltstone, sandstone, limestone, and quartzite clasts; includes smaller % of igneous and metamorphic lithologies from Canadian Shield	7.5YR 4/6 (strong brown) to 5Y 4/3 (olive)	0 - 5	24 to 37 m below grade	highly compacted and severly weathered	severley weathered, oxidixed colors	outwash deposited during MIS 6 or earlier
T6 alluvium	pebble sand; composed of quartz,chert, quartzite, sandstone,coal, limestone, and igneousand metamorphic clasts	10YR 4/2 (dark grayish brown) and 5Y4/2 (olive gray)	~2 - 6	20 to 24 m below grade	sediment caliber smaller than T7	oxidized colors	reworked MIS 6 outwash or MIS 5E meander belt alluvium
T5 alluvium	medium and coarse sand and fine pebbles; composed of quartz, chert, quartzite, sandstone, limestone, and granitoid rock fragments	10YR 4/2 (dark grayish brown) and 10YR 5/1 (gray)	~7 m	~10 m below grade	braided river deposits	unweathered coarse alluvium, only disguinishable from T4 by OSL dating	outwash deposited duriing MIS 3 or possibly MIS 4 outwash reworked during MIS 3
T4 alluvium (coarse)	coarse sand with lenses of pebble gravel; similar lithologies as T5	10YR 5/4 (yellowish brown) and 5Y 7/6 (yellow)	up to 35 m	from ~22 m below grade to ~13 m above grade	braided river deposits	unweathered coarse alluvium	MIS 2 outwash deposited by braided Ohio River
T4 alluvium (fine)	loamy sand and silty clay to clay	5Y 4/3 (olive), 10YR 3/1 (dark gray), and 5B 7/6 (light -blue)	14 m	from ~20 m below grade to 10 m above grade	lens shaped geometry	dark gray/reduced colors	fines deposited in in distributary channels, on leeward sides of bars, and in backwater areas formed during peak flow periods
T4 terrace	fill terrace, highest in Ohio Valle y	n/a	n/a	12 to 13 m above grade	braided terrace surface	n/a	surface of maximum aggradation during the LGM
T3 terrace and alluvium	cut terrace inset into T4 alluvium	10YR 3/3 10YR 4/6	n/a	5 to 3 m above grade	braided (upper levels) to anabranching (lower levels) channel morphology on surfaces	terrace risers between T4 -T3U and between T3U -T3L typically have low angles and are poorly expressed	inset terraces in T4 alluvium, climatically induced hiatuses in incision
T2 terrace and alluvium	silty clay loam underlain by moderately to well sorted medium and fine sand.	10YR 3/4 10YR 4/4	15-18 m	2 to 1 m above grade	meandering river deposits	n/a	transition to Holocene optimum
T1 terrace and alluvium	silty clay loam and silty clay that is underlain by massive, moderately sorted fine and medium sand	10YR 4/3 10YR 4/6	15-18 m	~1 m above grade	meandering river deposits	very weak soil development	Holocene climate
T0 terrace and alluvium	silt and silt loam	10YR 3/2 10YR 4/4	~4 m	grade	active floodplain level	no soil development	Holocene climate

true for the MIS 6 ice margin (Fig. 1.1) (Fuller and Ashley, 1902; Fuller and Clapp, 1904). Additionally, T7 alluvium is severely weathered and highly compacted compared to MIS 2 alluvium, which also suggests it is older, pre-Wisconsinan alluvium (Fig. 3.5b). Whether T7 is MIS 6 outwash or was deposited during an older glacial stage could not be determined. Regardless of its age, T7 alluvium is thin (1–5 m thick), suggesting there was significant erosion of alluvium deposited prior to or during MIS 6 (Fig. 3.5c).

T6 alluvium

The 114 ± 11.5 ka age of T6 alluvium, based on a single OSL age, spans from the end of MIS 6 to MIS 5d. Because the MIS 6 glaciation was more severe than the MIS 2 glaciation, the thickness of MIS 6 outwash should be comparable to that for MIS 2. However, the combined thickness of T6 and T7 alluvium was less than 10 m where observed (Fig. 3.5d). The age and thickness of T6 deposits suggest that T6 represents MIS 6 outwash that was reworked at the beginning of the last interglacial.

Though much of the MIS 6 alluvium appears to be missing from borings in the main valley where preservation potential is low, deposits of MIS 6 age are preserved in the tributary valleys, which lacked the stream power to significantly erode them. These deposits serve as a proxy for MIS 6 aggradation in the lower Ohio River valley. In cores, these deposits are easily identified by the presence of the Sangamon paleosol, a diagnostic marker horizon in the midwestern U.S. that developed on the surface of MIS 6 deposits during MIS 5. In the Highland Creek tributary in Union County, Kentucky, at the edge of the main valley, the Sangamon paleosol was present ~8 m below the modern floodplain (~18 m above the T7 alluvium). This landscape position indicates that at least 18 m of MIS 6 alluvium was eroded from the main valley before T6 alluvium was deposited/reworked.

No other MIS 5 or MIS 4 OSL ages were obtained within the study area, suggesting that there was a significant time gap between the deposition of the T6 and T5 alluvium. The Ohio River appears to have meandered during most of MIS 5 without significant phases of aggradation or incision, just as the Mississippi River did during this time interval (Rittenour et al., 2003). None of the deposits we dated had MIS 4 ages, so this meandering regime may have continued through MIS 4; if there was aggradation during MIS 4, the deposits were reworked or scoured from the valley.

T5 alluvium

The landscape position (10 m above T6 alluvium) and the OSL ages (38.8 ± 2.4 ka and 38.4 ± 5.9 ka) of T5 alluvium indicate significant aggradation occurred after T6 alluvium was deposited. The T5 alluvium is interpreted to correspond to aggradation ~38 ka during an MIS 3 ice advance (Fig. 3.5e). The absence of MIS 3 glacial landforms in the lower Ohio River basin does not preclude the advance of ice, as these landforms would have been overridden by the MIS 2 glaciation. This interpretation is supported by OSL ages of proglacial lake sediments deposited in a central Indiana cave during MIS 3 (Wood et al., 2010), which suggest that a MIS 3 ice margin exists near the cave. Alternatively, the MIS 3 age of T5 alluvium may represent reworked or incised outwash deposited during a MIS 4 ice advance. The interpretation of a MIS 3 ice advance is preferred, owing to the presence of the Roxana silt in the lower Ohio valley (Johnson, 1965; Ray, 1957, 1963, 1965; Ruhe and Olson, 1978, 1980), a ubiquitous, time-transgressive loess sheet deposited from ~60 to ~30 ka (Leigh and Knox, 1993; Rodbell et al.,1997; Markewich et al., 1998; Forman and Pierson, 2002).

T4 alluvium

The oldest T4 alluvium (LORV-48) present in the study area, located near the valley margin (samples LORV 49–50, Fig. 2), was ~12 m lower in the landscape than the older T5 alluvium (Fig. 3.6). This suggests there was major incision that removed a significant portion of T5 alluvium from the main valley at the end of MIS 3 and before the Laurentide ice sheet first advanced into the upper Ohio River basin (e.g., Clark et al., 1993; Szabo et al., 2011).

T4 terraces

The timing of maximum advance of the Laurentide ice sheet into the Great Miami River valley, which is the nearest source of meltwater input to the study area, was defined by Lowell et al. (1990) at ~23.5 ka

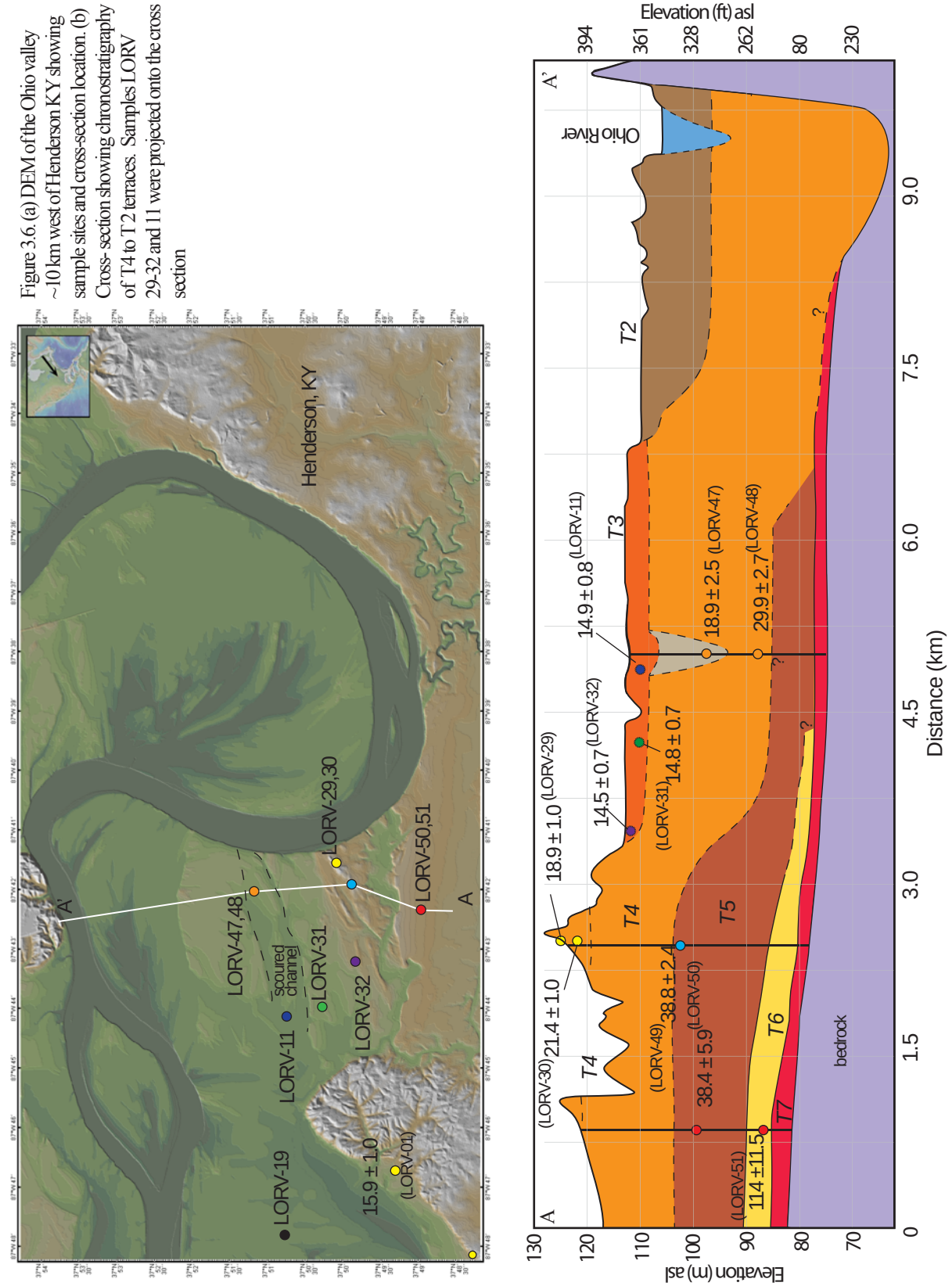

Figure 3.6. (a) DEM of the Ohio valley ~10 km west of Henderson KY showing sample sites and cross-section location. (b) Cross- section showing chronostratigraphy of T4 to T2 terraces. Samples LORV 29-32 and 11 were projected onto the cross section

(19,670 ± 68 radiocarbon yrs BP). This is somewhat younger than the oldest T4 terrace age of 21.4 ± 1.0 ka (Fig. 5f). However, terrace ages are based on the age of sand-rich alluvium below the surface soil and are, therefore, minimum ages, so the formation of the T4 terrace appears coincident with the LGM, indicating the high T4 terrace represents maximum aggradation in the lower Ohio Valley. There was as much as 35 m of fluvial aggradation in the valley in the period from ~30 ka up to the LGM (Fig. 3.5f).

T4 and T3 fill-cut terraces

Sediment input was significantly reduced as ice retreated, and the Ohio River began to incise the LGM outwash. The incision was not continuous; a series of fill-cut terraces were formed in the T4 outwash as the Laurentide ice sheet retreated (Fig. 3.5g-h). Fill-cut terrace ages are 21.2 ± 1.0 to 18.6 ± 0.9 ka for T4, 16.7 ± 1.0 to 14.5± 0.7 ka for the upper T3 terrace, and 13.5 ± 0.3 ka to 12.7 ± 0.6 ka for the lower T3 terrace (Fig. 3.6). Relict braid-bar morphology is preserved on the surfaces of T4 and upper T3 terraces, though lower T3 terrace surfaces transition to an anastomosing pattern, suggesting a significant flow regime shift ~ 14 ka.

T2–T0 terraces

The terrace surface morphology changed to a meandering pattern for T2 terraces, showing a shift from a braided/anastomosing to meandering flow regime. This change, indicated by the 11.5 ± 0.6 ka age of the oldest T2 terrace, shows that the change in fluvial regime took place at the beginning of the Holocene. The sedimentology/geomorphology and OSL ages indicate meandering persisted until ~6.2 ±0.3 ka (Fig. 3.5i). After 6.2 ± 0.3 ka, the Ohio River incised ~1 m into the T2 terrace (Fig. 3.5j), forming the T1 terrace. After the T1 terrace formed (5.8 ± 0.4 to 5.0 ± 0.3 ka), the Ohio River incised at least 4 m into it (Fig. 3.5k). The timing of this incision corresponds to a major shift in climate during the mid-Holocene (e.g., Dorale et al., 1998; Steig, 1999; Mayewski et al., 2004). This climatic shift has also been recognized in the dune deposits/landforms on the Great Plains (Dean et al., 1997; Foreman et al., 2001; Miao et al., 2007), in major changes in the pollen record reflecting vegetation changes in the eastern U.S. (Jackson et al., 2000; Foster et al., 2006), and in foreland basins of the Appalachian Mountains, recorded by abrupt shifts in $\delta^{13}C$ in soil organic matter (Driese et al., 2008) and rapid shifts in floodplain sedimentation rates (Driese et al., 2005, 2008).

Aggradation began ~4.3 ka after the incision of the T1 terrace (Fig. 3.5l). The timing of this aggradation might reflect response to drought in the midcontinental U.S. (e.g., Booth et al., 2005) or possibly global cooling that initiated the expansion of many mountain glaciers during the Neoglaciation (e.g., Wanner et al., 2008). Since ~4 ka, 4 m of vertical aggradation has occurred, with aggradation rates ranging from 0.75 m/ka to 4 m/ka over this time interval (Fig. 3.7).

3.6. Comparisons of the Ohio River and the lower Mississippi River valley

The timing and nature of fluvial adjustments of the Mississippi and Ohio Rivers are similar but not identical (Fig. 3.8a). The oldest dated alluvium deposits in the Mississippi valley are MIS 5a channel belt deposits (~84 ± 7 ka), which indicate the Mississippi River was a meandering system during MIS 5 (Rittenour et al., 2007). This chronology is comparable to the lower Ohio River valley, where, by MIS 5d (~114 ± 11.5 ka), the Ohio River had incised at least 18 m of MIS 6 outwash and presumably meandered during MIS 5, (based on the lack of any sediments of MIS 5 age or the Sangamon paleosol in the main valley(Fig. 3.8b). Rapid aggradation began in the Mississippi River valley near the end of MIS 4 in response to ice advancement into the basin (Rittenour et al., 2007). However, no direct fluvial evidence exists for MIS 4 aggradation in the Ohio River valley. Aggradation continued in the Mississippi valley through the middle of MIS 3, and the Melville Ridge braid belt (42 ± 3 to 35 ± 3) in the Mississippi valley correlates to Ohio River T6 alluvium (38.8 ± 2.4 ka), implying that rivers responded synchronously to environmental conditions by the middle of MIS 3.

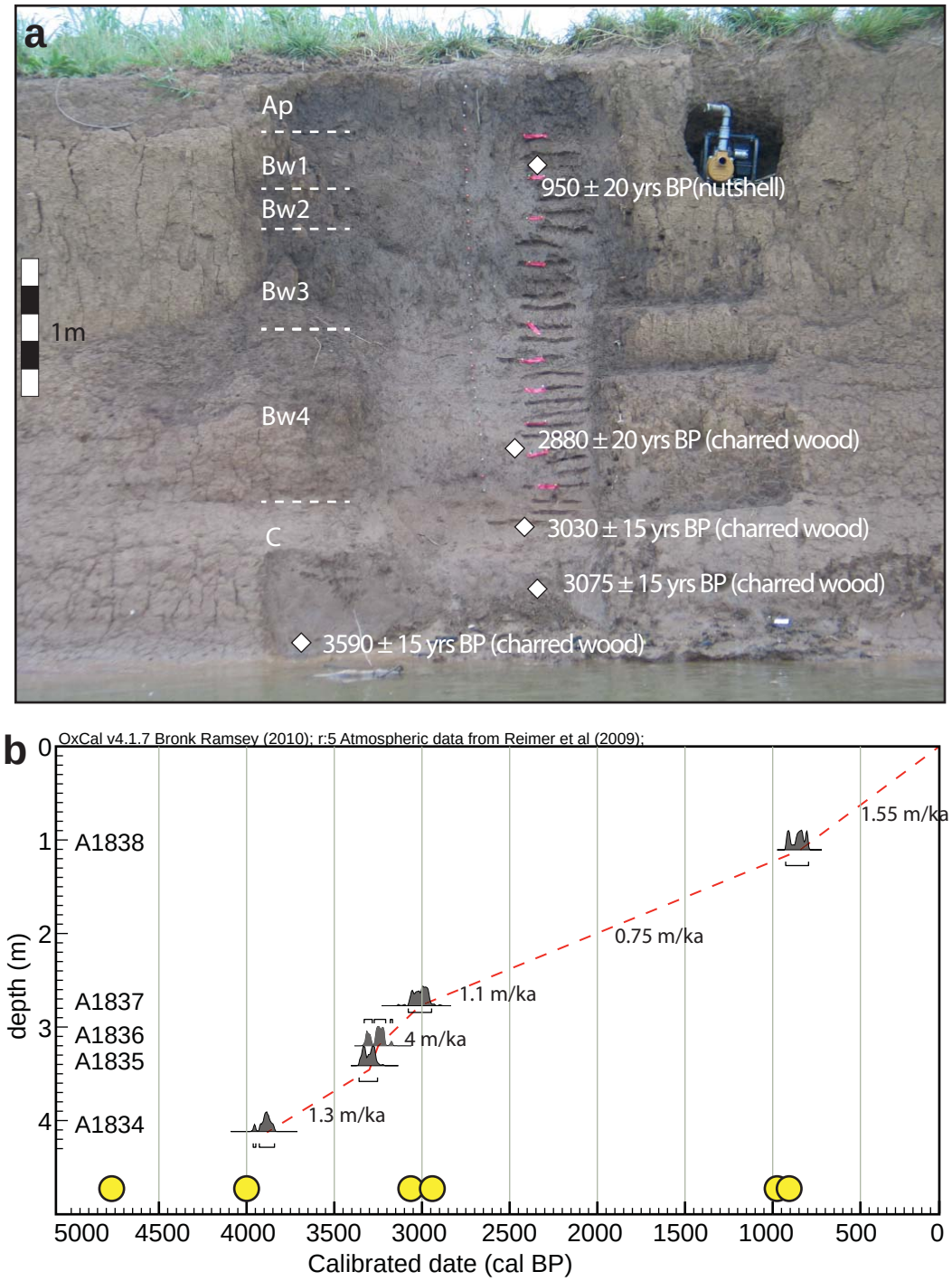

Figure 3.7. (a) Natural exposure of T0 alluvium with ^{14}C ages reported in radiocarbon years. Terrace has very weak soil development and is primarily silt loam and silt. (b). Aggradation rates calculated from calibrated radiocarbon ages show rapid aggradation occurred between ~4 ka and 3 ka. OSL ages for T0 (yellow circles) are consistent with calibrated radiocarbon ages.

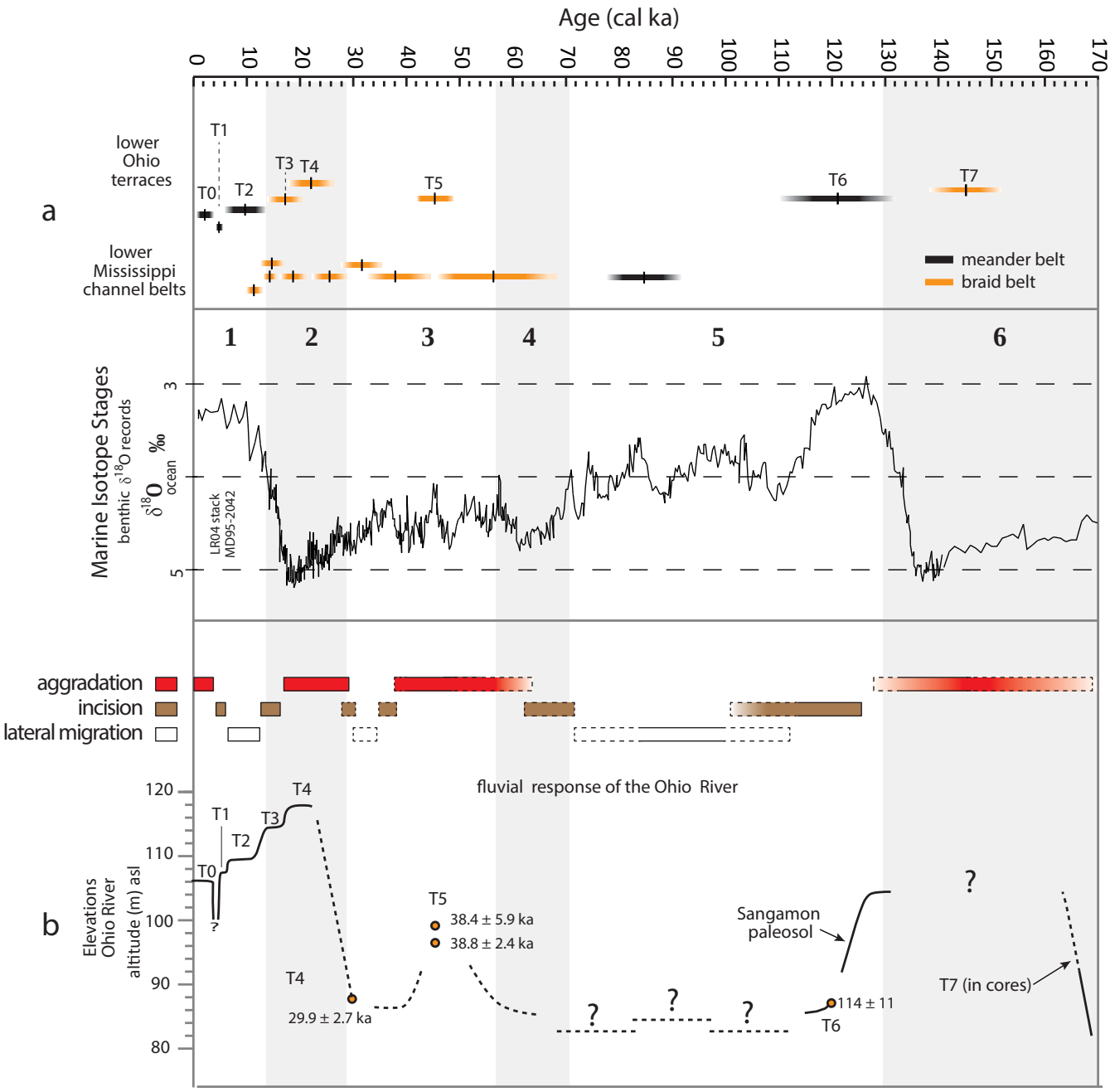

Figure 3.8. Comparison of Ohio River terrace chronology to the Mississippi fluvial system and to marine and terrestrial proxy records of climate change. (a) The channel belt chronology of the Ohio River and Mississippi River (Rittenour et al., 2007) compared to the benthic δ18 O foram record (Lisiecki and Raymo, 2005). (b) A fluvial response model for the lower Ohio River valley indicating phases of aggradation and incision are climatically modulated.

The oldest T4 alluvium in the Ohio valley, deposited at the end of MIS 3 (29.9 ± 2.7 ka), correlates to the Ash Hill braid belt in the Mississippi valley (27 ± 2 ka to 25 ± 2 ka). Following MIS 3, the fluvial responses in the Mississippi and Ohio valleys were largely synchronous. The T4 terraces (20.0 ± 1.0 to 17.6 ± 0.9 ka), upper T3 terraces (16.7 ± 1.0 to 15.4 ± 0.8 ka), and lower T3 terraces (14.8 ± 0.7 to 12.7 ± 0.6 ka) of the Ohio River correspond to Sikeston braid belt (19.7 ± 1.6 to 17.8 ± 1.3 ka), the Kennett braid belt (16.1 ± 1.2 to 14.4 ± 1.1 ka), Brownfield and Blodgett braid belts (14.1 ± 1.0 to 13.0 ± 0.9 ka) of the Mississippi River (Rittenour et al., 2007). The Ohio and Mississippi Rivers also shifted from braided to meandering flow regimes at nearly the same time; after 11.3 ± 0.9 ka on the Mississippi River and by 11.5 ± 0.6 ka on the Ohio River (Fig. 3.8a).

Fluvial responses of the Ohio and Mississippi Rivers are expected to be largely synchronous because of the similar climatic and glacial-hydrological forcing. Both rivers drain basins in the eastern U.S. that were covered by the late Wisconsinan Laurentide ice sheet. Additionally, the course of the modern Mississippi River, from Cairo, Illinois, to Memphis, Tennessee, was formerly occupied by the Ohio River until the Mississippi River was diverted through Thebes Gap ~12 ka (Rittenour et al., 2007), so some of the chronostratigraphies developed for the Mississippi valley are likely ages for lower Ohio River deposits.

4. Geoarchaeology of Angel Mounds

Angel Mounds is one of the largest Mississippian (ca. AD 1000–1400) towns in the lower Ohio valley (Fig. 4.1). It was established prior to AD 1100, grew in prominence, and was abandoned by AD 1450. The site has been investigated since 1937, including extensive excavations of earthworks, habitation areas, and sitewide geophysical surveys and core sampling (Figs. 4.1, 4.2, 4.3, and 4.4. As a result of this combined research: 1) the locations of most building and the traces of most palisade walls have been mapped, 2) the internal structure and construction sequences of the two major earthworks (Mounds A and F) are known, and 3) the stratigraphy and order of house construction and palisade walls are well-constrained by several large block excavations (Fig. 4.1), and their crosscutting or stratigraphic interrelationships have been identified and placed within Bayesian framework and modeled using OxCal software. The chronology of Angel Mounds is well controlled by more than 70 radiocarbon ages from key cultural contexts.

Angel Mounds is an agricultural town and figures importantly in the contemporary reconstruction of late prehistoric settlement systems in the midwestern region. The site lies on a T2 terrace of the Ohio River. When this terrace formed is known based on an OSL age from fluvial sand and gravel that occurs ~1.5 m below the surface south of Mound A. This age (10 ka) indicates that the terrace began to form in the early Holocene as lateral accretion deposits. However, the landform probably continued to develop during the early-middle Holocene through vertical accretion (i.e., overbanking). Minor sediment deposition probably continued throughout the middle and late Holocene, as even today the largest floods (e.g., 1937 flood) occasionally overtopped the site and only the earthworks lie above floodwaters. Sedimentation was probably very minimal during the middle and late Holocene. Consequently, the landform on which the Angel site lies was essentially established well before the establishment of Angel Mounds.

The focus of our visit to the site will be on the formation and construction of Angel Mounds, particularly its earthworks and structures. We will also discuss the chronology of the Mississippian occupation at the site and how these data enhance our understanding of Mississippian settlement in the lower Ohio Valley. We will focus on two major topics: 1) how geophysical methods, solid-earth coring, and chronology can be combined to reconstruct the age, internal properties, and construction methods and chronology earthworks at the site (see Monaghan and Peebles, 2010; Monaghan et al., 2013) and 2) the evidence and implications for earthquakes within deposits at Angel Mounds.

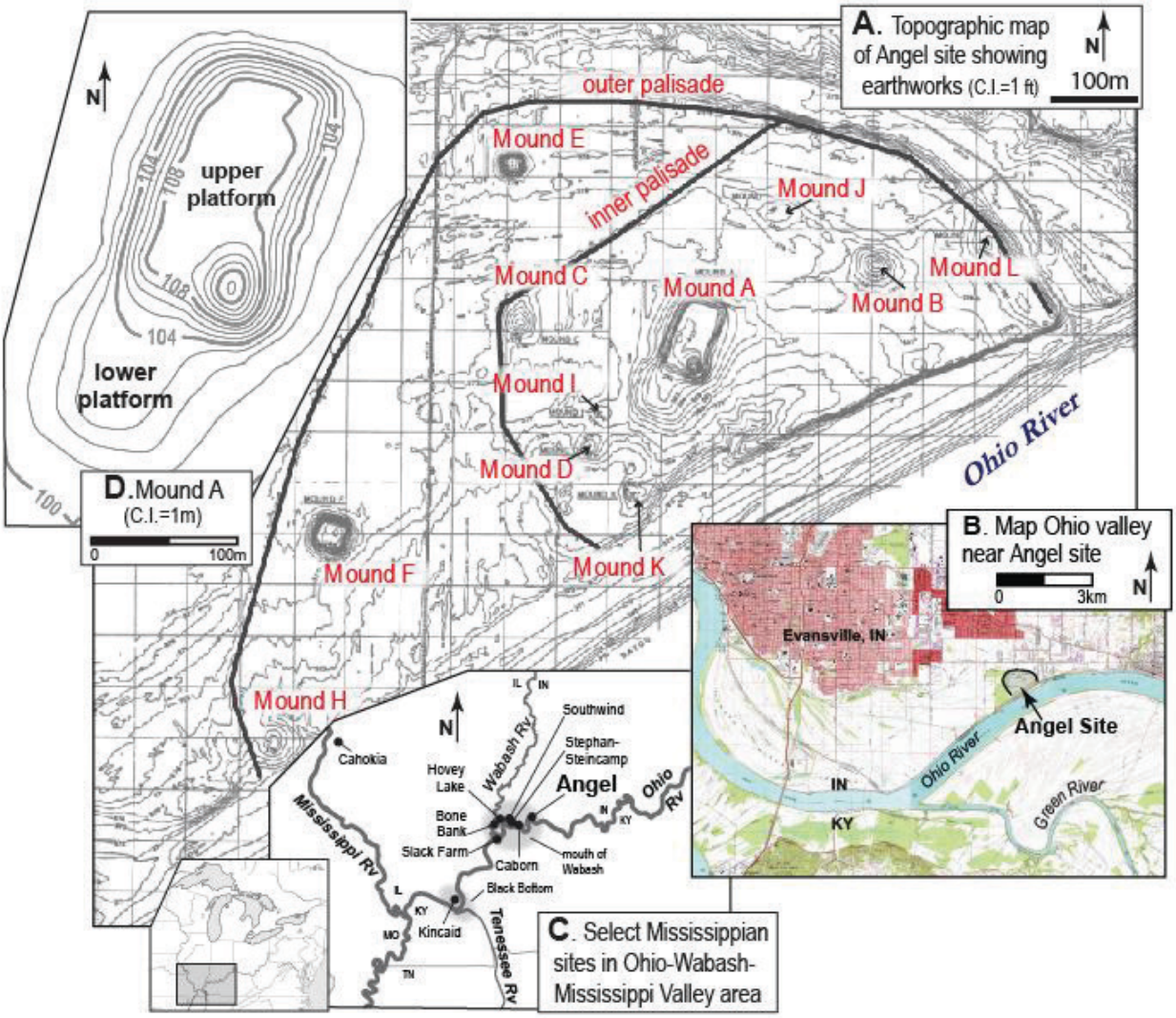

Figure 4.1 Maps showing the location of the mounds and earthworks at the Angel site as well as the locations of other nearby, significant Mississippian sites within the Wabash, Ohio and Mississippi valleys mentioned in the text. A) Topographic map of the Angel site showing locations of mounds (labeled) and other earthworks (after Black 1967; topographic base map provided courtesy of the Glenn A. Black Laboratory of Archaeology and Board of Trustees, Indiana University). B) Parts of the Evansville South and Newburgh 7.5′ Quadrangle map showing the Ohio River floodplain and location o the Angel site. C) Map of middle Mississippi and lower Ohio River valleys showing locations of the Mississippian Period archaeological sites mentioned in text. D) Detailed topographic map of Mound A (topographic contours based on relative datum of 100m).

4.1. Minimal and noninvasive methods applied to the study of earthworks and mounds

The process of recovering and contextualizing cultural information from strata is the heart of archaeological research but, given the size of earthworks, is no longer practical. Mound A at Angel Mounds, for example, measures ~200 x 125 m and is up to 16 m high (Fig. 4.5), and so is one of the largest Middle Mississippian earthworks found anywhere. The mound is complex and consists of two platforms: a "lower" (~75 m long by 4 m high) and an "upper" (~125 m long by 8 m high). Additionally, a small (~15 m diameter), conical offset rises about 6 m above the southeast corner of the upper platform (Fig. 4.6). Previously,

Figure 4.2 WPA crew sitting on the "primary mound surface" (Feature 2) after completion of Mound F excavation (November 1941)

the only excavation on Mound A was a shallow trench (3 x 9 m, 1.5 m deep) excavated in 1955 by Black (1967, p. 357–367), which literally only scratched the surface of Mound A. Additionally, beyond sheer size and expense to excavate, prehistoric earthworks are often unexplored, not only because of their linkage with burial and religious beliefs of modern Native Americans, but also because the archaeological community is reluctant to allow their alteration by even exploratory excavation. Clearly, its size and complexity provide some significant challenges for understanding when and how it was built, and even the most rudimentary questions regarding mound composition, stratigraphy, construction methods, and chronology are unanswered. How do we study such important archaeological landscape features given all of these constraints?

To address these questions, a long-term, multifaceted project was undertaken between 2007 and 2010. The project was designed to minimize damage to the mound (16-m-deep excavations were not possible), so several different, noninvasive or minimally invasive methods were used to investigate the subsurface configuration of Mound A. We focused on mapping the Mound's internal strata by combining fine-scale, point-source data collected through small-diameter solid-earth coring (Geoprobe) using geophysical methods (72-probe electrical resistivity [ER] profiler, Figs. 4.7 and 4.8). The cores provide ground truth information necessary to realistically interpret the resistivity profile data. The geophysical survey data provide the ability to link the cores and create a grounded and realistic reconstruction of the mound interior. Importantly, organic samples collected from the cores provide absolute chronology from well-understood contexts for episodes

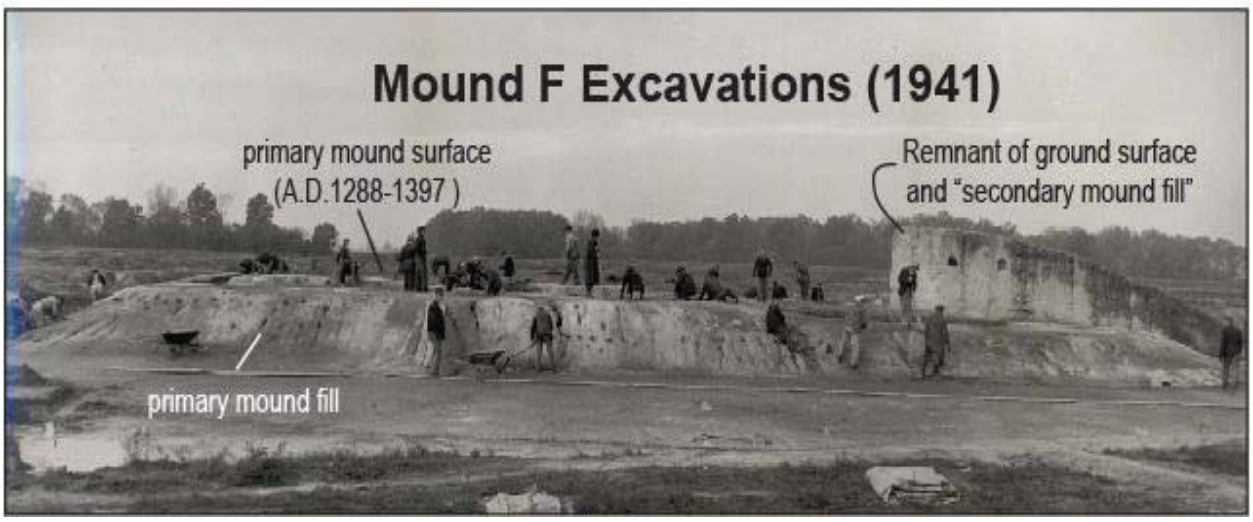

Figure 4.3 Photograph of WPA archaeological crew exposing the "primary mound surface" in 1941; remnant of "secondary mound fill" and original ground surface labeled. Age of primary mound surface based on calibrated pooled mean average of 14C ages (see Table 2 [Context "Mound F"]); ages shown are 2σ range of calendar years.

of mound building. Information from cores, including texture of the fills or pollen preserved within them, can also provide insights into the engineering knowledge and local environmental conditions at the site. The ability to "see" underground and create 3-D reconstructions of the subsurface is critical for developing more efficient and effective research plans and more targeted excavation strategies.

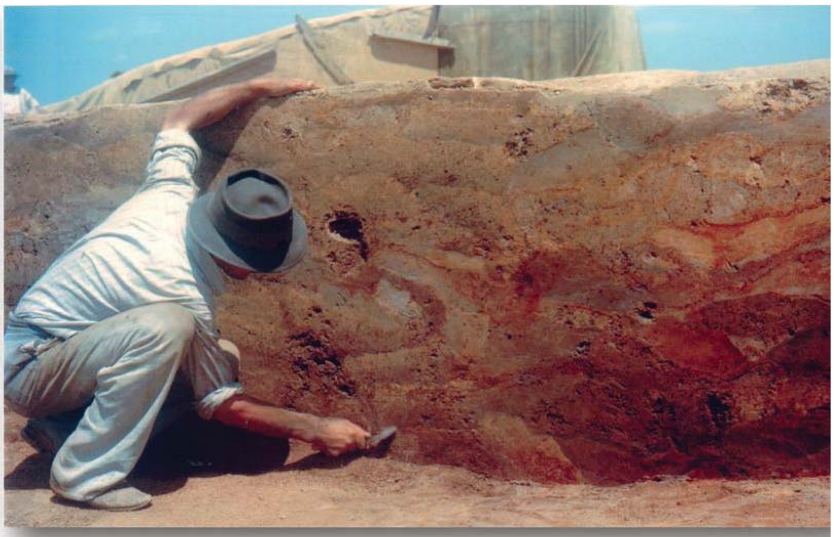

Figure 4.4 Complexity of fill underlying Secondary Mound fill, Mound F

4.2. The Mound A Project: using multiple methods to enhance our understanding of mound construction and chronology without significantly altering or disturbing the mound

Solid-earth cores were collected from the mound using a GeoProbe (model TR-54) and a Dual-tube (model DT21) sampling system (Fig. 4.7). The dual-tube sampler drives a core-casing along with the sampler to prevent the collapse of the borehole during sampling. A clear sample tube 122 cm (4 ft) long by 3 cm (1.125 in) diameter was placed within the core-casing and driven into the mound. The core sample tube was extracted, labeled, and saved. Another section of core-casing was attached to the top of the previous casing and a new sample tube with drive rod attached placed into the casing. This new segment was then driven 122 cm into the mound and the sample tube was extracted. In this manner, continuous cores (in sections) were collected until the mound base was penetrated. The core sample tubes were opened in the lab and described with regard to soil and sediment colors, textures, inclusions, and so on. Samples of any organic material that might provide an absolute chronology to construction horizons were also collected.

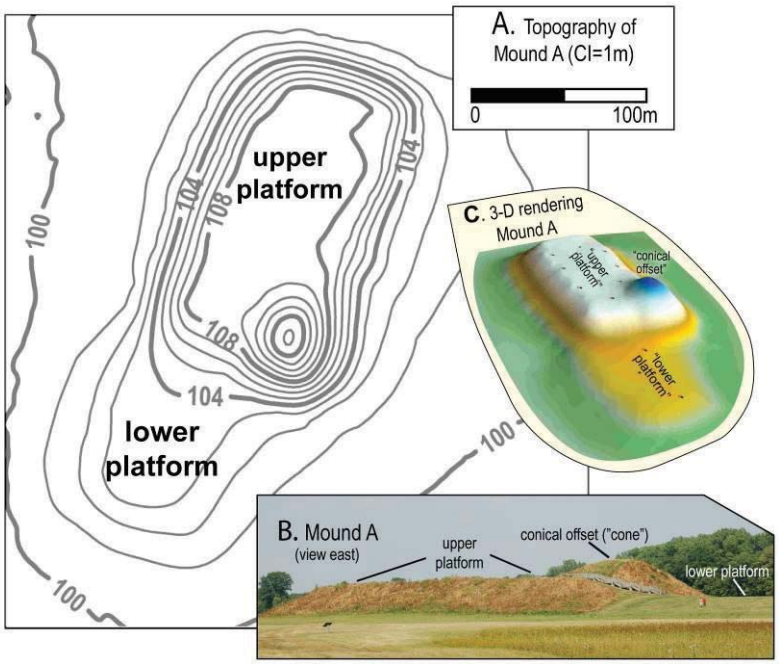

Figure 4.5. Maps of Mound A showing configuration of platforms. A) topographic map, B) 3-Dimensional rendering, C) photo of Mound A looking east.

ER multiprobe profile systems are most commonly used to define vertical sections of the subsurface and trace the stratigraphy of natural sediment and soil horizons, but they can also be used to map broad,

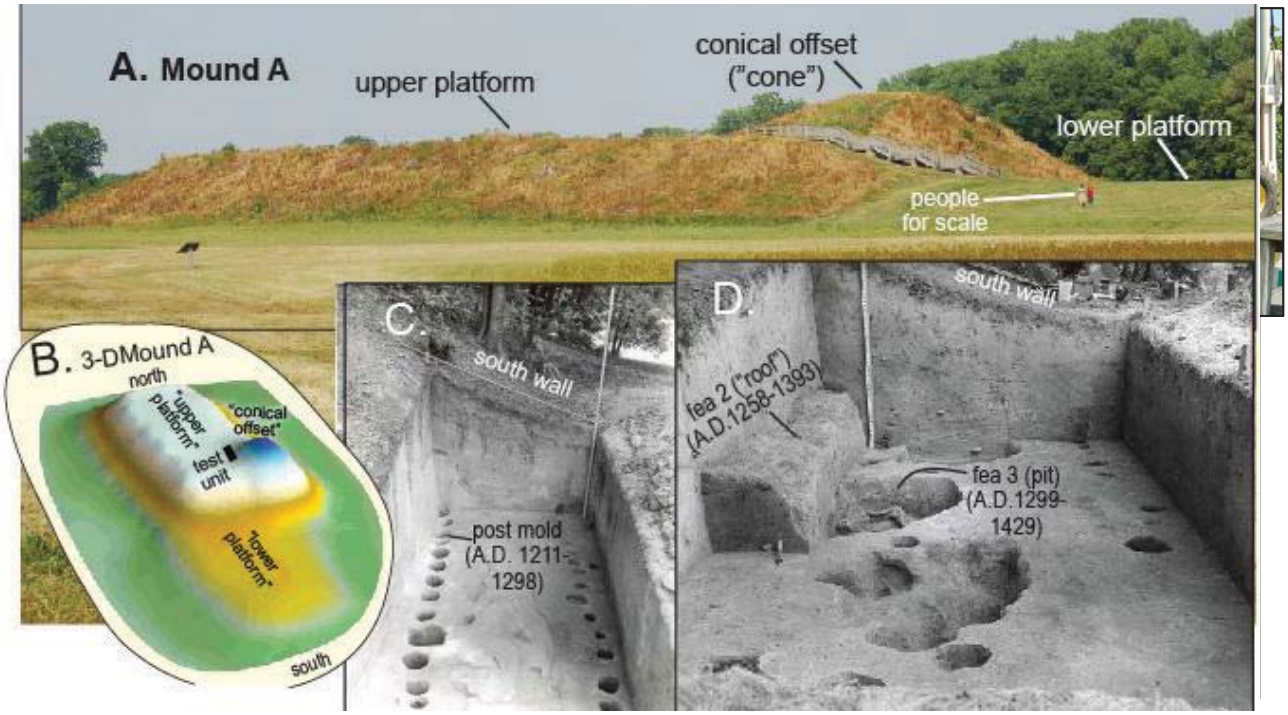

Figure 4.6 A) Photograph of long axis of Mound A (view east, north on right side of diagram). B) Three-dimensional rending of Mound A, locations or traces of cores and ER profiles shown and labeled. C) Photo of post molds at base of 1955 Mound A test excavation (view south); ^{14}C- dated post-mold labeled (see Table 1 [Group "B"]). D) Southern end of 1955 excavation block showing the locations and ^{14}C ages of Feature 2 ("roof") and Feature 3.

culturally derived mound fills. Implicit in this notion is that, similar to alluvial deposits, mound fill units are also structured, orderly, and composed of distinct and discrete layers selected by the builders based on their physical properties. How much of this selection reflects convenience or aesthetics and how much relates to their engineering properties is an open but important question. In general, the resistivity (i.e., a measure of the Earth's ability to inhibit electrical flow) of sediment and soil is controlled by three main properties: texture, moisture, and compaction. Fine-grained, moist, and compact materials conduct electricity more easily and, therefore, have low resistivity. Coarse-grained, dry, and loose materials are poor conductors and, therefore, have high resistivity. These factors are not independent. For example, fine-textured sediments also tend to hold moisture better than coarser-grained deposits for unsaturated profiles, accentuating the electrical differences between these layers. For most shallow profiles in unconsolidated materials, texture is the most important property and seems to broadly correspond to the observed ER profiles in Mound A.

A Syscal Pro multichannel ER profile system with an attached 72-probe linear array was employed in the Mound A project. The array was arranged with probes spaced 1 m apart and situated both parallel and perpendicular to the long axis of the mound. Both Wenner and Dipole-Dipole arrays were used to collect data. The depth and resolution of subsurface images is a function of probe spacing and the total length of the linear array: the longer the array, the greater the depth, and the closer the probe spacing, the greater the resolution. Consequently, a finite number of probes more closely spaced will yield more detailed resolution of the subsurface but will also produce shallower images. With the configuration employed in the Mound A study (i.e., 1-m probe spacing, Wenner and Dipole-Dipole array) maximum depths that equal about 15 to 20% of the total array length could be imaged (e.g., 10–14 m depths), and only layers that were >50 cm thick were resolved.

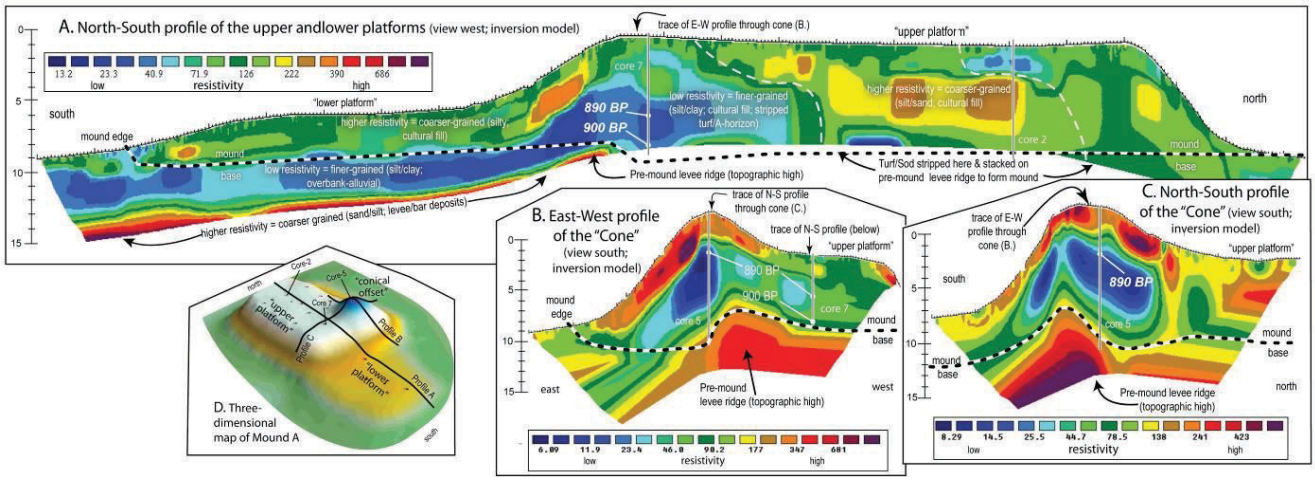

Figure 4.8 Electrical Resistivity Profiles collected from Mound A showing the subsurface configuration

Several resistivity profiles were taken from Mound A and three showing the general structure of the mound are displayed here (Fig. 4.8). Part A is a long north-south ER profile along the long axis of the mound showing the structure underlying the "upper" and "lower platforms." The approximate location of Core 7 and depths of associated radiocarbon ages (BP) is labeled. Part B shows an east-west ER profile through conical offset and upper platforms. Part C shows a north-south ER profile through the conical offset. This pair of relatively short E-W profiles shows the structure and general relationship between the "conical offset" and the platforms. The locations of Cores 5 and 7 and depths of associated radiocarbon ages are shown and labeled. Part D shows a three-dimensional rending of Mound A, locations or traces of cores, and ER profiles shown and labeled.

The profiles show differences in relative electrical resistance between various horizons, which is controlled by compaction, soil moisture, and texture. Of these, moisture and texture are dominate but not independent of each other. Thus, fine-grained and moist sediments have low resistivity while coarse-grained and dry soils are high. Moreover, finer-grained sediments (silt/clay) also retain moisture, which accentuates textural differences. In the Mound A profiles, the "darker" blue and green colors are the least resistant layers and probably mark finer-textured (silty to clayey) sediment and soil. The "brighter" yellow and red colors are the most resistant and mark coarser-grained (sandy) deposits.

For example, core data show that the basal, high-resistivity zone (Fig. 4.8) corresponds to bedded coarse-grained (sand) deposits, which likely represent bar or channel sediments. In cores, these sediments grade upwards into interbedded sand and silt and into more massive silt and clay alluvium near the mound base. This pattern matches the change from high- to low-resistivity sediments from well below the mound to near the base of the mound. Such near-surface low-resistivity horizons are particularly obvious underlying the lower platform (i.e., southern half of Mound A; Fig. 4.8). Such a fining-upwards sequence is typical of vertical accretion deposition and is often associated with levee construction processes; it probably relates to ridge and swale landform development prior to human occupation at the Angel site. In profile, the coarser-grained basal deposits appear to form a relative high palimpsest where the upper and lower platforms join with the conical offset (Fig. 4.8), suggesting that Mound A may have been placed on a topographic high associated with a preexisting levee ridge. While placement of the mounds or other earthworks on a preexisting prominent landform feature is not uncommon, the fact that the upper and lower platforms and conical offset join on top of this ridge may also have cultural or ceremonial significance. A "mound" of low-resistivity deposits also appears as palimpsest on this ridge. Although it may appear as a continuation of

the underlying fine-grained alluvial sequence, cores show that it actually is composed of layers of culturally derived fill related to Mound A construction. The similarities in ER and soil properties between these natural and cultural deposits indicate that cultural fills palimpsest on the levee ridge likely derived from areas that included sediments and soils having similar physical properties. By comparing the sedimentological and pedological characteristics observed in cores with the resistivity profiles, the origin, construction methods, and developmental sequence of the mound are evident. These relationships and details of the physical properties of mound fill are particularly clear where the underlying levee, upper and lower platform, and conical offset join.

By considering all of these various data, a general construction plan can be outlined (Fig. 4.9). We suggest that Mound A construction began on a preexisting levee ridge where the cone and platforms join. Beginning ~900 BP (2-sigma Cal AD 1030–1230), "turf" blocks were cut from elsewhere (possibly under the upper platform) and stacked ~2 m high on the ridge. Initially, Mound A was small, possibly a cone surrounded by a small platform, and may have been oriented E-W rather than N-S as today. More profiles, cores, and dates may clarify the chronology, stratigraphy, and engineering of Mound A .

4.3. Construction chronology of Mound A

The chronology of Mound A construction is based on Accelerator Mass Spectrometry ages of organic matter found within the cores (Fig. 4.10). Only annual plant samples associated with well-understood constructional or cultural contexts were selected to determine when the mound was built (Table 3). In contrast, many radiocarbon ages from the site have been reported as unacceptable dates by Black (1967) and Hilgeman (2000) and generally reflect either poor sample contexts or selection of inappropriate samples from the contexts. For example, charcoal from the Secondary Mound F (i.e., final fill/capping layer of Mound F) provided an age that was 300 to 500 years too old (e.g., M2, 1340 ± 120 BP; Table 4), given the ages from surfaces found below the Secondary Mound F. This sample was probably originally detrital charcoal within the alluvial sequence from which the fill derived and may accurately reflect the age of alluvial deposition rather than an episode of mound construction during the Mississippian occupation (Black, 1967). Two other bad dates from Mound F were obtained on shell from good Mississippian contexts within Feature 12 (primary mound surface; Black, 1967). These are 800 to 1000 years too old (M9 and M10; Table

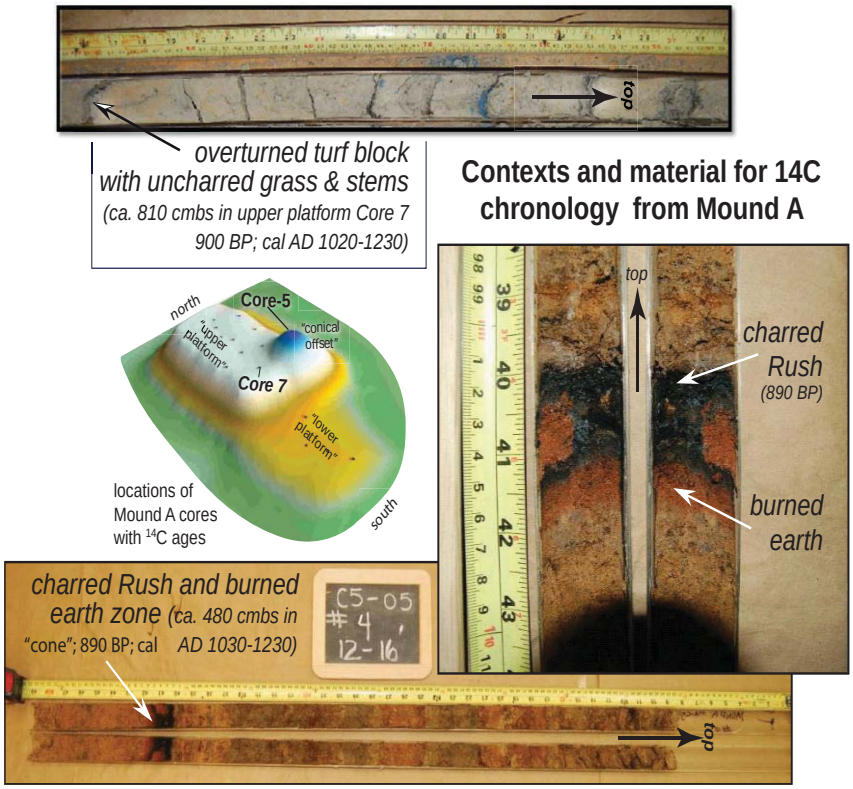

Figure 4.9. Pictures and locations of cores that have provided ^{14}C chronology for Mound A.

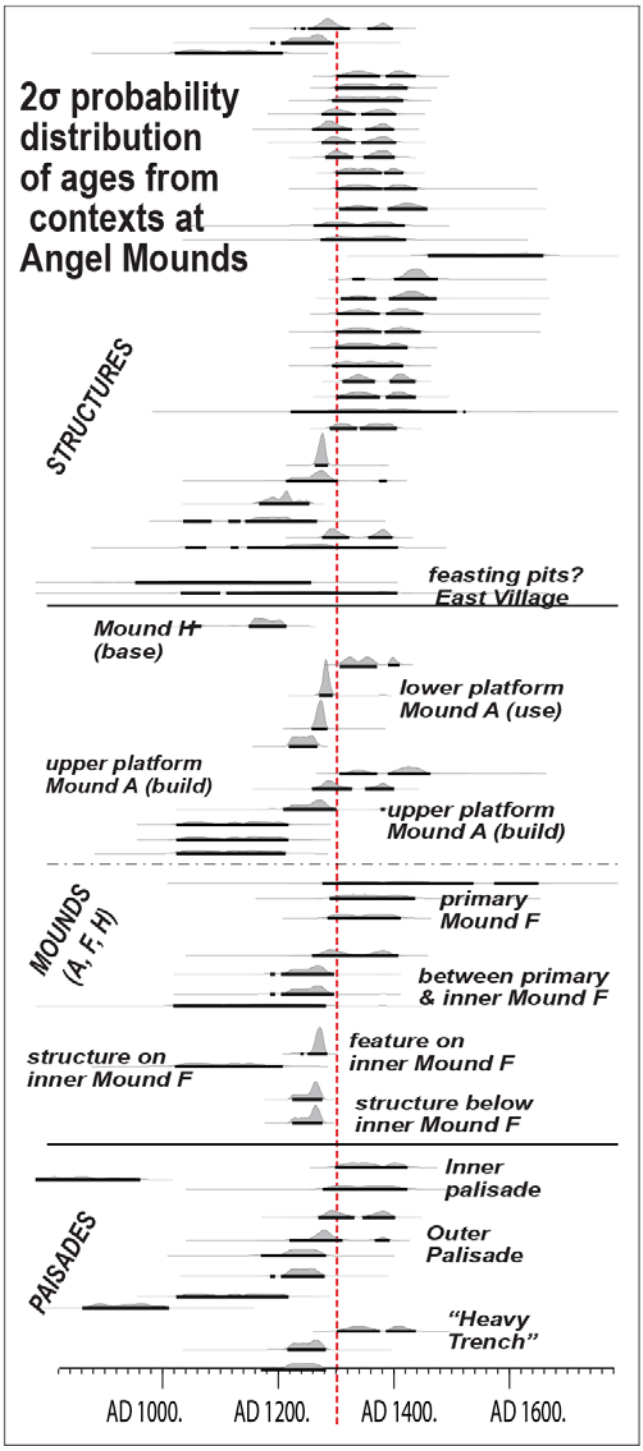

Figure 4.10. Chronology of Angel Mounds based on probability distribution of calibrated ages from specific archaeological contexts. Note that structures and palisades are concentrated after AD 1300 and mound construction before AD 1300.

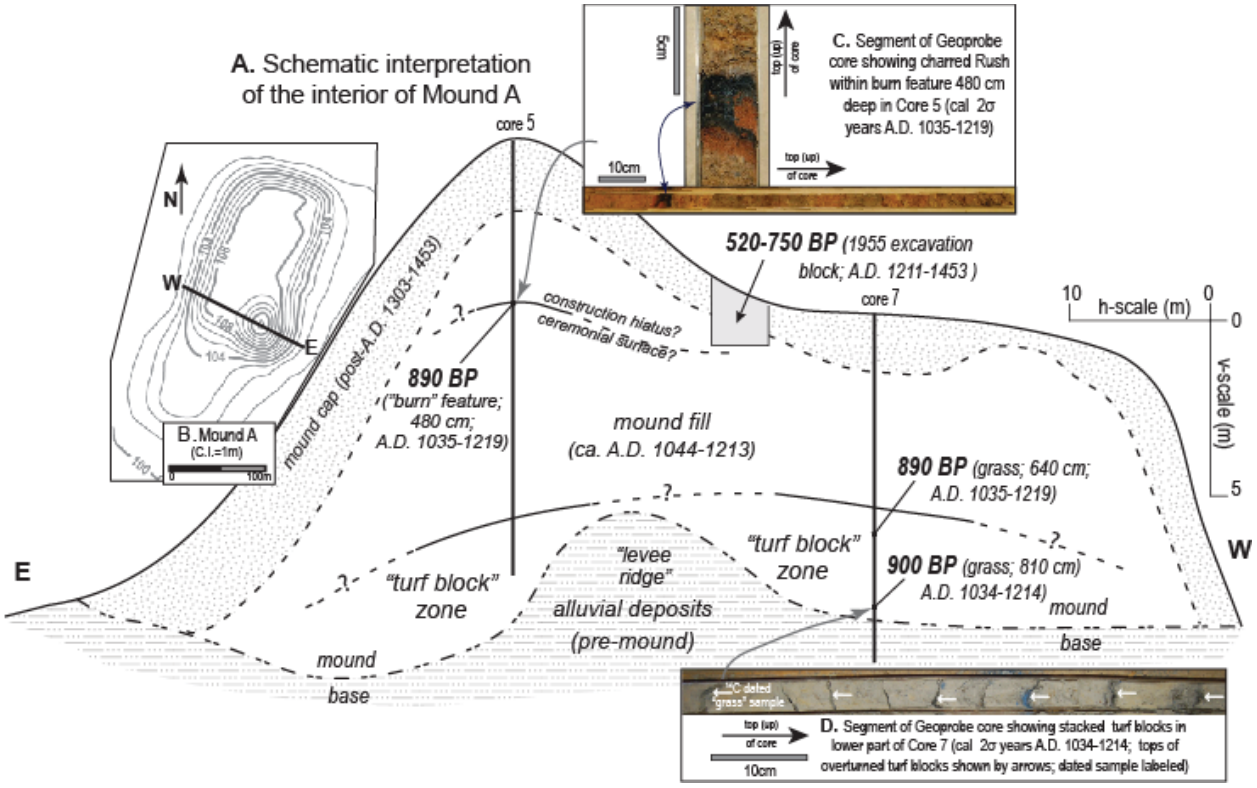

Figure 4.11 Interpretive diagrams summarizing the Mound A interior. A) East-West (east and west [E and W, respectively] labeled, view south) profile showing generalized fill sequences that comprised Mound A. Fill distribution and contacts based on cores and resistivity profiles (see previous figure). Chronological controls based on ^{14}C ages of organic materials in Cores 5 and 7 (labeled on diagram); position of organic samples shown on core; material dated and ages shown as ^{14}C years BP; calibrated 2σ range in calendar years shown in parenthesis; calibration after Stuiver and Reimer (1993), Hughen et. al. (2004) and Talma and Vogel (1993). B) Topographic map of Mound A showing location of profile shown in A. C) Photograph of Rush sample (Beta-237767, Table 1) related to burn feature in Core 5. Note redden earth under charred Rush in close-up of core (left side of C) showing intensive burning. D) Photograph of dated grass sample from near base of Core 7 (Beta-232870, Table 1). Contacts between overturned turf blocks, which is where preserved grass occurs, are indicated by arrows on core (lower part of 4D). Up-directions of cores in C and D labeled and indicated by an arrow adjacent to cores.

2) and may either reflect problems with the use of shell during the early years of radiocarbon dating or might also accurately indicate the age of shell but not the time that it was used.

Our research provides several new, important observations about the construction methods, material, engineering, and chronology of Mound A (Figs. 4.10 and 4.11). The ER profiles reveal several broad resistivity zones that can be traced across Mound A. These generally include a basal zone that has very high resistivity overlain by a low-resistivity zone that is, in turn, overlain by various zones of moderate and low resistivity. This layering roughly reflects the natural configuration and stratigraphy of pre-mound deposits, as well as the cultural stratigraphy of mound-fill units. Even though a variety of different earth models might explain this pattern of resistivity layering, the natural and cultural contexts and origins of these layers are constrained by the detailed stratigraphy, pedology, and sedimentology derived from solid-earth cores. These data can be used to deduce the history of Mound A construction, as well as the geomorphological configuration, pedological alterations, and sedimentological origin of the pre-mound landform that underlies the mound with minimal impact to the deposits.

5. Paleoliquefaction and earthquakes in the midcontinental USA

Evidence for late Holocene seismicity in southwestern Indiana and Angel Mounds

Multiple seismic sources having the potential to generate liquefaction-inducing earthquakes occur throughout lower Ohio valley, particularly near the mouth of the Wabash River. The most active area is referred to as Wabash Valley Seismic Zone (WVSZ) (Figure 5.1), an informally defined region of diffuse seismic activity that is centered on the lower Wabash River in southwestern Indiana, southeastern Illinois, and western Kentucky (Nuttli et al., 1974; Nuttli, 1979). The WVSZ has produced eight earthquakes of M5.0 to 5.5 and dozens larger than M4.0 within the past 175 years (Dart and Volpi, 2010) (Figure 5.2). Most of these earthquakes were deep and originated in the Precambrian basement; only one of the instru-

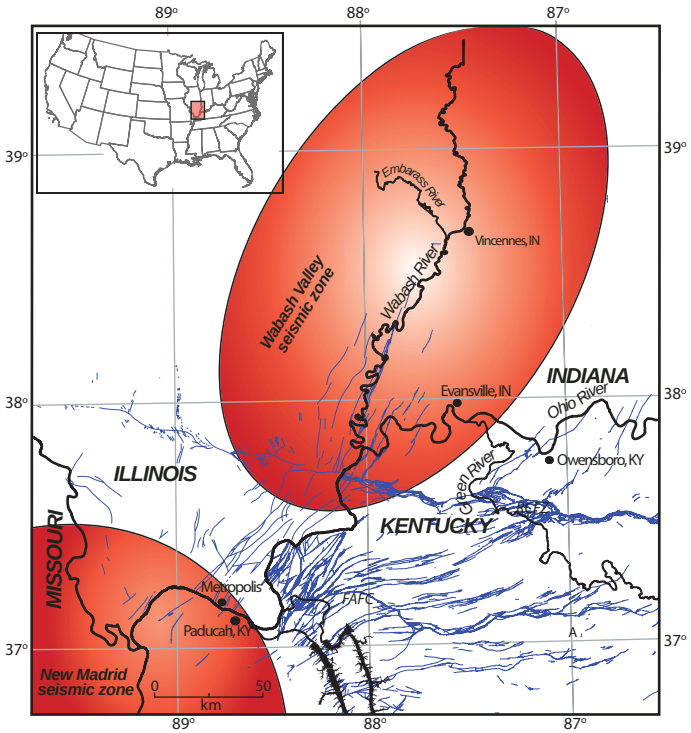

Figure 5.1 The Wabash Valley Seismic Zone and surrounding features. The blue lines are mapped bedrock faults. RCFZ and FAFC are the Rough Creek fault zone and the Fluorspar Area fault complex, respectively.

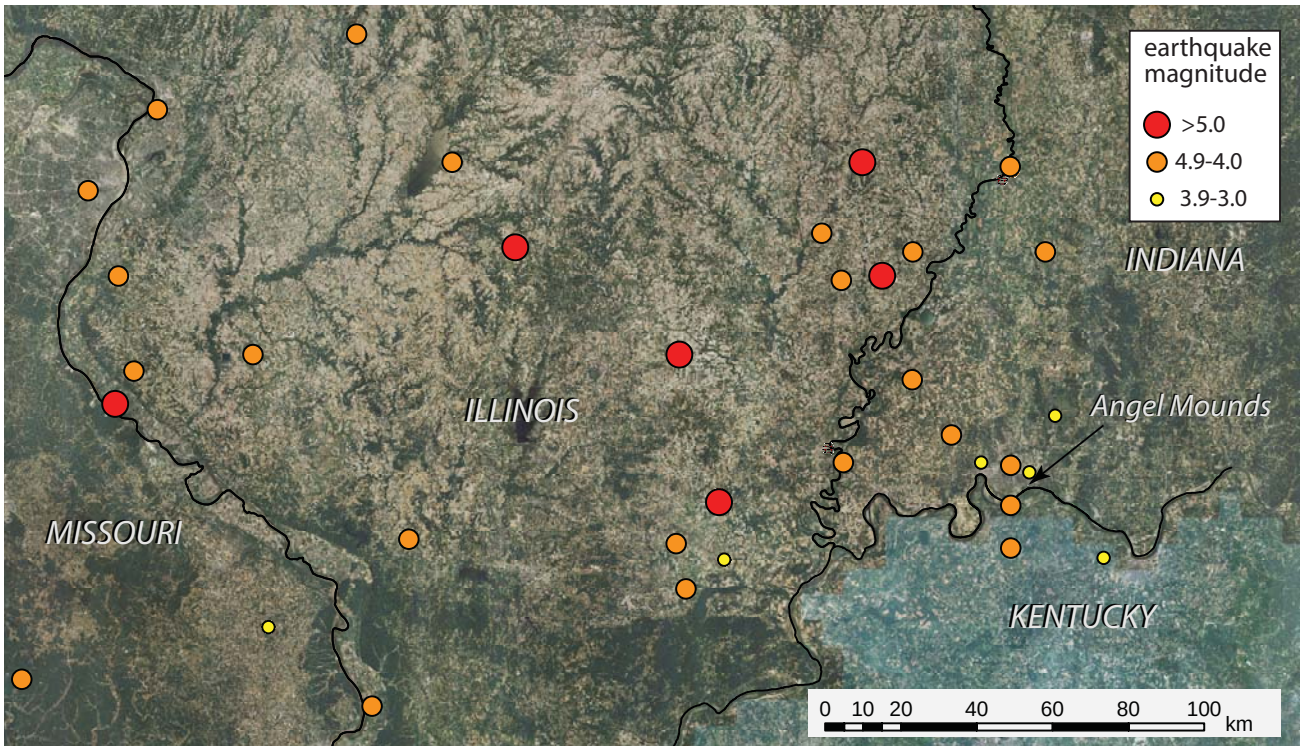

Figure 5.2. Distribution of moderate (M 3.0-5.5) historic and instrumentally recorded earthquakes in the lower Wabash Valley seismic zone.

mentally recorded earthquakes occurred on a mapped fault (Taylor et al., 1989; Mitchell et al., 1991; Bear et al., 1997; Kim, 2003), indicating there are many unknown seismogenic faults in the WVSZ. Fault-plane solutions indicate that offset on the faults are both strike-slip and reverse motion (Taylor, 1989; Mitchell et al., 1991; Kim, 2003). Some researchers believe that strain from the New Madrid Seismic Zone has been transferred to the WVSZ, which explains the apparent increase in frequency of M4.0–5.0 earthquakes, and they speculate that the next large earthquake in the central U.S. will be from the WVSZ (Li et al., 2005, 2007).

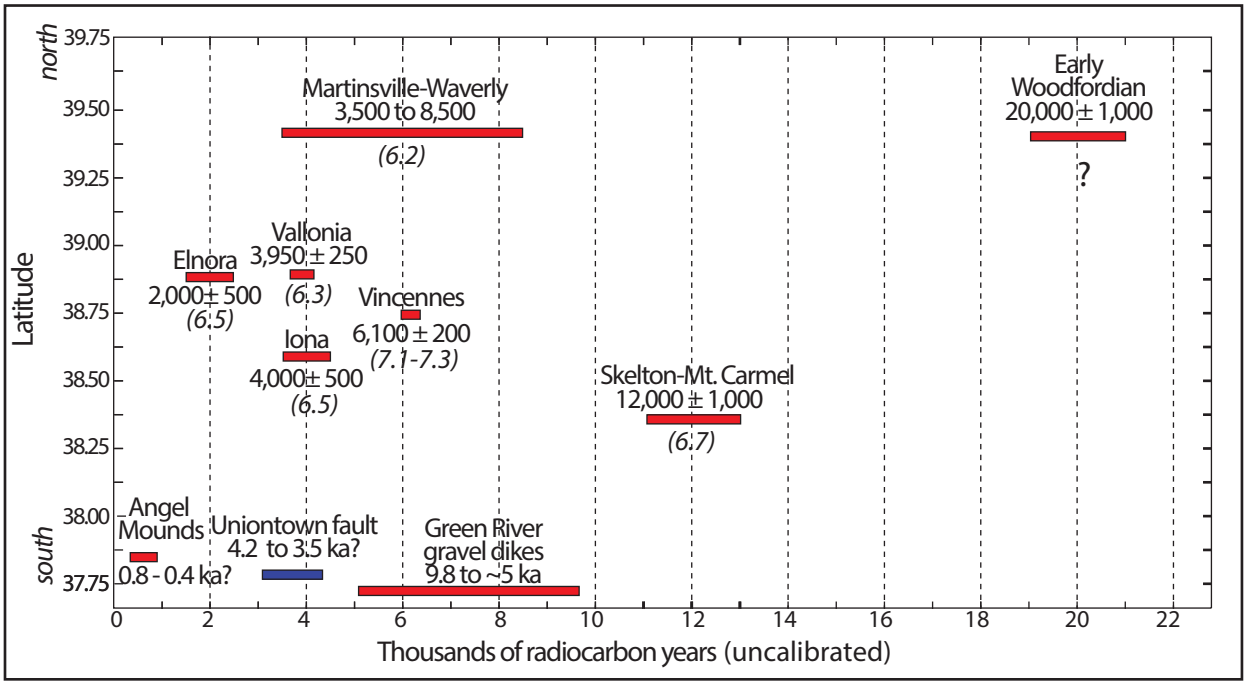

Figure 5.3. The paleoseismic record of the Wabash Valley seismic zone, based primarily on meisoseismal areas defined by paleoliquefaction (red) and one fault study. Recent research in the lower WVSZ has identified multiple sites with offset unconsolidated Quaternary reflectors above bedrock, but these features have no geochronology associated with them and are not included in this figure.

Paleoseismic studies indicate that the WVSZ experienced at least eight earthquakes with magnitudes >M6.0 within the past 20,000 years (Fig. 5.3), with the majority of them occurring during the Holocene (Obermeier et al., 1991, 1993; Munson and Munson, 1996; Munson et al., 1997; Obermeier, 1998; Olson et al., 2005; Counts et al., 2008). All but one of these studies were based on the size and distribution of paleoliquefaction features, which are indicators of very strong shaking (Obermeier, 1996, 2009), but paleoliquefaction features reveal only the meisoseismal area of an earthquake and not its source (Obermeier, 2009). Stop 5 on Saturday will discuss the Holocene history of the Uniontown fault, a part of the Hovey Lake fault system that appears to have diverted the course of the Ohio River within the past ~4 ka.

Angel Mounds, which was occupied between ca. AD 1100 and 1450 occurs within the southern region of the WVSZ, and archaeological excavations have uncovered evidence that the site has experienced intense seismic shaking in the past. Moreover, several clastic gravel dikes, large sand dikes, and

many small liquefaction features are less than 20 km away on the Green River (Fig. 5.4); also, Angel Mounds is less than 40 km from the Uniontown fault, which we will discuss at Stop 5 on Saturday.

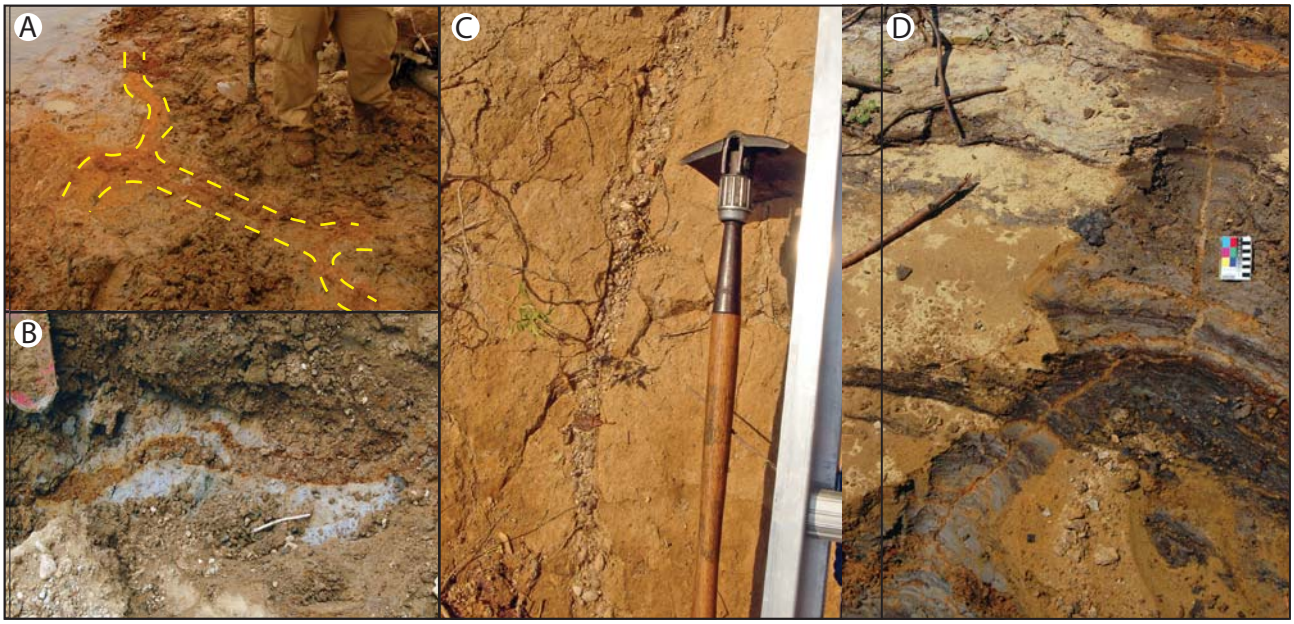

Figure 5.4. Paleoliquefaction features found within 20 km of Angel Mounds, exposed in the banks of the Green River to the south, include (A) large-scale clastic sand dikes (plan view), (B) and (C) large-scale gravel dikes, and (D) numerous smaller sand dikes.

6. Saturday Field Stops

6.1 Angel Mounds (37.944682°, -87.452052°)

The Angel Site Landform: Mound G, Angel Mounds, and Ohio River terraces

Mound G, although administered as part of the Angel Mounds State Historic Site, is actually not part of the occupation of the Middle Mississippian (ca. AD 1000–1400) Mississippian town that comprises Angel Mounds. It is likely considerably older and has long been believed to have been built during either the Middle Woodland (Hopewell/Havana, ca. 200 BC–AD 400) or Early Woodland (Adena, ca. 500–200 BC) periods. Artifacts of both these periods (as well as Archaic, Late Woodland, and Mississippian) have been recovered from near the mound, but few formal excavations have been undertaken. Several years ago the Indiana State Museum excavated into the west side of Mound G, but it proved inconclusive, and no diagnostic artifacts or organic material were found in contexts useful for settling the age of this mound. More recently we began a program to understand the age and structural configuration of Mound G; we will be discussing this project to introduce geoarchaeology topics (Day 2 in the field guide).

In addition to Mound G, we will also discuss the Ohio River terrace system near Angel Mounds, what is known about its age, and how the site (as well as Mound G site) area fits into the overall landform configuration.

Description:

Mound G is a conical mound, sometimes referred to as a “beehive” mound, that rests on an earthen

platform (Fig. 6.1.1). This mound shape is common throughout the Midwest and is also typical of the Hopewell and Adena mounds in Indiana and Ohio. In fact, its shape, more than anything else, is the reason Mound G is usually associated with these cultural periods. Moreover, the shape of Mound G is very different from the platform style of mounds that are common and more characteristic of the Mississippian Period. These occur on the Angel Mounds site proper. For example, Mound A (Day Two) is a large platform and we will discuss similar issues about construction and how to characterize mound interiors without destroying them.

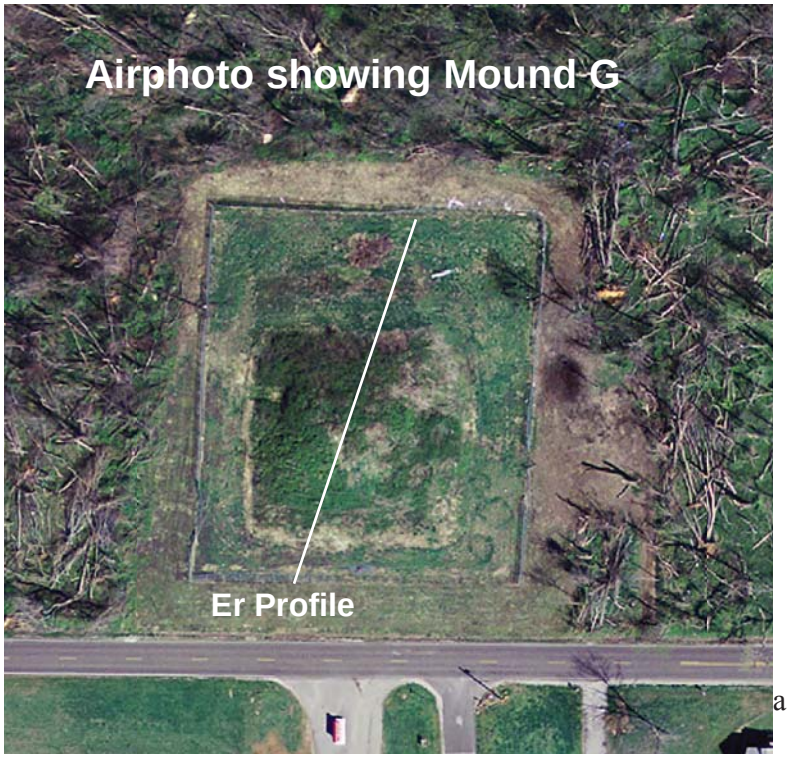

Figure 6.1.1 Air photo from 2006 showing Mound G and location of an Electrical Resistivity profile shown below.

From a geomorphological standpoint, Mound G actually occurs on well-defined ridge, the origin of which is probably partly as braded stream deposits and partly as an eolian ridge, probably a combination of loess and eolian fine sand (Figs. 6.1.1 and 6.1.2). The Mound G construction on this ridge is not coincidental and allows the mound to become "bigger" by using landscape prominent landscape features. The same is apparent for Mound A (Day Two), which was built on a levee ridge related to younger (early Holocene) terrace of the Ohio River.

Discussion topics:

We will discuss several issues while at Mound G. These relate to our study of the age and internal structure of the mound and the age and development of the floodplain, and how the Angel site fits into the scheme (Figs. 6.1.2 and 6.1.3). Our research plans for Mound G include placing a series of ER profile lines rotating around the center of the mound and developing a 3-D reconstruction of the interior of the Mound. From these data, we will develop a coring program to sample the mound, aiming, in particular, to penetrate the base of the mound and collect radiocarbon samples from contexts that provided chronology for mound construction episodes. Continuous, solid-earth cores have also been collected using a Geoprobe; these cores revealed no organic or other datable material but provided OSL samples to determine the age of construction. However, it is critical to select the correct context of such samples to reliably determine OSL ages, and determining such context is a very complex decision (see Day Two at Angel Mounds).

The terrace (T4) upon which Mound G was constructed is late Wisconsinan, based on an OSL age of sediment collected adjacent to the mound (Fig. 6.1.4). The OSL sample (and others noted below) was collected using a shielded GeoProbe core and its age, 21.8 ± 4.0 ka, suggests that the terrace probably formed in relation to the retreat from the late Wisconsinan terminal moraine. The age of the next lower terrace, 17.8 ± 0.9 ka, however, suggests that the glacial Ohio River underwent a readjustment during the retreat of the Laurentide Ice sheet from Ohio and Indiana.

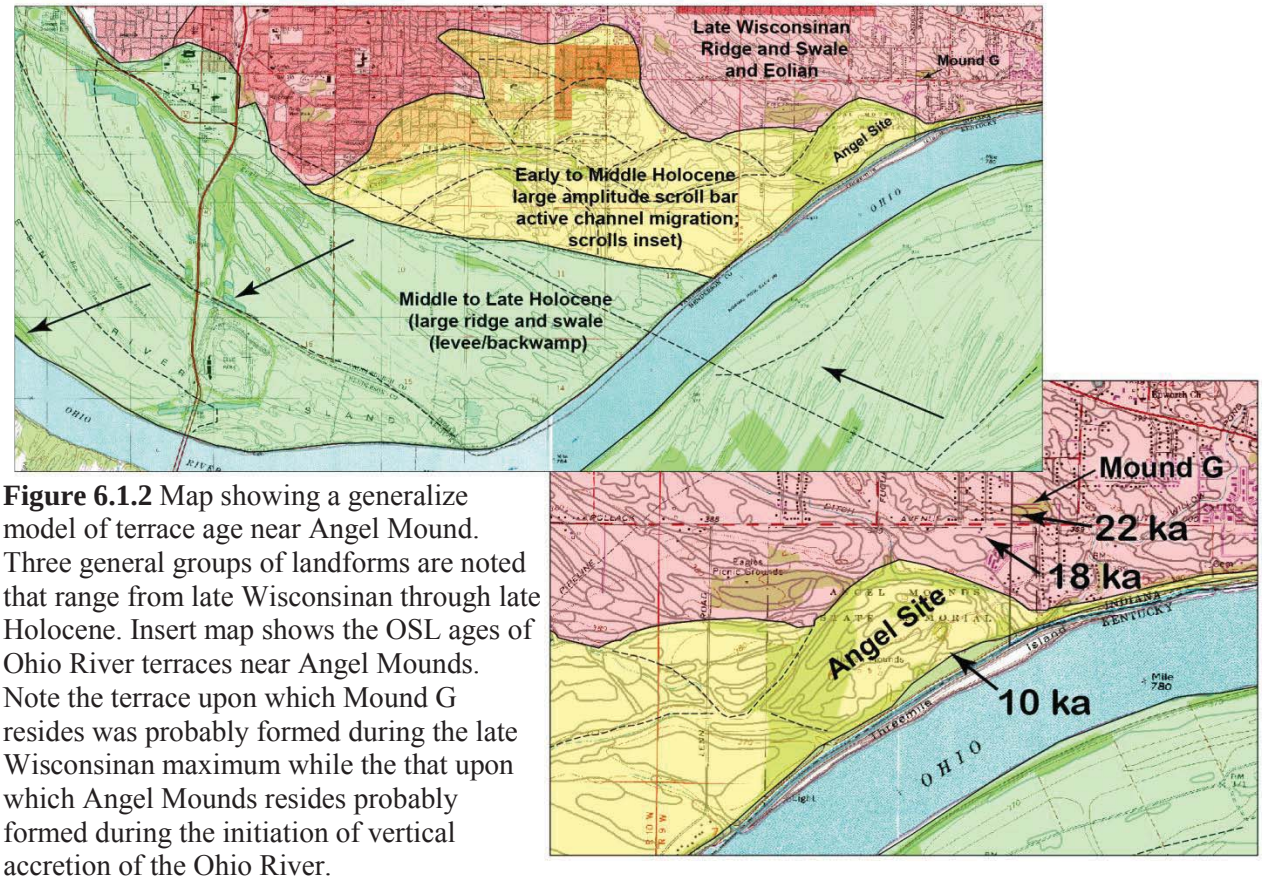

Figure 6.1.2 Map showing a generalize model of terrace age near Angel Mound. Three general groups of landforms are noted that range from late Wisconsinan through late Holocene. Insert map shows the OSL ages of Ohio River terraces near Angel Mounds. Note the terrace upon which Mound G resides was probably formed during the late Wisconsinan maximum while the that upon which Angel Mounds resides probably formed during the initiation of vertical accretion of the Ohio River.

The view south from Mound G shows the next lowest terraces (lower T4 and T3) and landform morphology near the Angel Mounds(Fig. 6.1.4). The terrace adjacent to Mound G is marked by a series of generally NW-SE trending ridges that are of MIS 2 age. OSL dating indicates that the terrace formed 17.8 ± 0.9 ka, which suggests a (probable) post-Erie Interstade Ohio River channel readjustment (Fig. 6.1.5). This morphological configuration continues south to the current location of the Angel Mounds Museum where a significant crescent-shaped slough marks another change in the terrace landform morphology (Fig. 6.1.3). The lower terrace (T2) is marked by sets of relatively tight meander scrolls that were eroded in the older Mound G landform. It is apparently part of a younger alluvial sequence upon which Angel Mounds was constructed.

The terrace (T2) landform configuration is characteristic for several miles east and at Angel Mounds, marked by basal sand and gravel that grade upwards in bedded fine sand and silt/clay alluvium. As such, these deposits represent vertical accretion rather than lateral accretion deposits, which characterize the other older terraces (T3 and T4) noted earlier. An OSL age, 10.0 ± 1.5 ka, collected from sandy deposits that mark change from lateral to vertical accretion of the Angel Mounds terrace suggests that it was formed during the early Holocene, which may also approximate the initiation of lateral accretion sedimentation along the lower Ohio River. What sedimentation or terraces may also exist between the Angel Mounds landform or terrace and those late Wisconsinan terraces between Angel Mounds site proper and Mound G will be the topic of the remainder of the field trip. The ages of these landform components and how such changes in the character of the Ohio floodplain morphology reflect the evolution of the Ohio valley is an interesting and important question and worthy of our discussion.

Paleoearthquakes and paleoseismicity, particularly related to the Holocene terraces and archaeological

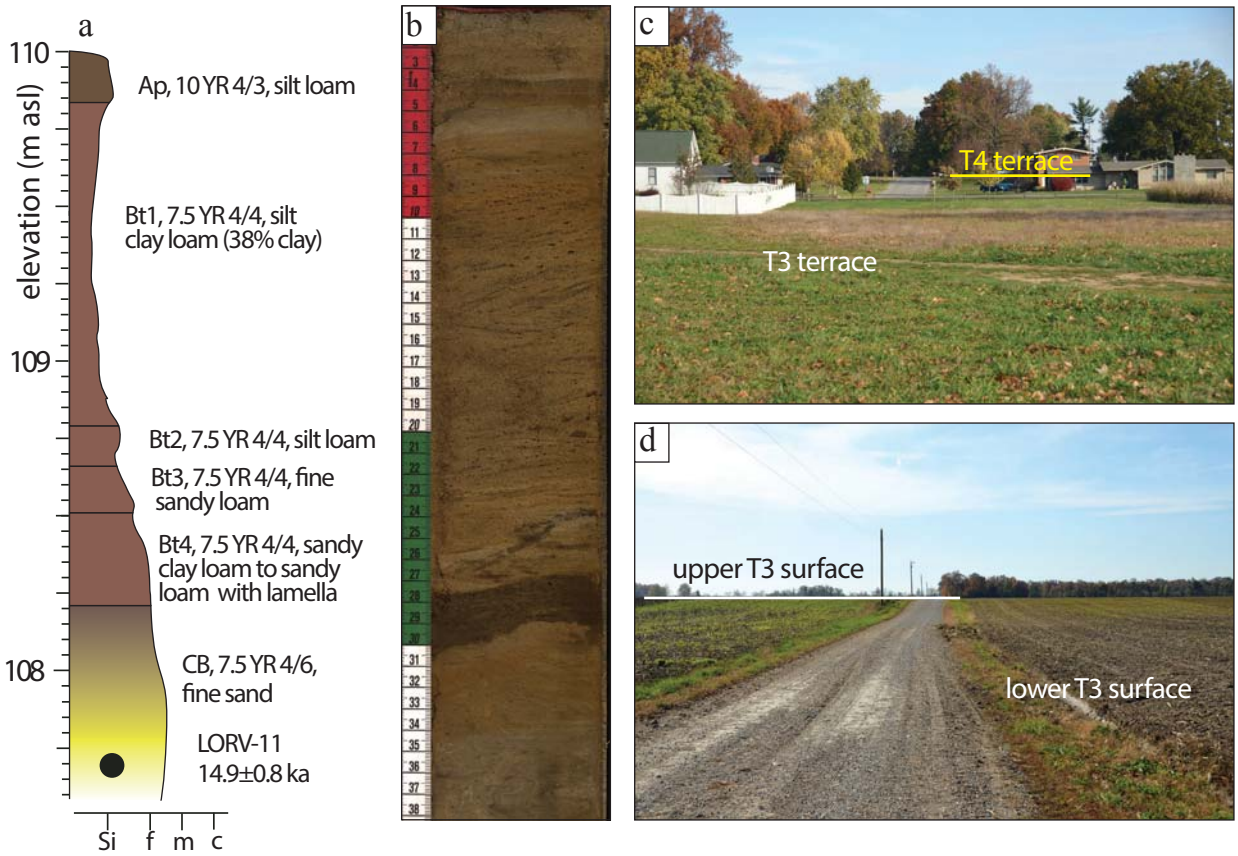

Figure 6.1.3. (a) Graphic sediment log of a core shallow core drilled on a T3 terrace and OSL age (LORV-05). (b) Digital linescan image of a T3 core; interval is 3.6 - 4.0 m below the land surface (color alternates every 10 cm in scale to the left). (c) Photo of a T3 terrace inset in a T4 terrace. The road in the distance shows the scarp, which is almost as tall as a 1 story house in this example. OSL samples LORV-26 and LORV-27 were taken from the T3 and T4 terraces shown in this photo. (d) Photograph of the eroded, low-angle scarp separating the upper and lower T3 terraces.

features, is an underlying theme of the trip. Seismic shaking can, in some cases, leave signatures in the sediments that can be detected using geophysical tools such as electrical resistivity. A resistivity profile through Mound G reveals some anomalies that are not easily explained (Fig. 6.1.6). These anomalies could be liquefaction that occurred sometime after the mound was built. This is suggested based on the "vertical" high-resistivity zone on the north side of the profile, which is the type of signature a sand injection from the underlying terrace sediments would have. Alternatively, the high resistivity may actually be related to cultural processes, such as alternating sandy and clayey materials in the mound-building sequence, or it could represent tombs within the mound. These questions can be addressed only through excavation. On Sunday we will discuss better evidence of an earthquake(s) at the Angel Mounds, including electrical resistivity profiles and other physical evidence of sand injections and faults beneath the Potters house, a physical profile under Mound F that includes sand injections, and a GPR profile over the lower platform of Mound A that includes features that might be sand dikes.

6.2 Epworth Road loess section and overview of tributary valleys (37.978065°, -87.436025°)

6.2.1. Loess

This stop is a borrow pit where loess and underlying weathered bedrock are actively being mined for fill material. The Peoria, Roxana, and Loveland loess units are present here, but they are all much

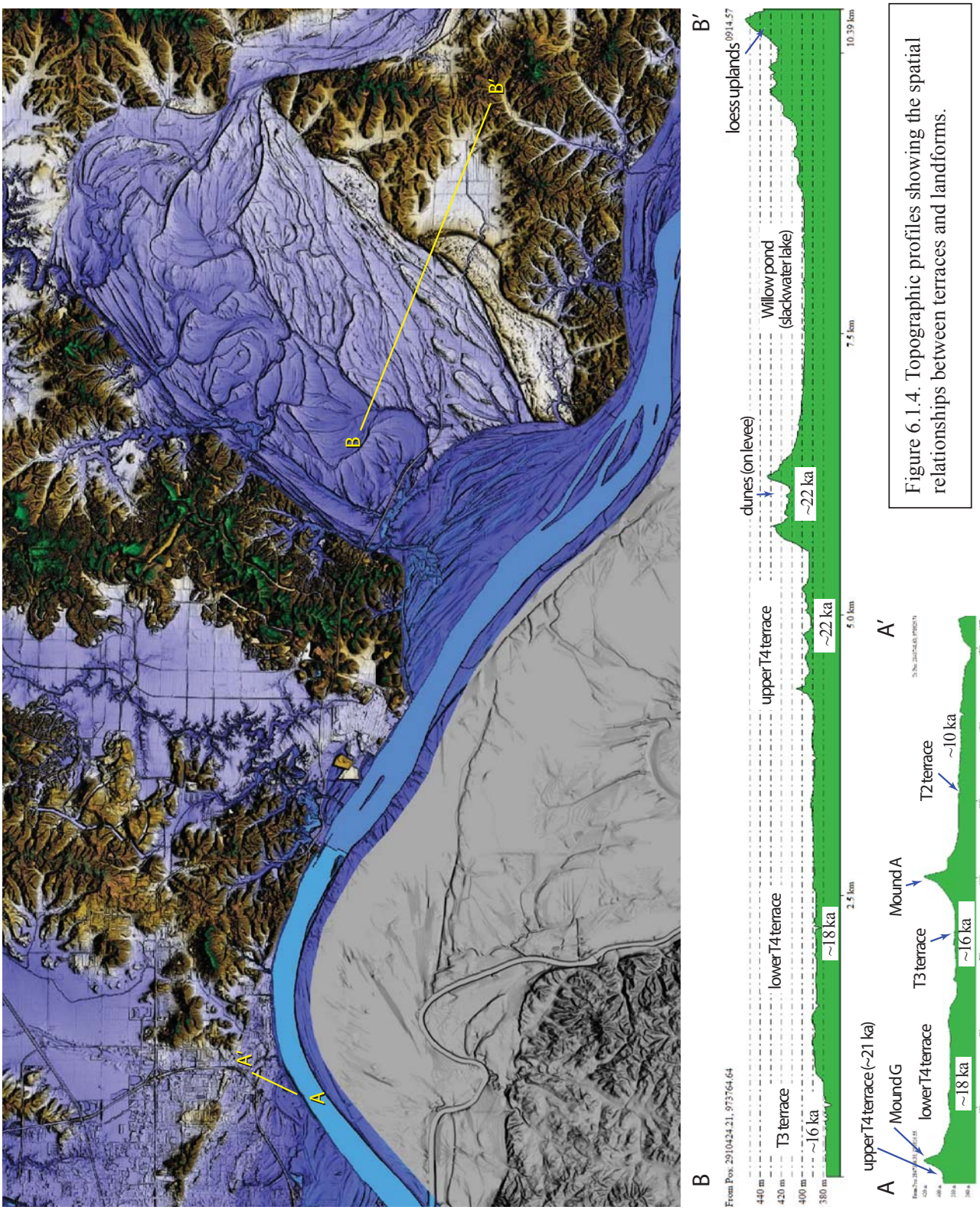

Figure 6.1.4. Topographic profiles showing the spatial relationships between terraces and landforms.

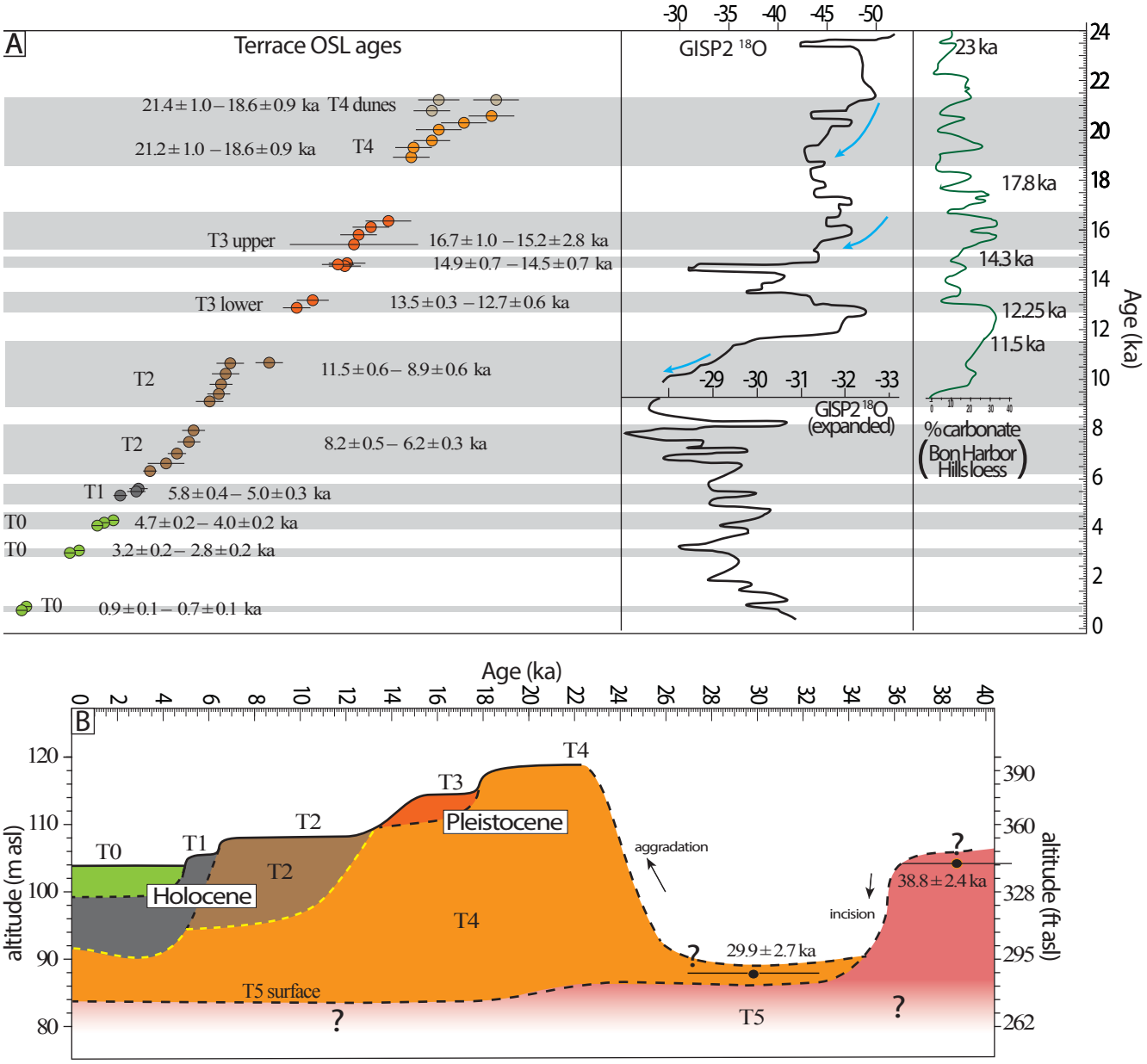

Figure 6.1.5. (A) Distribution of terrace OSL ages compared to the GISP2 ^{18}O ice core record and the carbonate content of Bon Harbor Hills loess (a proxy for weathering), tuned to the ice core record using the OSL and ^{14}C paleosol ages . Fill-cut terraces formed in the T4 outwash during transitions from cool to warm intervals. (B) chematic diagram showing the aggradation and incision history of the lower Ohio River for the past 40 ka, based upon the landscape position and OSL ages of deposits and terraces.

thinner here on the northern side of the valley compared to the loess section at the Bon Harbor Hills. The Loveland loess overlies bedrock and has a minimum age of >100 ± 15 ka (signal was at saturation limit). The Loveland is thin here (~2 m) and was pedogenically altered like the ~116 ka Loveland at the Bon Harbor Hills, so the age likely represents the development of the Sangamon paleosol on the Loveland loess. The thin silt overlying the Sangamon is the Roxana, but the transition from the Roxana to Peoria is difficult to identify in the field. A charcoal-rich horizon 1.7 m below the surface at the time of sampling (Fig. 6.2.1) was believed to be from the Farmdale paleosol, but it had an age of 20560 ± 440 yrs BP. This is younger than published ages of the Farmdale paleosol and likely represents organic material buried during the LGM. The OSL age of a sample of unaltered Peoria from a different part of the site was 18.3 ± 0.4 ka.

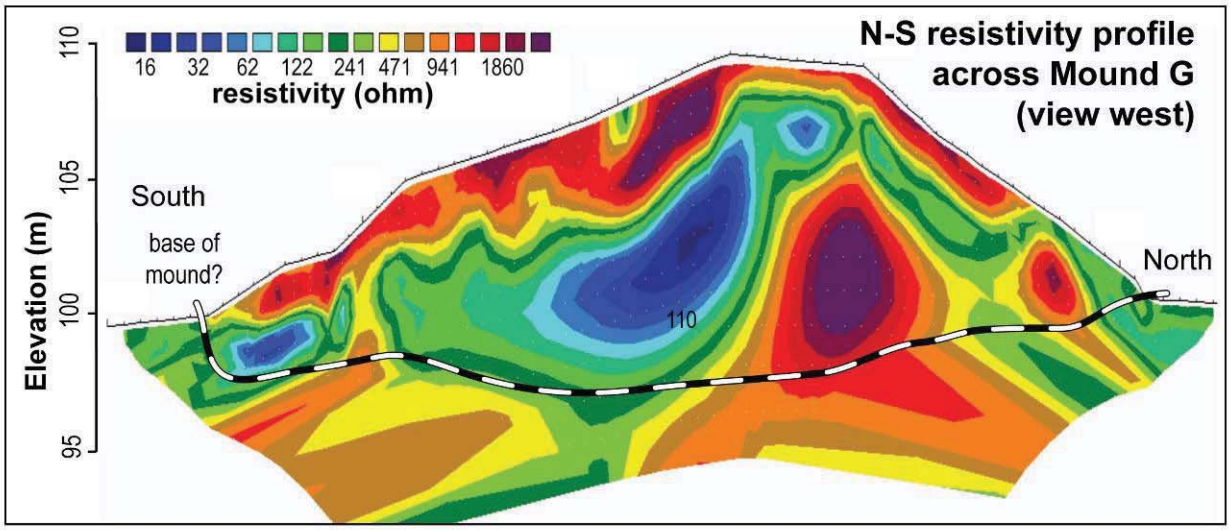

Figure 6.1.6 Electrical Resistivity profile collected across Mound G showing the subsurface properties of the mound fill. Probe spacing is typical (1m). These data were collected using a Syscal Pro Resistivity Profiler with 72 probes set at 1m spacing and "fired" using Wenner and/or Dipole-Dipole arrays. With such probe-spacing and array types, 10-14m of the mound subsurface was revealed. The location of the profile through Mound G is shown on the on the previous airphoto of the mound.

This sample was ~1 m below the land surface at the time of sampling, but some of the overlying material had been removed, and the original depth is not known.

6.2.2. Tributary Valley Fill

Stop 6.2 provides an overview of the Pigeon Creek watershed, one of the larger Ohio River tributaries. As the Ohio River aggraded, sediment blocked the tributaries and created an extensive network of lakes. The dominant landform in the tributary valleys appears to be that of an extensive lake plain or a backwater floodplain. However, the surfaces slope away from the river for several km and have the morphology of a large-scale natural levee (Fig. 6.2.2).

Many of the tributaries in the region are underfit streams that occupy extremely broad valleys filled with as much as 30 m of sediment. It is unclear whether the valleys were once meltwater outlets for pre-MIS 6 ice or were occupied by ice, but there is little doubt that major components of their current morphologies were inherited from older glacial landscapes. The tributaries do not have sufficient stream power to erode the sediments that fill their valleys, so older sedimentary records that are typically scoured from the main valley are often preserved in the tributary valleys (Fig. 6.2.3).

One study (Woodfield, 1998) proposed that some of the fill in the Pigeon Creek valley were flood "megasequences" from the Wabash River. A divide of the valley is adjacent to the Wabash River valley, but floodwater would have to overcome a 20-m-high divide, so this interpretation seems improbable for the MIS 2 glaciation. Although the MIS 6 glacial limit extends into the basin and it is tempting to identify the megasequences as MIS 6 meltwater pulses, the sediments associated with MIS 6 are lake deposits (Fig. 6.2.3). The OSL ages of the flood sequences near the base of the core indicate that aggradation occurred in the basin during MIS 3. Evidence for aggradation during MIS 3 or MIS 4 is also present in the main valley (Fig. 3.7).

6.3 Base of the Mumford Hills

The Mumford Hills is a large upland area in the middle of the Wabash valley that rises ~120 feet

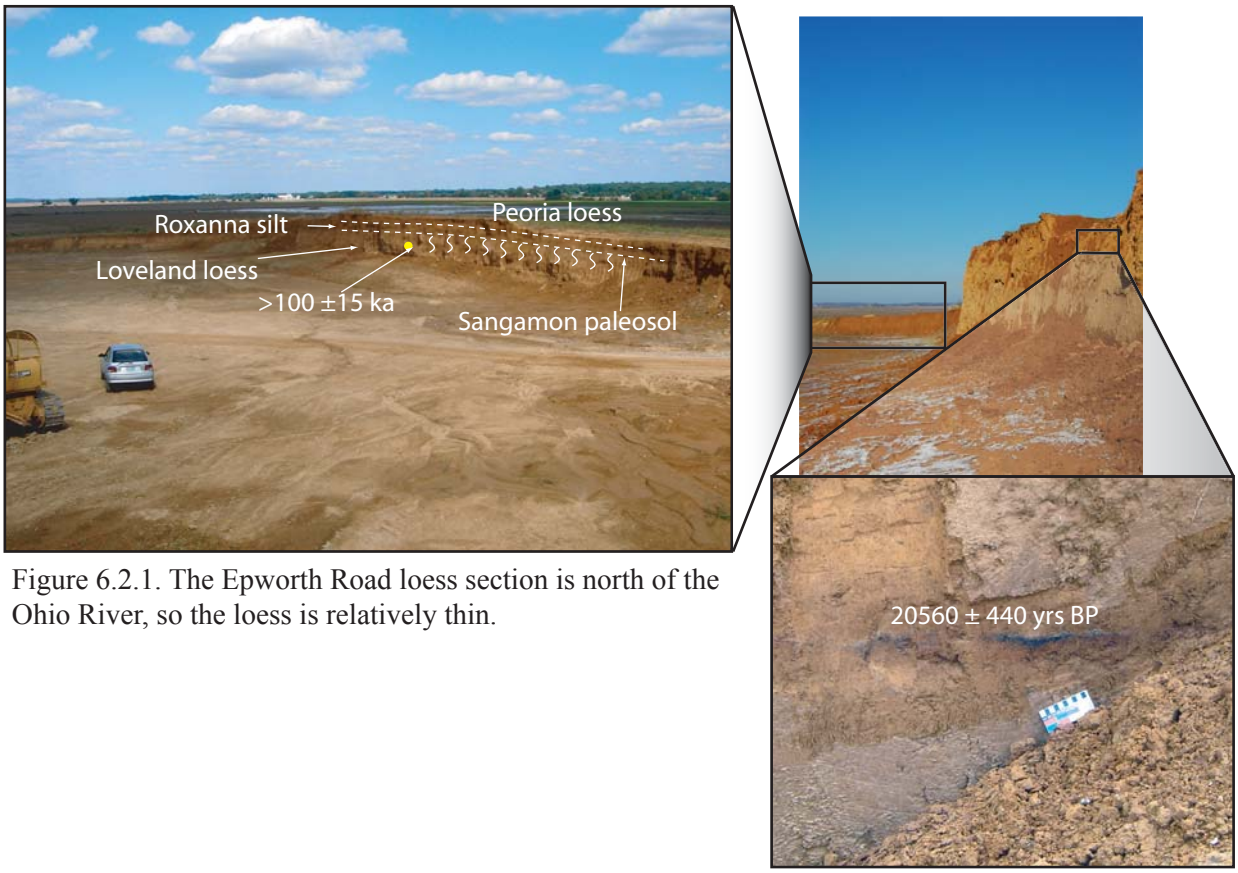

Figure 6.2.1. The Epworth Road loess section is north of the Ohio River, so the loess is relatively thin.

above the surrounding outwash plain. This is an interesting area that has exposures of diamicton, alluvium, and loess, but it is not the subject of any ongoing project and has only just begun to be studied. Other than one ^{14}C age, these sites have not been characterized or described in detail and nothing has yet been measured or sampled. Furthermore, the nearly all exposures are in stream channels, so the extremely wet spring made scraping and photographing exposures virtually impossible, so the deposits haven't even been photographed well. The next two stops will highlight some of the exposures in the Mumford Hills that we have only begun to study.

Floodplain and Eolian Deposits (38.211077°, -87.914694°)

At this stop at the base of the Mumford Hills you can see a 4 m thick section of floodplain deposits (Figure 6.3.1). The base of the exposure is riddled with large Krotovina and is denser, forming a subtle break in slope. The interval above this denser zone contains thin sand beds that are calcareous, and they react strongly with acid. This was unexpected because the sediments are within 2.5 m of the land surface and are in a channel that floods frequently. Another curiosity is that although there appears to be a mollic epipedon at the surface of the soil profile, there is no obvious B_t horizon.

About 100 m east of the floodplain exposure is a loess exposure in a small borrow pit (Figure 6.3.2). There is a thin sand body in the loess with many fine laminae. One OSL sample was collected from the sand body but it has not yet been analyzed. One the northern edge of this exposure there is very dark sediment that is more than 40 % clay that appears to drape the topography. This suggests the hill may have been covered by floodwaters frequently or for a long duration.

6.4 Mumford Hills (38.222624°, -87.921680°)

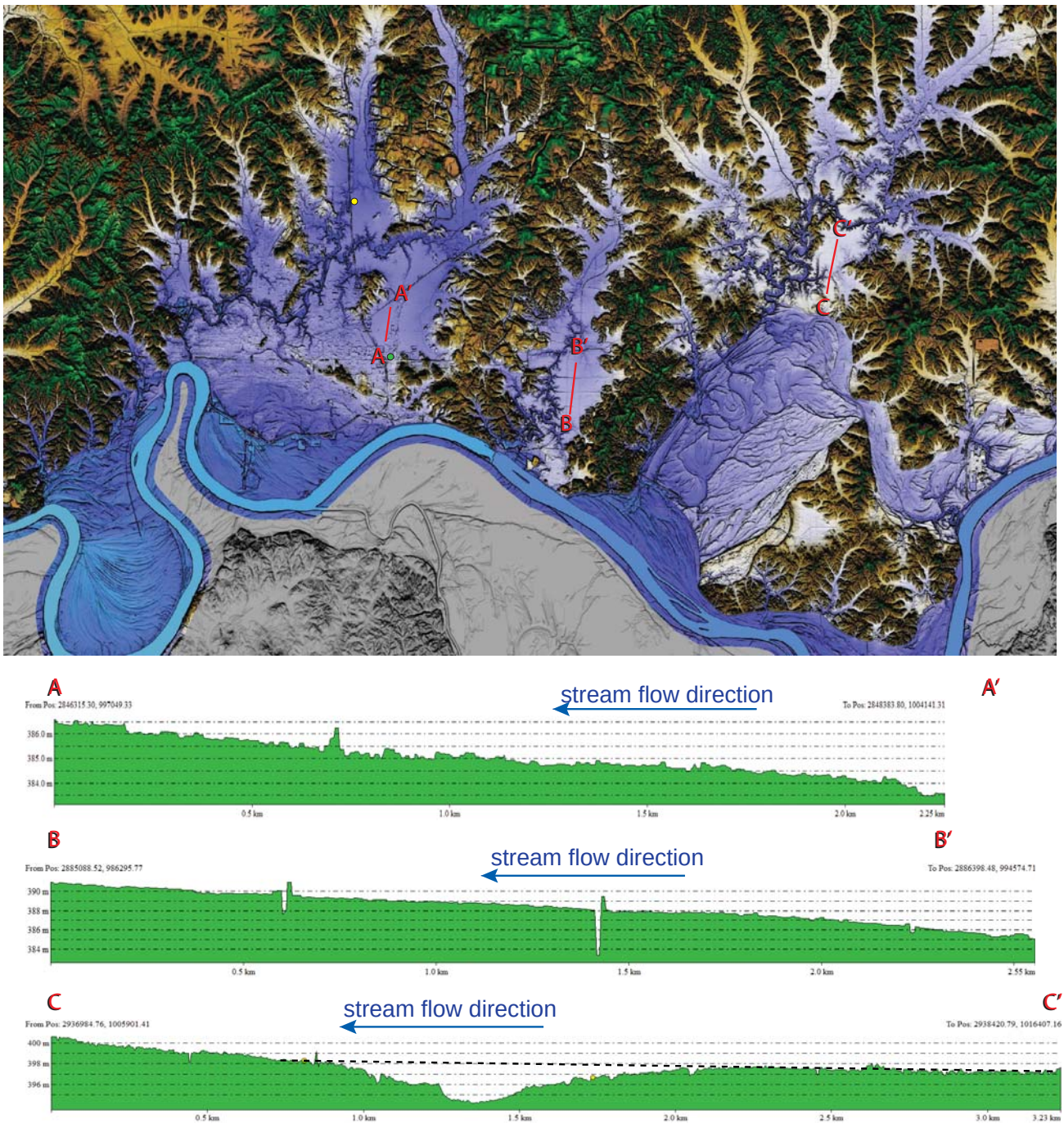

Figure 6.2.2. The surfaces of tributary valleys appear to be flat lacustrine plains, but they actually slope away from the river and are very large, dissected natural levees that formed as aggrading outwash spilled into tributary valleys and filled them with sediment. Green dot is Stop 2 on Saturday. Yellow dot is the location of the core depicted in Figure 6.2.2.

This stop has two exposures. One is a long, continuous trek along a stream channel. The other is on the opposite side of the ridge that the bus parks on, where a cutbank in the creek has created a large slumped section with small windows that allow you to see the underlying sediments. There should be time to visit both sites.

The surface of the hills to the north west is capped by small dunes, but the surface slopes to the southeast and has a morphology that is similar to a kame terrace (Fig 6.4.1). Yet the Mumford Hills are covered with as much as 10 m of Peoria loess, so perhaps the surface is the leeward side of a large dune form. Coring will answer this question.

Beneath the Peoria loess is an oxidized, ~ 1 m thick sandy clay (Fig 6.4.2). This unit could be the Sangamon paleosol developed on MIS 6 outwash. Alternatively, the reddish color could be due to the hydrologic interface between the sandy unit, which transmits water well, and the underlying clay.

The ~2 m thick underlying black clay is heterogeneous (Fig 6.4.2). Charcoal is abundant within it, as are sand lamina. A fairly complete mussel shell was found eroding from this unit. Charcoal sampled from a tree protruding from sidewall of the stream was 5470 ± 25yrs BP, (6231 – 6297 calibrated years), or mid Holocene. This age signifies that the stream channel was incised before 6ka, aggraded around 6.2 ka, and since then have been incising again.

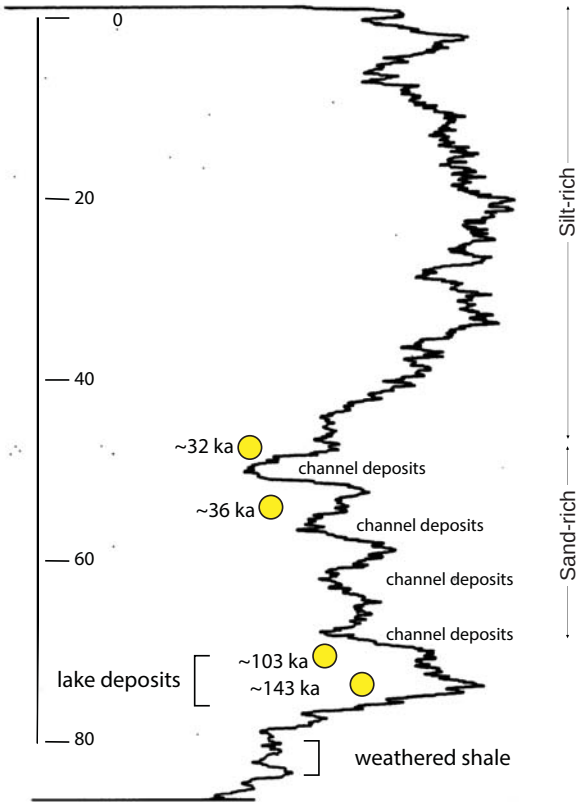

Figure 6.2.3. Natural gamma log and geochronology for an IGS core taken along Interstate 69 which shows the complexity of the tributary basin fill.

A green diamicton underlies the black clay (Fig 6.4.2). The diamicton has a loamy clay matrix with clasts of igneous and local sandstone and has halos of larger cobbles that are completely weathered away (Fig 6.4.2). The diamicton is inferred to be MIS 6 till.

The diamicton exposed in the creek bed at the exposure created by the slumping is thicker, denser, and reddened (Fig 6.4.3). It is not known if is part of the same unit or perhaps is a pre-MIS 6 till.

6.5 Hovey Lake (37.813170°, -87.961983°)

Neotectonics

Geologic and geomorphic mapping in northwestern Kentucky along the Ohio River identified several anomalies associated with a north-south trending, ~2 m high scarp in the Ohio River floodplain (Fig. 6.5.1). Several geomorphic relationships suggest there could be near-surface faulting. The most obvious indicator is the location of the scarp along the inside of an Ohio River meander bend, where there should be point bar deposition and not an erosional scarp (Fig. 6.5.1). East-west drainages on the terrace east of the scarp can be traced across the scarp onto the lower floodplain, though they are more subdued, as if they were formerly at the same elevation. On a larger scale, the morphology of the Ohio River meander loop around the scarp is significantly different than meanders upstream and downstream of this area. The river flows around the scarp in three prominent straight channel sections connected by ~90 degree bends (Fig. 6.5.2), suggesting there is structural control of the channel morphology. However, alluvium in this section of the river is ~40 m thick, so if there is structural control it is being transmitted through thick Quaternary

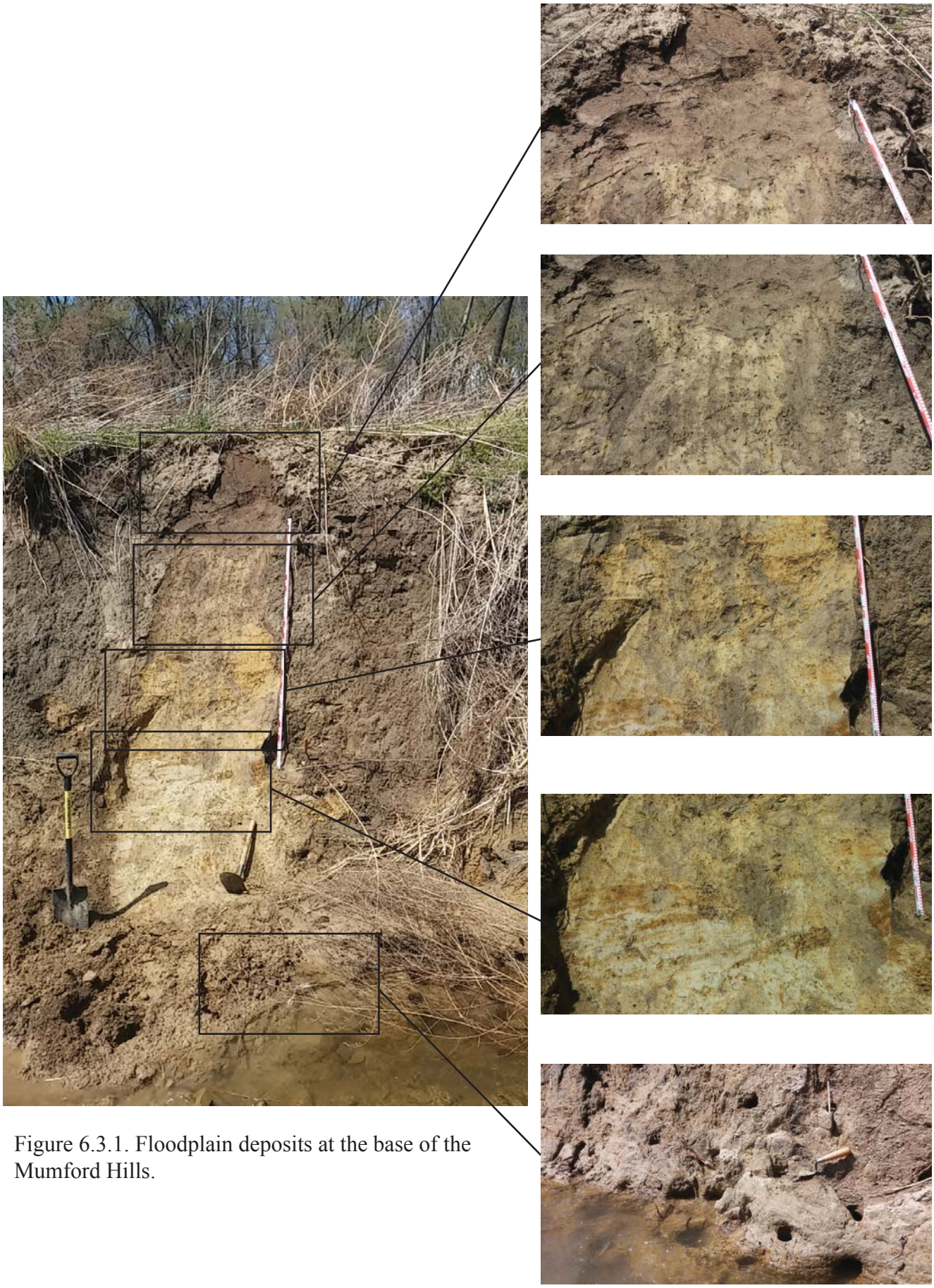

Figure 6.3.1. Floodplain deposits at the base of the Mumford Hills.

Figure 6.3.2. Loess exposure is primarily silt, but it does contains a lenticular shaped sand body that has lamina. At the far left side of photo 1, clay drapes the hill-shaped topography.

alluvium. Additionally, geomorphic mapping indicates that the course of the Ohio River abruptly shifted ~180 º at the scarp, taking its present route around the scarp and then returning to nearly the same location it occupied before its diversion (Fig. 6.5.2a). This is similar to how the Mississippi River is diverted around the Reelfoot Fault at the Kentucky Bend of the Mississippi River (Kelson, et al., 1996) and around the Charleston uplift near Cairo, Illinois (Pryne et al., 2013, Fig. 6.5.3). Furthermore, high resolution elevation data show the scarp is almost perfectly straight for 5 km (Fig. 6.5.2b), and longitudinal profiles of the floodplain and its terraces are deformed at the scarp (Fig. 6.5.4). There is no reasonable geomorphic explanation for the existence of this scarp as a fluvial landform given the current configuration of the Ohio River, the thickness of the alluvium, the surrounding landforms, and the surficial deposits in the surrounding area. However, vertical warping of the floodplain and terraces and channel diversions are known responses of alluvial rivers to surface deformation (Holbrook and Schumm, 1999; Schumm et al., 2000).

Seismic Reflection Across the Scarp

Shallow SH-wave seismic reflection profiles were acquired across the scarp in two locations to determine if underlying Quaternary alluvium and Paleozoic strata were displaced. Seismic data were collected with a 48 channel Geometrics StrataVisor seismograph. Geophones were spaced 1 meter apart, and the energy source was a steel piece of H-beam struck perpendicular to the array with a 1.4 kg sledgehammer. Both reflection profiles show down-to-the-west deflections in the bedrock surface, which is the same configuration as the surface topography. The reflection profiles also show offset reflectors in the alluvium above the bedrock surface, supporting a fault interpretation (Fig. 6.5.5). The fault appears to be a high-angle normal fault that that has been inverted with reverse motion.

Trenching across the scarp

A 33 m long, 1.25 m wide, and 3 m deep single-slot trench was excavated perpendicular to the scarp and above offset seismic reflectors (Fig. 6.5.6). Three sedimentary units and a paleosol were exposed in the trench. The eastern portion of the trench exposed a horizontal, 2.5 m thick bed of silt (unit B) overlying a massive horizontal sand (unit C) that continued below the trench floor an additional ~5 m as determined by coring. In the western portion of the trench, these beds are warped downward below the trench floor, where they are overlain by a younger silt deposit (unit A). The surface soil also dips down-

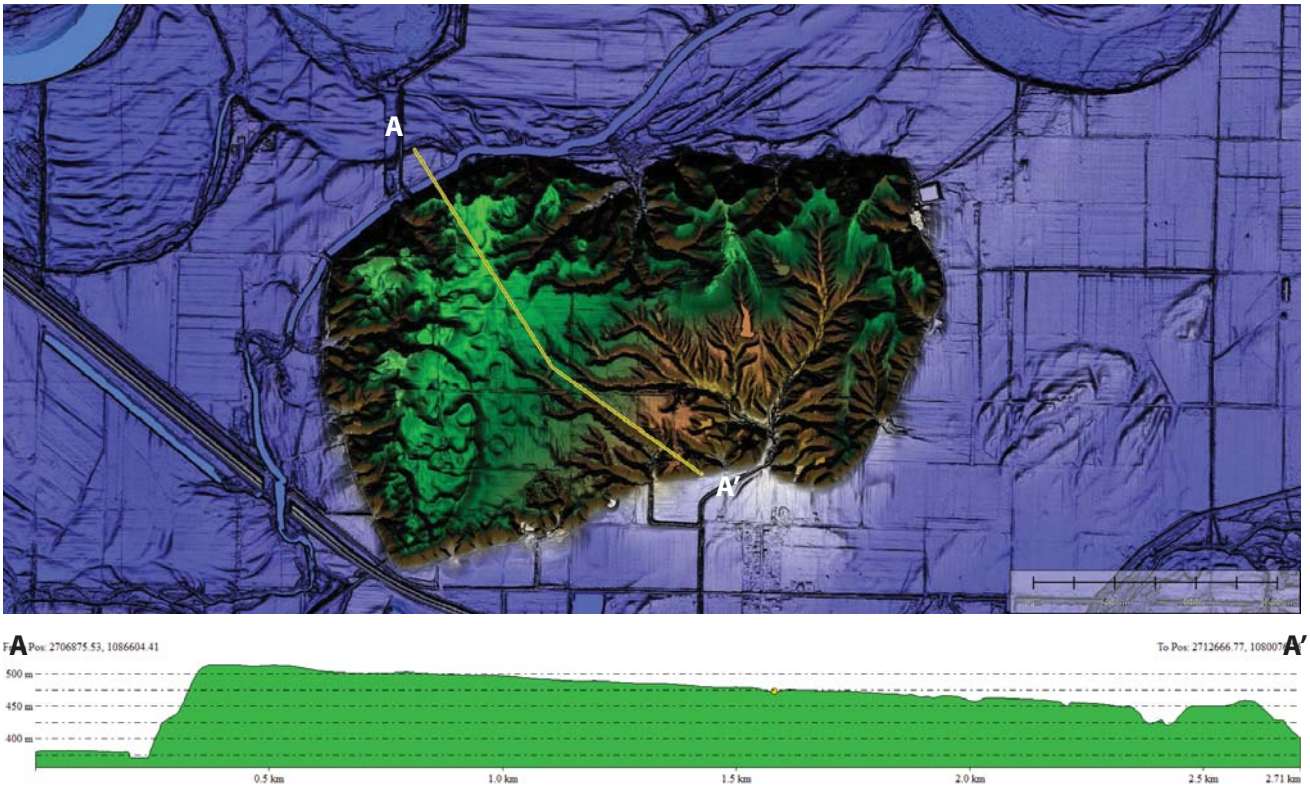

Figure 6.4.1. Topographic profile across the Mumford Hills.

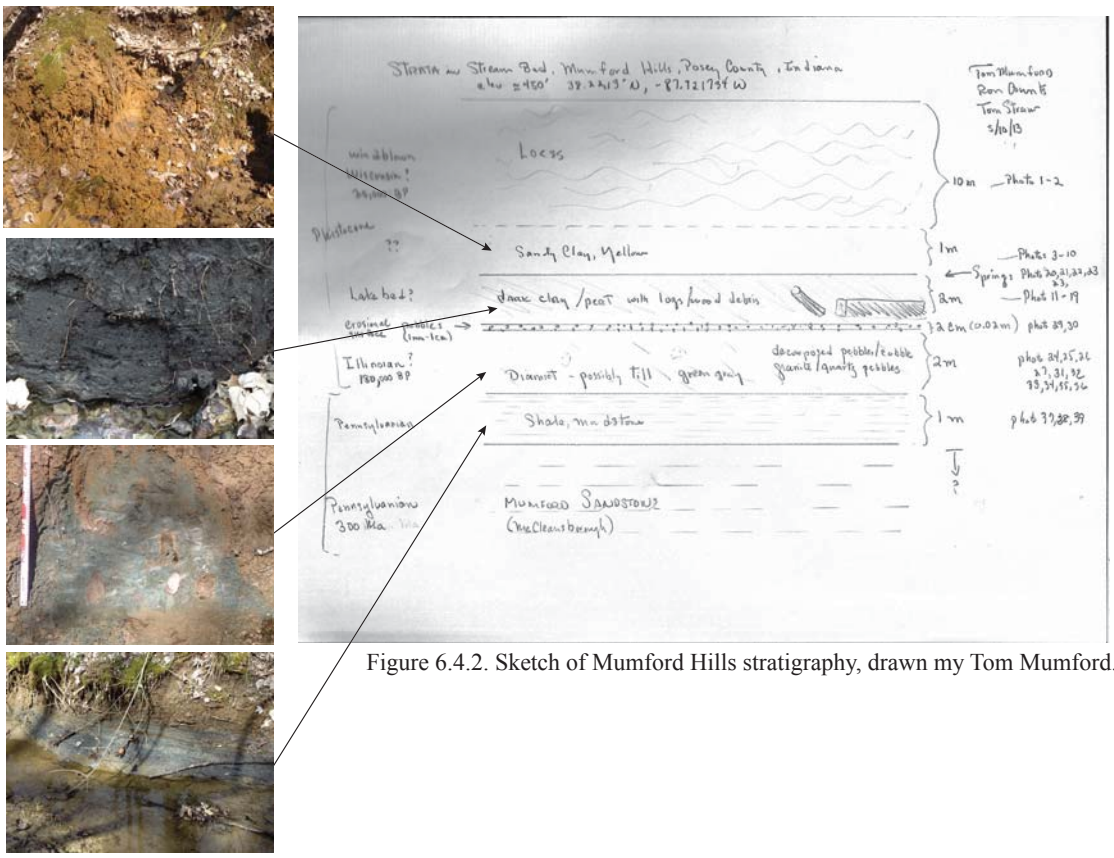

Figure 6.4.2. Sketch of Mumford Hills stratigraphy, drawn my Tom Mumford.

Figure 6.5.1. Hovey lake lies between the confluence of the Ohio and Wabash Rivers and an anomalous scarp in the Ohio River floodplain. Note the truck for scale in the inset photo.

ward and becomes a buried A soil horizon beneath unit A (Fig. 6.5.6). This geometry is interpreted as a monocline, where the buried soil and units B and C have been folded with 3 m of amplitude. Multiple large fractures are in Unit A above the zone where Units B and C are warped.

Absent from the trench were liquefaction features. Seasonal fluctuations of the water table in the region are significant, so even the largest earthquake may produce no liquefaction where the water table is depressed (Obermeier, 2009). However, a core taken from a higher terrace 12 km southeast of the trench contained multiple small-scale liquefaction features at depths from 5.5 – 8 m. It is unknown if these liquefaction features are related to the deformation of the monocline.

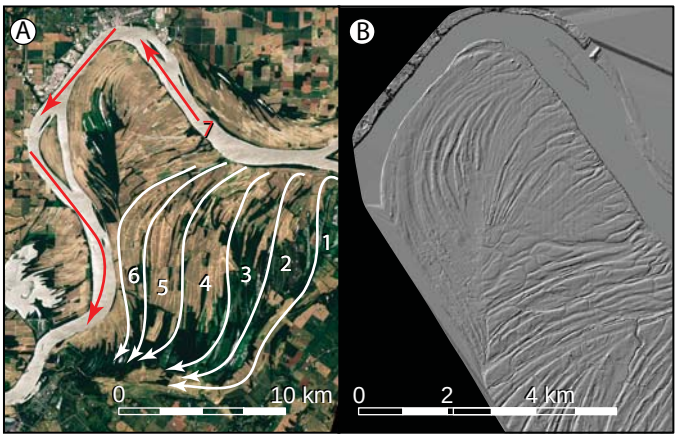

Figure 6.5.2. (A) Geomorphic mapping indicates the flow direction of the Ohio River abruptly changed nearly 180 degrees ~4ka to flow around the scarp. (B) The scarp as imaged in a high resolution data set.

Detrital charcoal was collected from each of the three units exposed in the trench. Radiocarbon analysis indicates the units are late Holocene, with calibrated 2 sigma calendar ages of 296–455 yrs B.P (Unit A), 4,224–3,988 yrs B.P (Unit B), and 3567–3420 yrs B.P. (Unit C). The ages for units A and B are similar but are stratigraphically inverted, illustrating uncertainties in radiocarbon dating from potentially redeposited older charcoal, contamination from plant roots, or bioturbation. A small area of the trench floor was excavated by hand and one optically-stimulated luminescence (OSL) sample was collected below the trench floor in unit C. The OSL age of unit C indicates the sand was deposited 4.7 ± 0.2 ka (Counts, 2013), confirming the folding of the alluvium occurred in the late Holocene. This paleoseismic investigation identifies the first known instance of surface deformation along the southern extension of the WVFZ on a previously unknown fault. This fault, named the Uniontown fault, is a splay fault that connects the Hovey Lake fault system to an unnamed fault complex lying 9 km south (Fig. 6.5.7). Trenching across the floodplain scarp revealed folded Ohio River alluvium, and radiocarbon and OSL dating show that the deformation occurred between ~4.7 and ~0.5ka. Slip on the Uniontown fault displace the Quaternary sediments near the bedrock surface , but younger near-surface sediments were folded into a down-to-the-west monocline with ~3 m of structural amplitude, and the scarp at the surface is interpreted to be a fault propagation fold above the Uniontown fault. The chronology of scarp formation is illustrated in Fig. 6.5.8; 1) deposition of a fluvial point bar sand and overlying overbank silt during flood plain construction at approximately 4.7 ± 0.2 ka; 2) soil formation on the overbank silt across the flood plain; 3) the flood plain sequence and overlying soil were monoclinally folded due to slip on the underlying Uniontown fault, resulting in a west-facing scarp; 4) erosion denuded the scarp thereby removing the surface soil and most of the overbank silt in the scarp; 5) a new soil developed on the denuded scarp; 6) sedimentation at ~0.29 ka (Unit A) buried the down thrown side of the scarp, preserving the buried soil as a paleosol; and 7) subsequent minor flexing along the scarp, possibly caused by minor fault reactivation, formed fractures in Unit A above the hinge of the monocline (Fig. 6.5.6).

The absence of liquefaction features in the trench and the presence of small-scale liquefaction at depth on a nearby higher terrace suggest that the water table was low during the paleoearthquake, and that the absence of liquefaction is not always indicative of aseismicity. Geomorphic mapping indicates that displacement on the fault was large enough to divert the Ohio River around the fault and permanently alter the course of the river. The INQUA Environmental Seismic Intensity scale (Reicherter et al., 2009) indicates that permanent river diversion, 5 km of surface deformation, , and at least 3 m of vertical displacement are indicative of a paleoearthquake of M ~6.0-7.0.

Geoarchaeology

A late Prehistoric village, which was occupied from about AD 1300 and also includes some European trade goods, occurs on the northwestern side of Hovey Lake. In 2013 we collected a core from the lake

Figure 6.5.3. USDA photography showing two examples of extreme flow direction changes due to neotectonic deformation in the Mississippi River valley. A) The Mississippi River makes a 180 degree change in flow direction and flows up valley for nearly 15 km to go around the Reelfoot scarp (after Kelson et al., 1996). B) The Mississippi River changes 180 degrees and flows up valley for nearly 10 km to get around the Charleston uplift (Pryne et al, 2013).

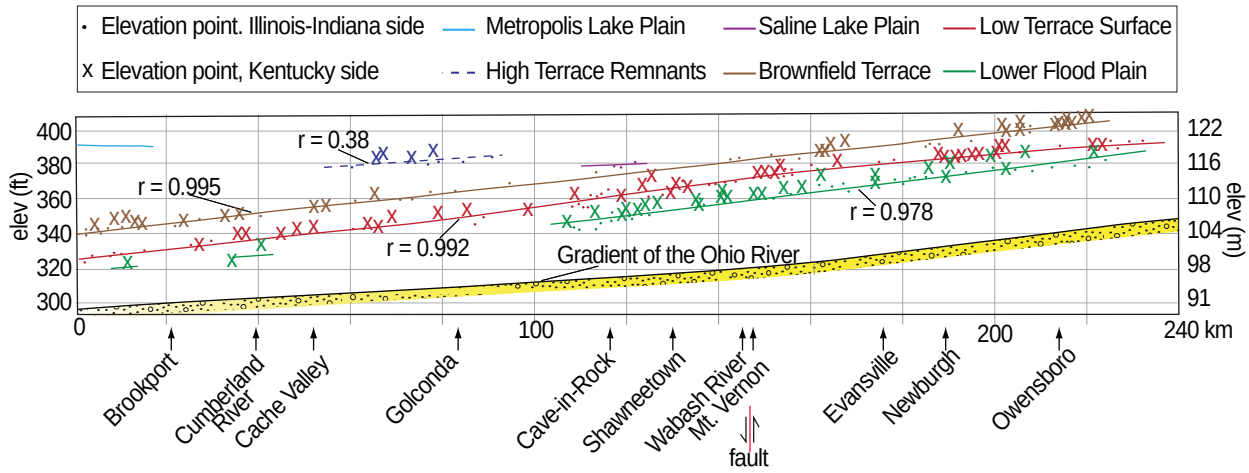

Figure 6.5.4. Longitudinal profiles of the Ohio River floodplain and terraces are arched around Mount Vernon, Indiana and the Uniontown fault to the south (modified from Alexander, 1974).The Wabash Valley seismic zone was not recognized at that time, so Alexander attributed the warped profiles to epeirogenic deformation from an unknown source.

using a Livingston sampler. The core was about 5 m long but only extended back to about AD 1600. We suspect that at least 10 m of sediment occurs within the lake. Preliminary analysis of this core (shown below) suggests that more work from this core will provide excellent data concerning sedimentation and flooding of the Ohio valley . For example, magnetic susceptibility in the core shows several, probably historically document, floods (Fig. 6.5.7). Other analyses, including pollen, stable isotopes, etc., from the core should give us an idea of land clearance and other paleoenvironmental information. We will return here in a few weeks and using a different coring setup will collect the remaining +5m of core and (hopefully) extend our data back to before the establishment of the Hovey Lake village.

Summary

- Ohio River tributary valleys are composite landscapes that owe much of their current morphologies to inheritance of pre-MIS 2 glacial landscapes (Fig 3.1).
- In northwestern Vanderburgh County, the MIS 6 ice margin lies at least 5 km farther south than it is mapped (Fig 3.1).
- The Ohio River responded rapidly to changes in Quaternary and Holocene climate by aggrading and forming terraces during cool intervals and incising during transitions to warm intervals (Fig 6.1.5).
- Responses of the Mississippi and Ohio Rivers to changing Quaternary climate were largely in phase with one another (Fig 3.9).
- There is a significant phase of aggrada-

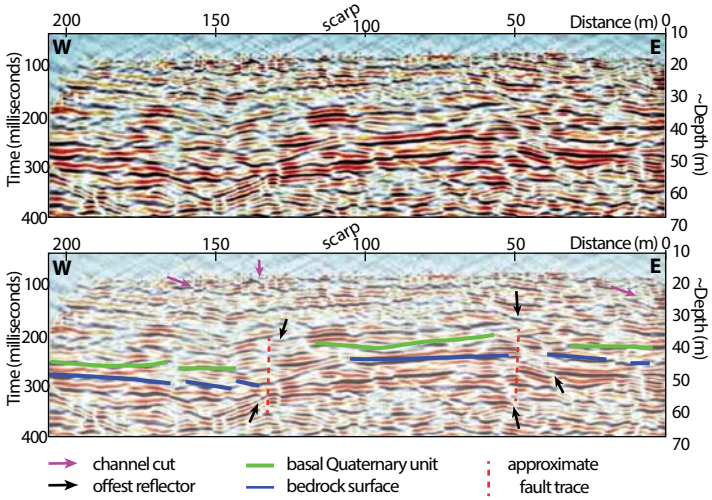

Figure 6.5.5. Seismic reflection profile (top is un-interpreted original) shows that below the surface scarp, there is a down-to-the-west drop in the bedrock surface and offset overlying alluvium reflectors. Seismic line location shown in Figure 6.5.1.Figure 6.5.6

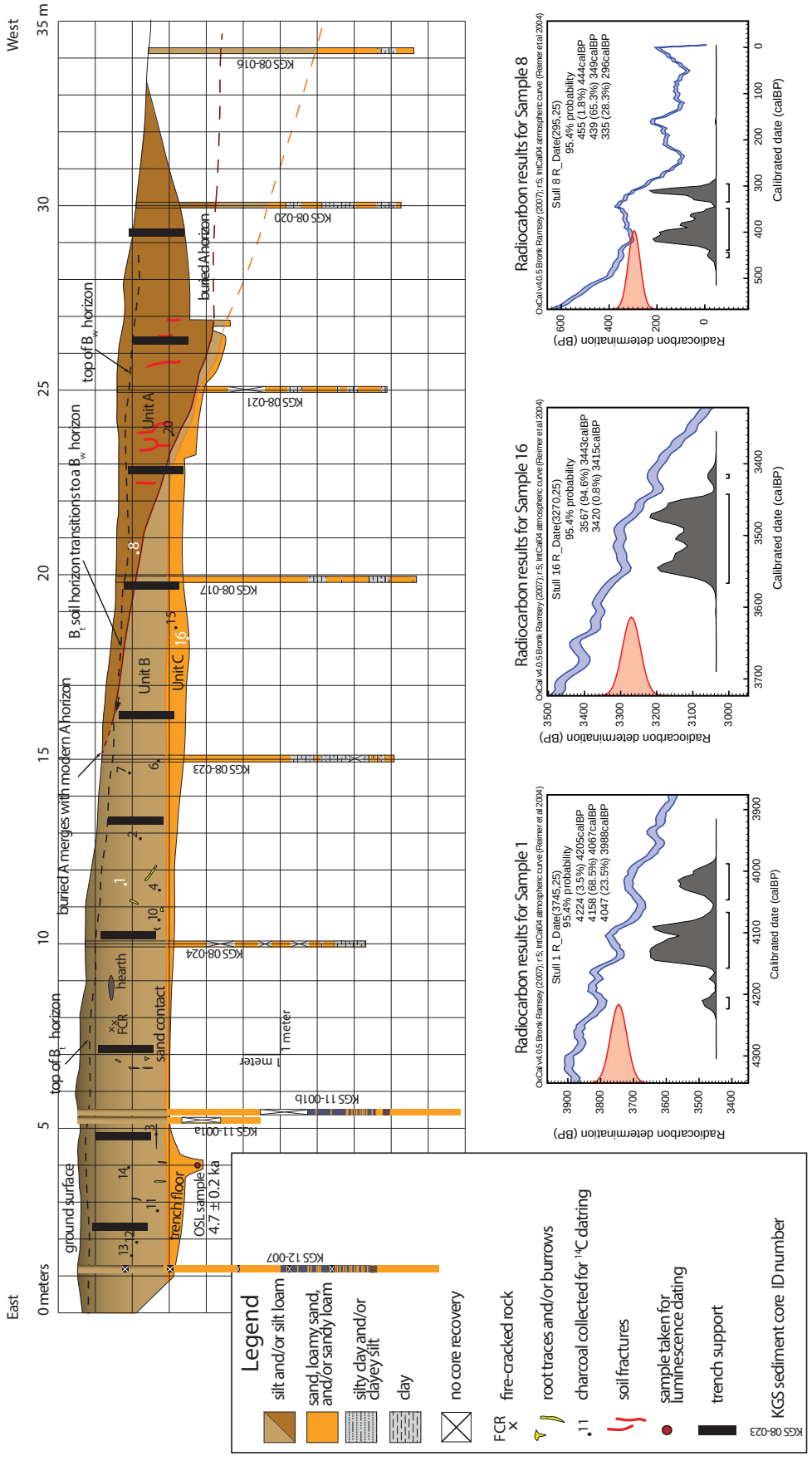

Figure 6.5.6. Complete trench log with geochronology age results. The fractures in unit A above the monocline hinge area suggess there was minor slip on the Uniontown fault within the past ~400 years. White numbers represent charcoal submitted for radiocarbon dating.

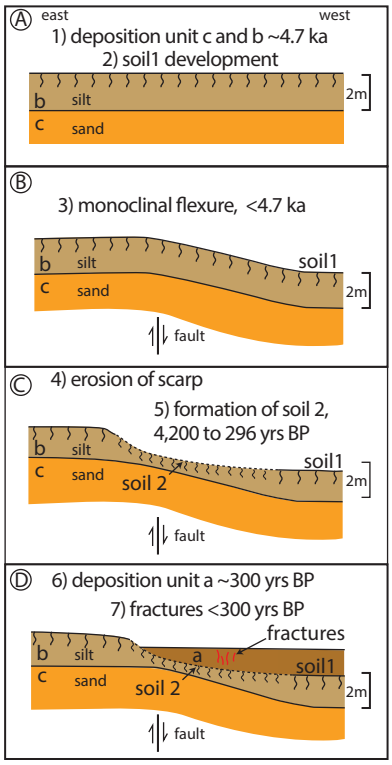

Figure 6.5.8. Model for the evolution of the Uniontown fault scarp: A. Well-developed soil at the surface before faulting. B. Sediments are folded. C. Scarp is eroded, and weak soil develops on the scarp. D. Deposition fills downthrown side of fault, weak soil develops on fill.Fractures indicate possible reactivation within the past few hundred years. Note that east is to the left, which represents the orientation of the trench wall that was logged.

tion in the Ohio valley during MIS 4 or MIS 3; this record is preserved in both the mainstem river and in the Pigeon Creek tributary valley (Fig 3.7,Fig. 6.2.2).

- There is a pre-Loveland silt in the Ohio River valley (Fig. 3.3, Fig 3.5).
- In thick Ohio River Peoria loess, total carbonate with depth correlates very well with the GISP 2 ice core record and seems to be a good proxy for temperature (Fig 6.1.5).
- The Ohio River is susceptible to neotectonic activity in the Wabash Valley seismic zone.
- There may be pre-MIS 6 diamict inder the Mumford Hills.

Much more work needs to be done regarding MIS 6 and older glaciations in southwestern Indiana.

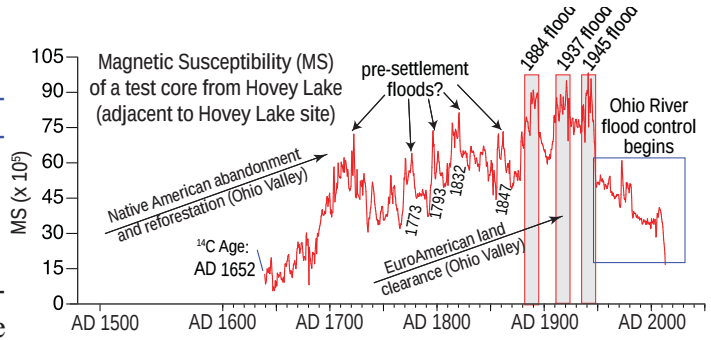

Figure 6.5.7. Magnetic susceptibility and a radiocarbon age for a 4 m core from Hovey Lake record Ohio RIver flooding history for the past 400 years.

7.1 Construction of the upper and lower platform of Mound A: reconstructing a Mississippian mound without destroying it

Introduction to research about Mound A:

The process of recovering and contextualizing cultural information from strata is at the heart of archaeological research. Extant earthworks are often unexplored not only because of their linkage with burial and religious beliefs of modern Native Americans but also because the archaeological community is reluctant to allow their alteration by exploratory excavation. Overcoming such limitations is our focus. The ability to "see" underground to reconstruct the subsurface is a worthy goal, but it must be linked to ground-truthed data. The purpose of our visit to Mound A is to discuss the results of modern work at the Mound within the context of the history and development of Angel Mounds town and its occupations.

Mound A is a good place to start because it is among the largest of Mississippian earthworks in the region, measuring ~200 by 125 m by ~16 m high (Figs. 7.1.1 and 7.1.2). It is a complex structure, consisting of two platforms: a lower (~75 m long by 4 m high) and an upper (~125 m long by 8 m high). A small (~15 m diameter) conical offset projects ~6 m above the southeast corner of the upper platform. Although construction was probably complex, except for a few shallow trenches, Mound A has not been excavated, and the first real investigations of the lower platform occurred only in 2013, through our NSF REU project. Thus, important questions, including mound composition, stratigraphy, construction methods, and chronology, remain unanswered.

Work in 2008–10 revealed that the upper platform was built rapidly at ~900 BP by stacking >60,000

Figure 7.1.1. View of Mound A looking East

m^3 of overturned turf blocks and basket loads in (probably) <10 years (Monaghan and Peebles, 2010) (Fig. 7.1.3). Mound strata of the upper platform were mapped by combining point-source data collected using minimally invasive solid-earth coring (Geoprobe) with subsurface geophysical methods (72-probe resistivity profiler and downhole geophysics). These data have been combined to create a 3-D model of what the mound interior looked like (Figs. 7.1.4 and 7.1.5). The cores and downhole geophysics provide ground-truth information necessary to realistically interpret the resistivity and GPR data. Additionally, organic samples from the cores provide absolute chronology to various episodes of mound building; such information as texture of the fills or pollen preserved within them can give insights into the engineering knowledge and local environmental conditions at the site.

When and how the lower platform was constructed remained unknown until our work in 2013. The sets of closely spaced solid-earth cores and geophysical profiles demonstrate that the upper platform was built earlier than the lower platform but underwent significant slumping and sheet-washing on its edges before the lower platform was constructed. Additionally, the 2013 work shows that the lower platform was expanded at least twice and underwent major episodes of erosion and repairs along its edges during use and after site abandonment.

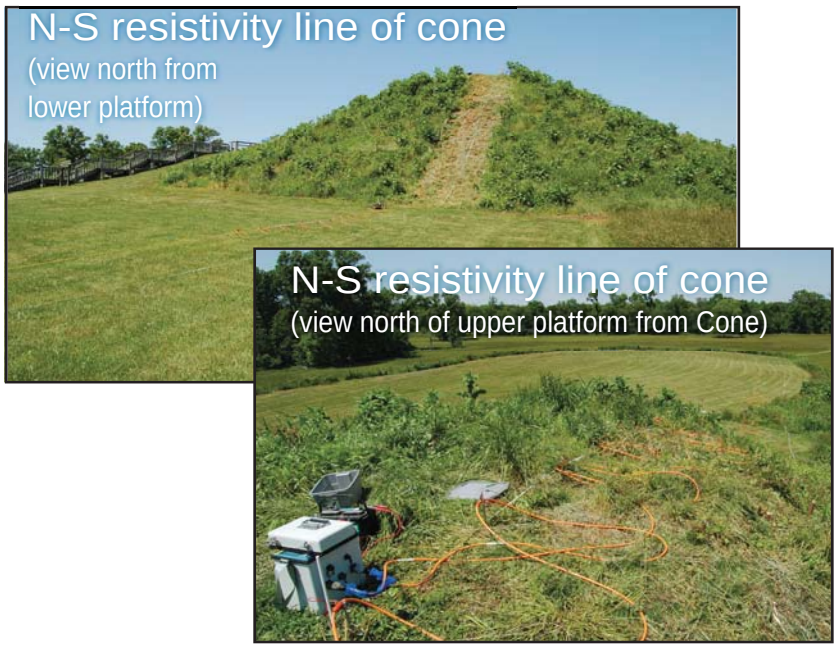

Figure 7.1.2 Examples of common setup of resistivity lines to construct ER profiles across the upper platform and conical offset. Probe spacing is typical (1m). These data were collected using a Syscal Pro Resistivity Profiler with 72 probes set at 1m spacing and "fired" using Wenner and/or Dipole- Dipole arrays. With such probe-spacing and array types, 10-14m of the mound subsurface was

Seven 1-x-1-m units were opened on the lower platform of Mound A, revealing over 30 features indicative of minimally two habitation levels covered with fill, possibly dating to the ceremonial closing of the site, and wash episodes likely related to post-abandonment mound degradation. Three units on the southwest mar-

Coring on the upper platform near conical offset (cone). Opened core shown on right

Figure 7.1.3. Solid-earth coring (Geoprobe). Coring on Mound A. Several continuous, solid-earth cores that penetrate the entire mound fill have been collected from various parts of Mound A using a Geoprobe with dual-tube sampler. Many of these await analysis, but several have been described in detail, one of which was taken were the cone and platforms join and is shown here. These cores serve to define and trace physical stratigraphy of fill and sediment sequences within Mound A and provide a ground-truth framework for the subsurface geophysics. They show the "real" mound subsurface in great detail and by delineating the physical properties of fills and natural sediments, constraints can be placed on the "virtual" subsurface defined by geophysical methods.

The core shown has of about 9.5m of mound fill consisting of stacked sequences derived from near-surface soil horizons. The base consists of a ~2m-thick sequence of stacked 10-20cm-thick block of A-horizon soil that sometime contain preserved grass (or "turf") along their upper surface. Grass, which is an annual plant, from the top and bottom of the sequence yielded nearly identical 14C ages (890 BP and 900 BP; 2-sigma Cal AD 1020-1230) and indicates that Mound A was probably rapid built beginning soon after AD 1000. The "turf" blocks are clearly overturned and are distinct from the in situ soil sequence under the mound fill. These are overlain by stacked 10-20cm-thick blocks of B- or BC-horizons that are generally stacked by color, with alternating "redbrown" and "yellow/grey" horizons. Whether this sequence has "cultural meaning" or reflects collection methods and engineering properties is interesting but speculative. Very few constructional hiatus were noted in any of the cores, which support rapid construction. Additional 14C dates may provide a clearer idea of the timing and rates of mound building. Other analyses, such as palynology of fill and in situ soil at the mound base, as well as their geochemistry, may provide other important cultural and engineering data about the mound and Angel town environment.

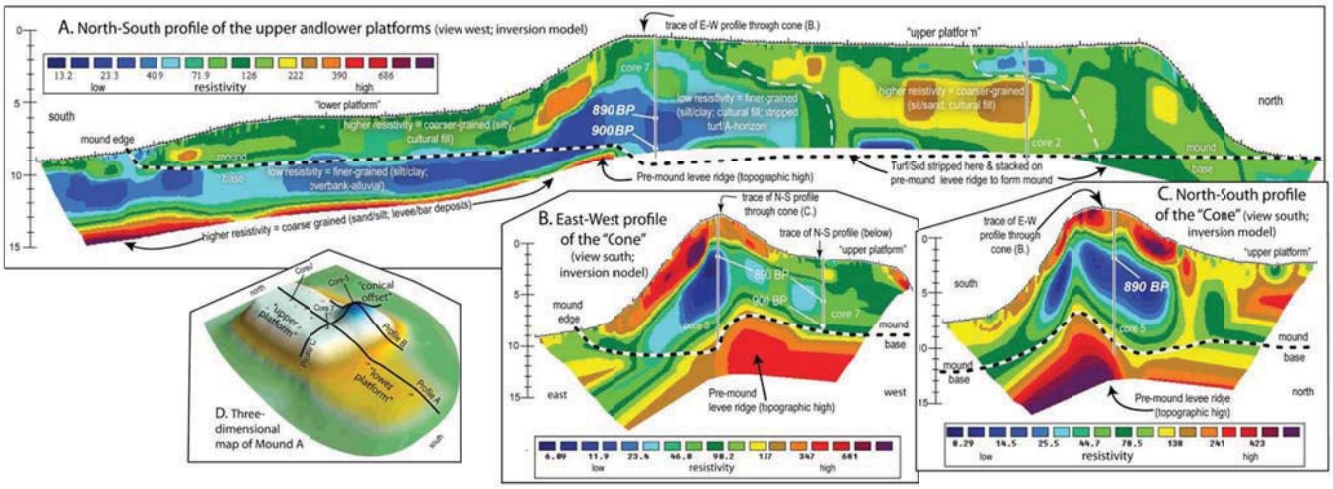

Figure 7.1.4 ER Profiles collected from Mound A showing the subsurface configuration.

Several resistivity profiles revealing the electrical properties of the subsurface were taken from Mound A and three showing the general structure of the mound are displayed here. Part A is a long north-south ER profile along the long axis of the mound showing the structure underlying the "upper" and "lower platforms." The approximate location of Core 7 and depths of associated ^{14}C ages (BP) is labeled. Part B shows an east-west ER profile through conical offset and upper platforms. Part C shows a north-south ER profile through the conical offset. This pair of relatively short E-W the structure and general relationship between the "conical offset" and the platforms. The approximate location of Cores 5 and 7 and depths of associated ^{14}C ages (BP) are shown and labeled. Part D shows a three dimensional rending of Mound A, locations or traces of cores and ER profiles shown and labeled.

The profiles show differences in relative electrical resistance between various horizons, which is controlled by compaction, soil moisture and texture. Of these, moisture and texture are dominate but not independent of each other. Thus, fine-grained and moist sediments have low resistivity while coarse-grained and dry soils are high. Moreover, finer-grained sediments (silt/clay) will also retain moisture, which accentuates textural differences. In the Mound A profiles, the "darker" blue and green colors are the least resistant layers and probably mark finer-textures (silty-to-clayey) sediment and soil. The "brighter" yellow and red colors are the most resistant and mark coarser-grained (sandy) deposits.

By considering various data, a general construction plan can be outlined. We suggest that Mound A construction began on a preexisting levee ridge where the cone and platforms join. Beginning ~900 BP (2-sigma Cal AD 1030-1230) "turf" blocks were cut from elsewhere (possibly under the upper platform) and stacked ~2m high on the ridge. Initially, Mound A was small, possibly a cone surrounded by a small platform and may have been oriented E-W rather than N-S as today. More profiles, cores and dates may clarify the chronology, stratigraphy, and engineering of Mound A.

gin of the lower platform provide evidence for an expansive burning episode on the southwest margin of the lower platform that was quickly buried during a reconstruction/renewal episode. Initial construction of the lower platform occurred between AD 1220 and 1267 with a subsequent burning episode between AD 1270 and 1292 and a burnt structure dating to AD 1304–1402. The latter is the radiocarbon age from a structure excavated in 1955 on the upper platform of Mound A. Wall trenches and corresponding post holes mark the former locations of mound-top structures in several locations on the lower platform, and in combination with geophysical mapping, provide an approximate view of the lower platform's use and function.

Results and Discussion:

Our work on the upper platform of Mound A highlights several important observations related to the construction methods, materials, and engineering of Mound A, as well as the chronology of mound building

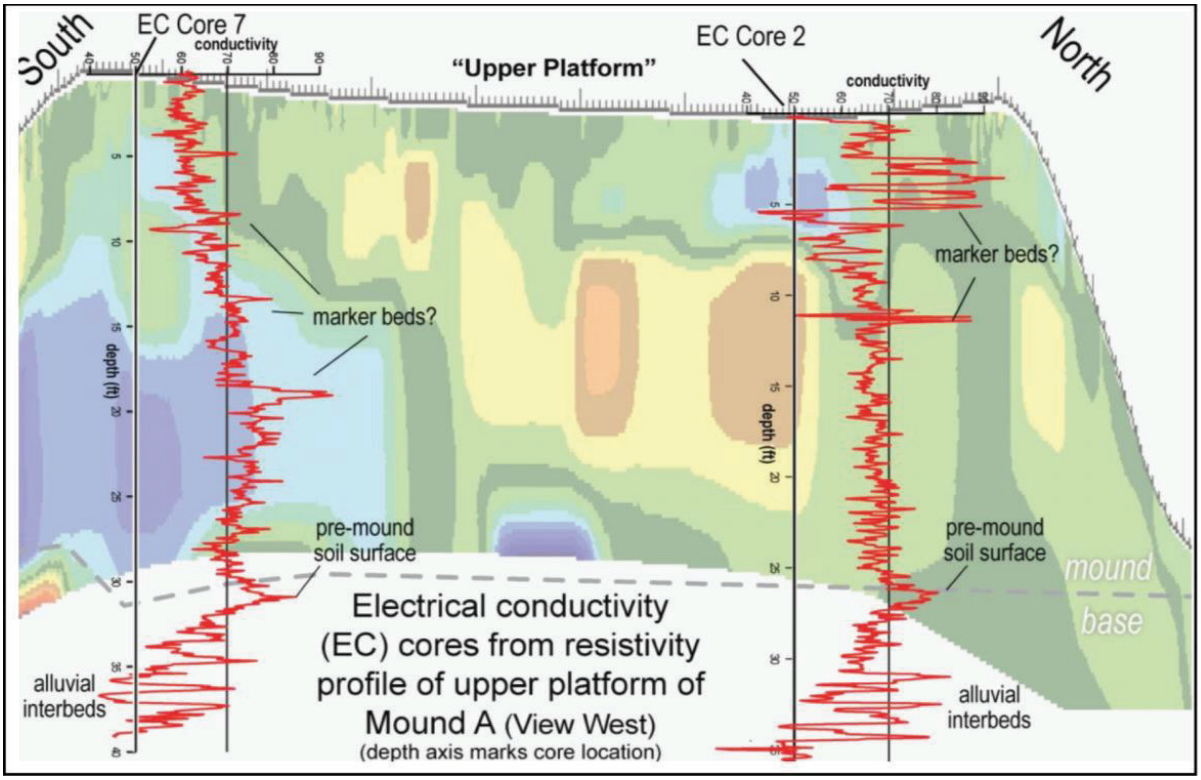

Figure 7.1.5 Comparison of downhole conductivity traces from cores with resistivity profile from the upper platform.. Several down-hole electrical conductivity (EC) logs were taken from Mound A adjacent to the locations of GeoProbe cores and because they directly measure the EC of sediment at 2cm resolution, they show much more detail than resistivity profiles. EC is the inverse of resistivity and works similarly. Typically, silt and clay have high conductivity while sand has low conductivity. By taking several EC logs along a resistivity profile, broader subsurface resistivity profiles can be calibrated to detailed, but more point-source measurements of electrical properties, and also can be directly related to the actual sediment or soil sampled and described from the GeoProbe cores.

Two of the EC logs are plotted above to directly compare with the resistivity profiles. One (left) is adjacent to the dated sequence at the southern margin of the upper platform while the other log (right) was taken about 20m from the northern end of Mound A. The EC logs broadly agree with the coarser resistivity profiles. The base of the mound is evident by a characteristic "kick" in EC and the basal levee deposits are indicated by interbedded coarse- and fine-grained interbeds (alternating "high" and "low" EC layers). The 10-15cm-thick layers marked by variations in EC represent minor fill units within in the mound. A few of these may have EC properties that are distinct enough to represent marker horizons within specific components of the mound.

and its context within the larger framework of Middle Mississippian settlement of the Ohio/Wabash valley (Fig. 7.1.6).

- Resistivity can be used to map broad units of mound fill. Implicit in this notion is that the mound is structured, orderly, and composed of distinct and discrete layers selected by the mound builders based on their physical properties. How much of this selection reflects convenience or esthetics and how much relates to their engineering properties is an open but important question.

- The mound is composed of stacked sequences of sediment that were mainly derived from near-surface soil horizons. These were mainly 10- to 20-cm-thick blocks from the A-horizon, which sometimes pre-

served turf (or grass) along their upper surface, and B- or BC-horizons. These were often stacked by

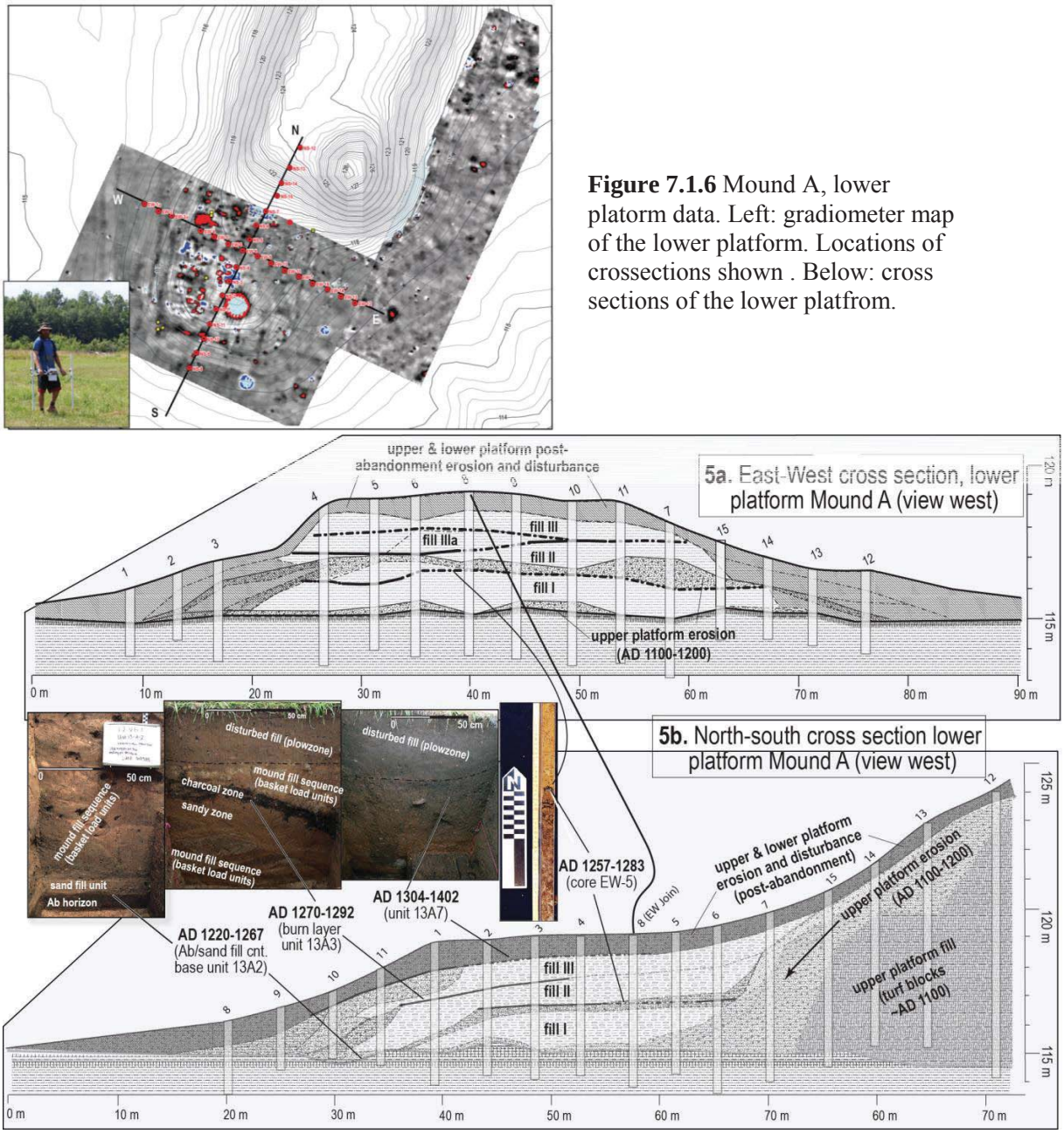

Figure 7.1.6 Mound A, lower platorm data. Left: gradiometer map of the lower platform. Locations of crossections shown . Below: cross sections of the lower platfrom.

color, with alternating red/brown and yellow/grey 10–20-cm-thick Bt/Bg horizons.

- The A-horizon stacks from the basal part of the mound are generally overlain by similarly thick stacks of B-horizon. Whether this sequence is general across the mound and reflects a simple unroofing process as the surface soils horizon are cut first and stacked on the mound, exposing B-horizon soils that are then cut and stacked on the A-horizon, is connected to religious and aesthetic principles or relates to specific engineering properties of the soil types remains speculative.
- Mound A construction began in the central portion where the upper and lower platform joins and was

built outward from where turf blocks were stacked ~2 to 3 m high on a preexisting high area (levee).

- Grass, an annual plant, preserved near the top and bottom of this turf stack in the mound core yielded radiocarbon ages of 89 0± 40 BP (2-σCal AD 1030–1230) and 900 ± 40 BP (2-σCal AD 1030–1220), which are very early in the Angel site chronology. The dates suggest that occupation of the town likely began soon after AD 1000 and that earthwork construction was one of the first building tasks at Angel town.
- Turf blocks were probably used to make steep-sided margins of the mound, which failed when the grass and roots decayed. Slumping from this failure probably accelerated over the first century after construction of the upper platform. Sheetwashing was common within the lower platform sequence.
- No turf blocks were found in the lower platform but were common at the margin of the upper platform.
- Rush collected from a burn feature about 4.5 m below the top of the cone (approximately coinciding with the surface of the upper platform, if it were projected through the cone), yielded a statistically identical date of 890 ± 40 BP (2-σCal AD 1030–1230). Together, the dates suggest that the mound was not only constructed early but also very rapidly, implying a massive and purposeful immigration of whole populations to Angel town with a clear town plan rather than some form of *in situ* cultural development.
- The regional chronology of Middle Mississippian sites suggests a rapid expansion of towns into and up the Ohio/Wabash valleys soon after AD 1000, followed by relatively sudden abandonment (collapse?) of these towns by AD 1450. While the fate of the inhabitants is unknown, some affiliation with or migration to Caborn-Welborn sites is often suggested. Some researchers have also proposed that Caborn-Welborn sites were populated by descendants of Angel and other Middle Mississippian towns and represent cultural development after the Angel Chiefdom collapse (Pollack, 2004).

7.2 Evidence for Paleoearthquakes and Seismicity at Angel Mounds (still on Mound A)

Liquefaction within a 25-m-long profile of Mound F?

A profile of Mound F left intact after the 1965 excavations was exhumed in 2013 and revealed two anomalous sand units (Figs. 7.2.1, 7.2.2, 7.2.3). One unit, located at the mound base, is a horizontal, 2- to 4-cm-thick bed of medium sand and is the source of a small (~0.5 cm wide by ~100 cm long) clastic dike that upwardly penetrated the overlying fine-grained mound fill by hydraulic fracturing. In some places the sand appears to have vented onto the Inner Mound surface, but disturbances from the 1965 excavation confuse this relationship. Although feeder dikes were not exposed in the trenches, the two sand units are interpreted as seismogenic liquefaction features. The mound is too small to have produced such liquefaction via slumping, and staged mound construction was not rapid enough to induce a sudden loading to generate hydraulic fracturing.

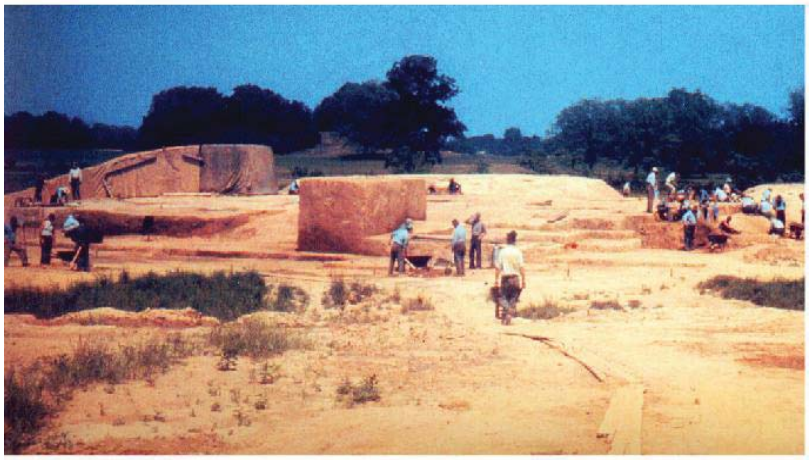

Figure 7.2.1. Excavation of Mound F during the WPA era.

These data suggest that a large earthquake occurred at Angel Mounds after 1100 AD. Forthcom-

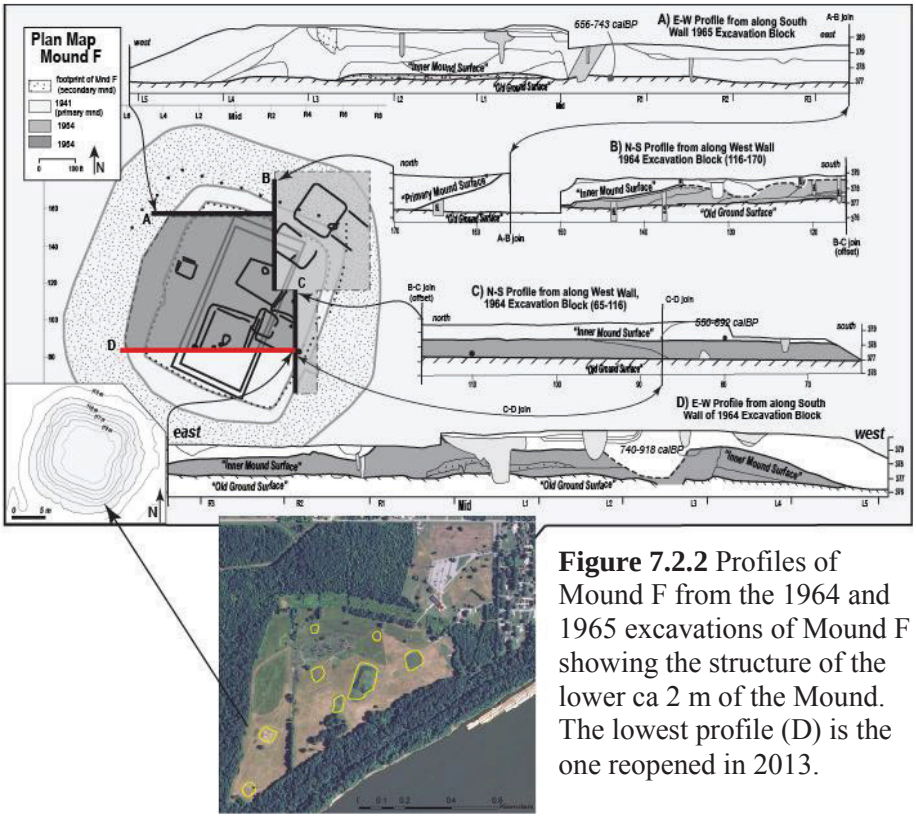

Figure 7.2.2 Profiles of Mound F from the 1964 and 1965 excavations of Mound F showing the structure of the lower ca 2 m of the Mound. The lowest profile (D) is the one reopened in 2013.

ing OSL ages, however, will improve our understanding of the site's history, including whether sand vented onto the Inner Mound surface. Large, mid-Holocene sand/gravel dikes and at least one Holocene fault, likely associated with the Wabash Valley Seismic Zone, occur within ~20 to 40 km of the site and demonstrate that large-scale, Holocene seismicity is common in the area. Seismicity at Mound F likely affected the occupation and mound construction at Angel Mounds and may have contributed to the post-AD 1450 site abandonment.

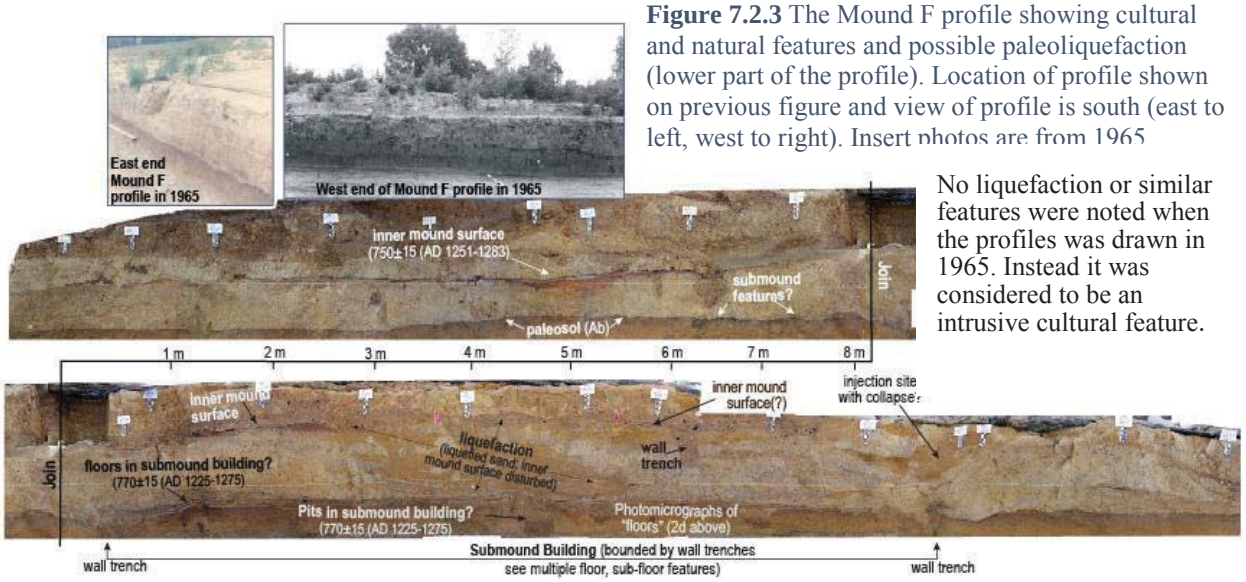

Figure 7.2.3 The Mound F profile showing cultural and natural features and possible paleoliquefaction (lower part of the profile). Location of profile shown on previous figure and view of profile is south (east to left, west to right). Insert photos are from 1965

No liquefaction or similar features were noted when the profiles was drawn in 1965. Instead it was considered to be an intrusive cultural feature.

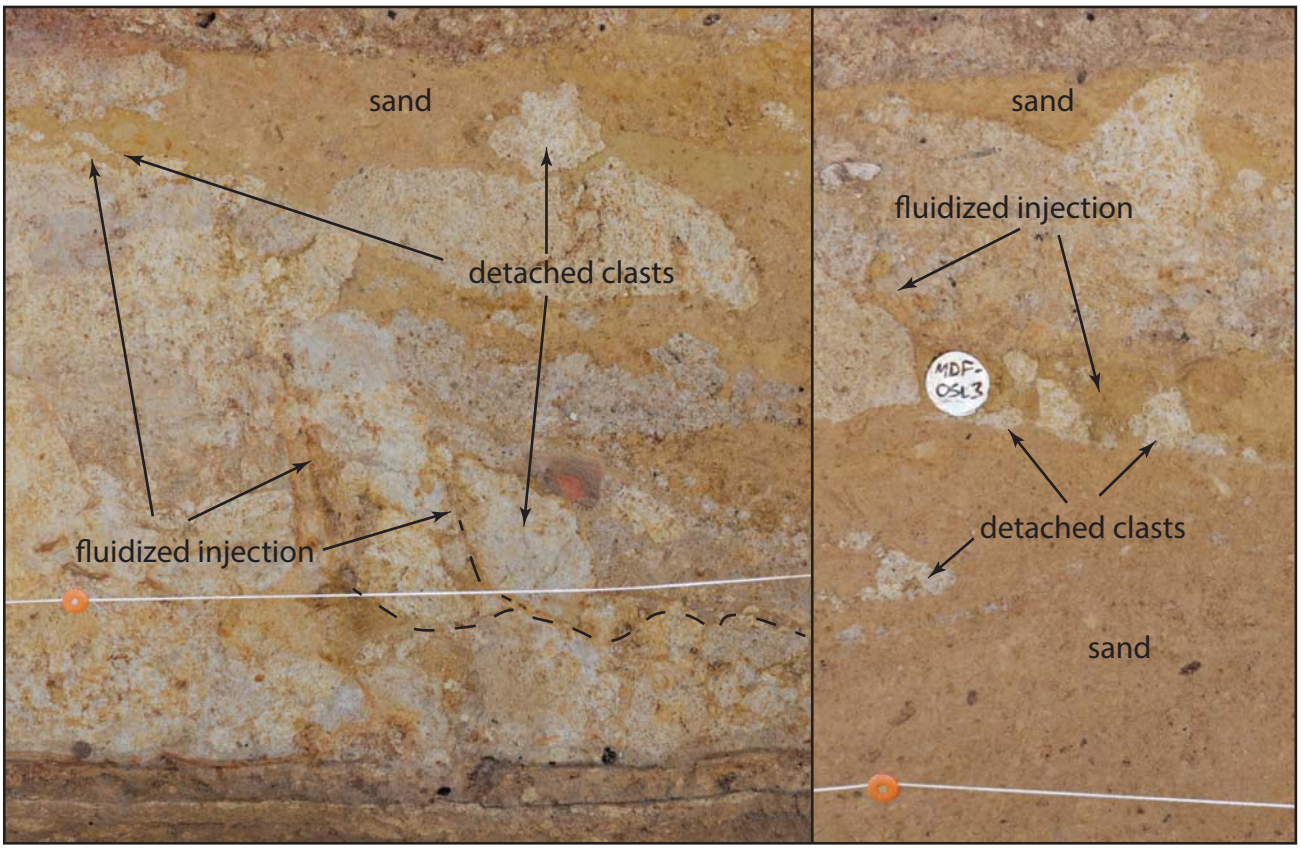

Figure 7.2.4. Many fluidized injections in the mound profile originated from larger liquefied sand bodies. During seismic liquefaction, the forceful injection of sand into fine-grained units fractures the fine host unit, and clasts of the fine unit are often detached and transported by the fluidized sand. When shaking stops, the clasts become "frozen" in the sand.

Injected sands in the Mound F profile at Angel Mounds:

Mound F was almost completely excavated between 1940 and 1965 (Figs. 7.2.1 and 7.2.2). However, a partial profile was left intact after the 1965 excavations and was exhumed in 2013. Once the exhumed profile was cleaned, two anomalous sand units were noted (Fig. 7.2.3). One unit, located at the mound base, is a horizontal, 2- to 4-cm-thick bed of medium sand and is the source of a small (~0.5 cm wide by ~100 cm long) clastic dike that upwardly penetrated the overlying fine-grained mound fill by hydraulic fracturing. A second, larger sand body (~1 m high by ~4 m wide) is lenticular and contains many detached fragments of mound fill (Fig. 7.2.4). This sand unit is clearly not part of the mound building fill because in many places it disrupts/truncates the mound fill, the mound surface, and other cultural features. Moreover, sand was rarely used as mound building material elsewhere at the site and is certainly anomalous within the basket loads that were used to build the mound. Loose sand would have been more difficult to transport in baskets, would not stay in place on mound slopes, and, except for deeply buried sediment, there is not a readily available source of sand at the site.

In some places, the sand from the large, 1- by 4-m unit appears to have vented onto the Inner Mound surface, but disturbances and poor mapping of the profile from the 1965 excavation confuse this relationship. Although feeder dikes were not exposed in the trenches, the two sand units are interpreted as seismogenic liquefaction features. The sand units in Mound F exhibit characteristics that are typical of hydraulic fracturing and liquefaction; most notably they are continuous in three dimensions and they contain abraded

clasts of the host material that they were injected into (Fig. 7.2.4). Processes that can create the types of liquefaction features observed in Mound F include slumping or landsliding, rapid sediment loading, artesian (pressurized) groundwater, and seismic shaking. The mound was not large enough to significantly slump and, although the site is adjacent to a river, it is on a flat surface with no relief to induce large-scale landsliding. The mound was not constructed fast enough to induce sediment loading needed to liquefy sediments, and the top of the local groundwater aquifer is the water table, so it is unconfined and not under pressure. Seismic shaking is the remaining logical mechanism for the liquefaction. Additionally, unlike natural floodplain deposits, mound fill is much more chaotic and is only ~700 years old. Consequently, it is loose and not as compacted as the 10 ka terrace deposits. This arrangement and structure may be weak enough to hydraulically fracture at lower shaking thresholds than natural floodplain deposits and may explain why it appears there is not widespread liquefaction at the site.

The injection features in the Mound F profile are characteristic of seismic liquefaction features, which do not appear to have been widespread at the surface of Angel Mounds. So far it has been directly observed only in one mound excavation and potentially in several geophysical surveys of mounds and one of the structures at the site. The fact that the liquefaction seems to be restricted to the mounds could be attributed to either increased soil moisture or elevated water tables beneath the mounds during dry conditions (compared to the floodplain), or to the chaotic and disorganized mound fill being much weaker than the natural floodplain cap, lowering its threshold for hydraulic fracturing.

Data from Mound F suggest that a large earthquake occurred at Angel Mounds after AD 1100–1200. Forthcoming OSL ages, however, will improve our understanding of the site history, including whether sand vented onto the Inner Mound surface. Regardless, the paleoseismic and historical seismic record indicate that the Evansville area has experienced moderate to strong shaking in the past. Large mid-Holocene sand/gravel dikes and at least one Holocene fault, likely associated with the Wabash Valley Seismic Zone, occur within ~20 to 40 km of the site and demonstrate that large-scale Holocene seismicity is common in the area. Seismicity at Mound F likely affected the occupation and mound construction at Angel Mounds and may have contributed to the post-AD 1450 site abandonment.

Other liquefaction features at Angel Mounds

Was liquefaction widespread at the Angel site? Possibly. We know that outwash and channel/bar sands are ubiquitous 2 to 3 m below the fine-grained floodplain deposits, so we would expect widespread liquefaction from a major earthquake. However, the site was heavily modified by natives and then cultivated by European settlers well into the 20th century, so if sand vented onto the surface, it is no longer visible. But there are other indications of liquefaction at the site. An excavation of a potter's house in the East Village revealed a cultural feature that was displaced downward, possibly by densification of the underlying sand (Fig. 7.2.5). An electrical resistivity profile over the East Village shows features beneath the potter's house that appear to be sand injections (Fig. 7.2.5), supporting our interpretation. An ER profile over Mound G (Fig. 6.1.5) and a GPR profile (Noggin Plus with 250 MHz antennae) over the platform south of Mound A (Fig. 7.2.6) both identified features that could be sand dikes.

7.3 Mound C: Integrating Occupational History and Demography of Angel Mounds into a Regional Framework

Data from the small mounds, Mounds C and H

We used similar methods and procedures to investigate Mound C as used in the upper and lower platforms of Mound A. Using a gradiometer, four 30-x-30-m grids were surveyed, the centers of which were

Insert photo on left (view north) show a downward displaced cultural horizon exposed in an excavation of a Potters house, presumably by densification or liquefaction of the underlying sand. Arrow points to approximate location of photo on the resistivity profile. Note red knife for scale.

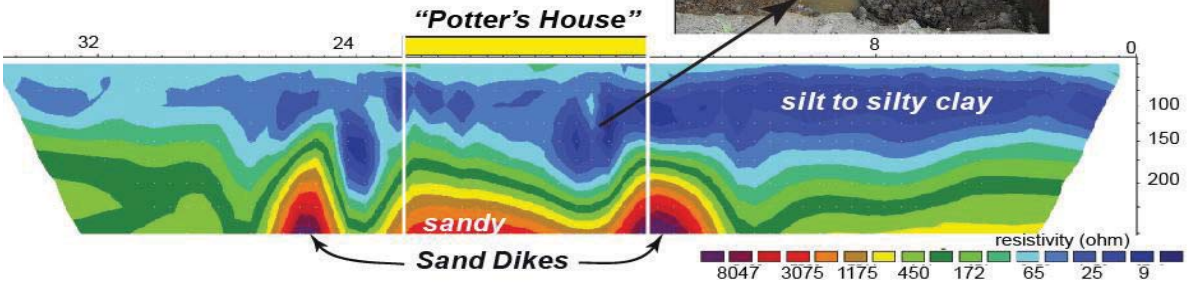

Figure 7.2.5 Electrical resistivity profile through the East Village and near the Potter' s house (unit A) shows upwardly displaced sand in several areas, including the region below the cultural horizon displaced in Fig. 5. Data acquired with a Syscal Pro Resistivity Profiler using 72 electrodes spaced 50 cm apart. Note: OSL date of 10 ka was derived from this locale within the basal sand/gravel deposits.

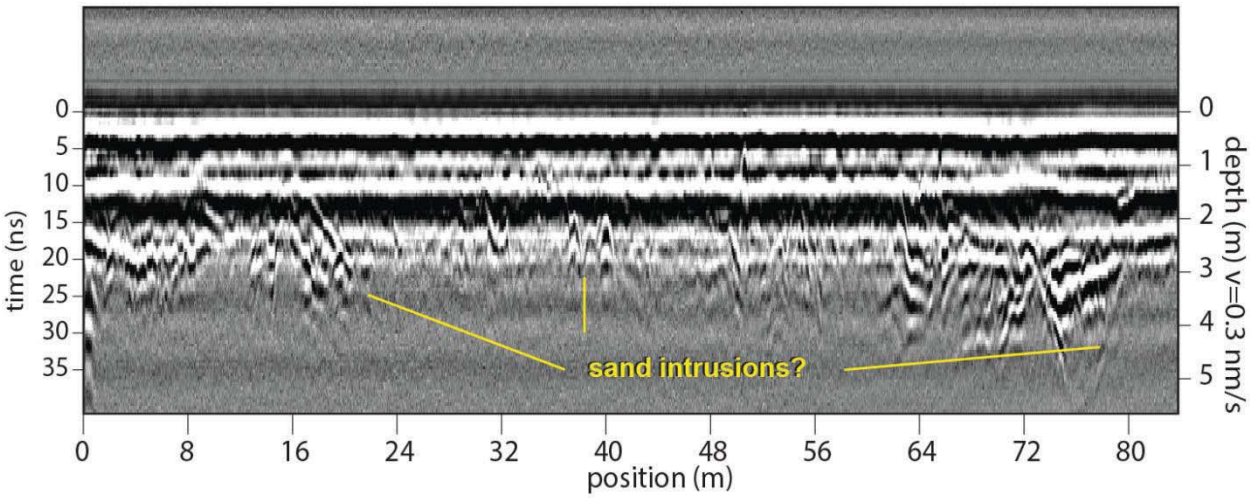

Figure 7.2.6. GPR profile across the low platform on the southern side of Mound A. Disturbed radar reflectors are too deep to be horizons that were disturbed by natives. Data acquired using a Sensors and Software Noggin Plus GPR unit with a 250 MHz antennae. GPR transect location shown as the red line in attached airphoto)

placed on the topographic apex or centers of the mounds, but which were aligned so they best fit the shapes of the mounds (Fig. 7.3.1). Gradiometer data was collected on 50-cm transects with a sampling interval of 12.5 cm along transects (sample density of 12.5 x 50 cm). Raw survey imagery was processed in the Terra-Surveyor software package using standard processing algorithms including destriping, despiking, destaggering, spatial interpolation, and spectral clipping to correct for operator error and clarify magnetic anom-

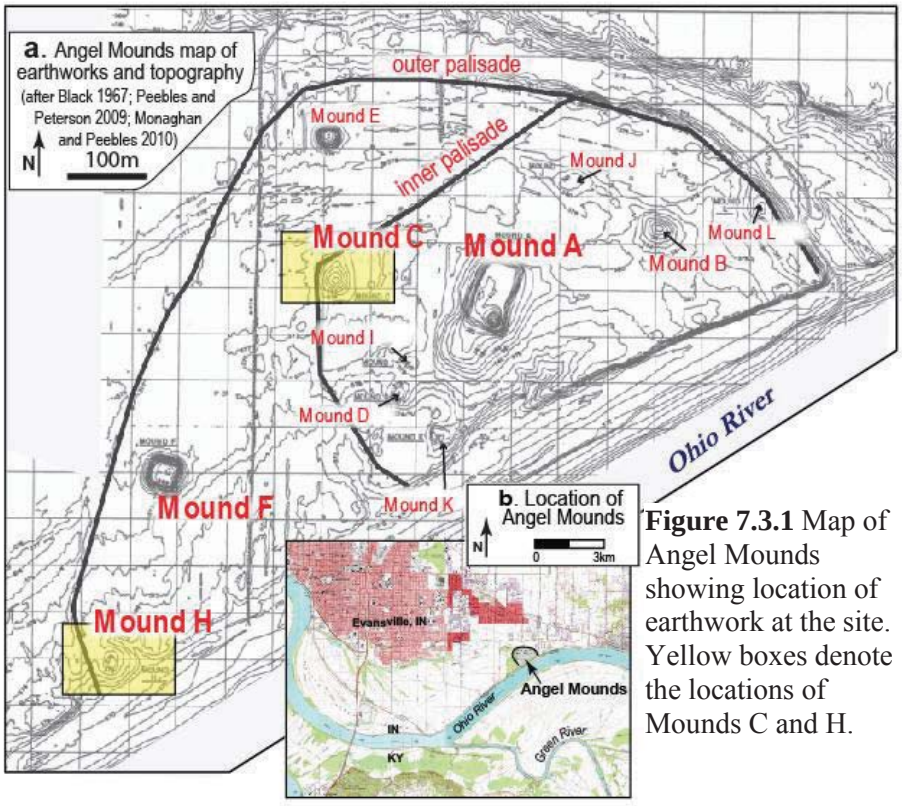

Figure 7.3.1 Map of Angel Mounds showing location of earthwork at the site. Yellow boxes denote the locations of Mounds C and H.

alies related to the mounds. Continuous solid-earth cores were collected with a Geoprobe (TR54) using a dual-tube sampler. On Mound C, cores were collected every 5 m along NW-SE (C and H) and E-W and N-S transects. Cores were placed to best sample anomalies from the gradiometer survey and provide a cross section of the subsurface in the mound (Fig. 7.3.2). Cores were opened in the laboratory and descriptions included color, texture, consistency and inclusion. Particular attention was paid to changes in fill types and possible mound surfaces.

Gradiometer surveys of Mounds C and H

The gradiometer image of Mound C (Fig. 7.3.3) is very clean with a high density of linear and rectilinear anomalies. The origin of some anomalies were readily apparent, including the NE-SW trace of the Inner Palisade and associated bastion. A rectilinear anomaly NW of Mound C is consistent with a Mississippian wall trench building. A large rectilinear anomaly (~10 x 20 m) under Mound C may represent a large, submound structure. The interpretation of the other palimpsest of linear anomalies is less straightforward. Their general shape and extent suggest a preliminary estimate for the original boundary of the mound, and many of the parallel lineations may be a result of successive episodes of post-abandonment (historic) mound erosion. More

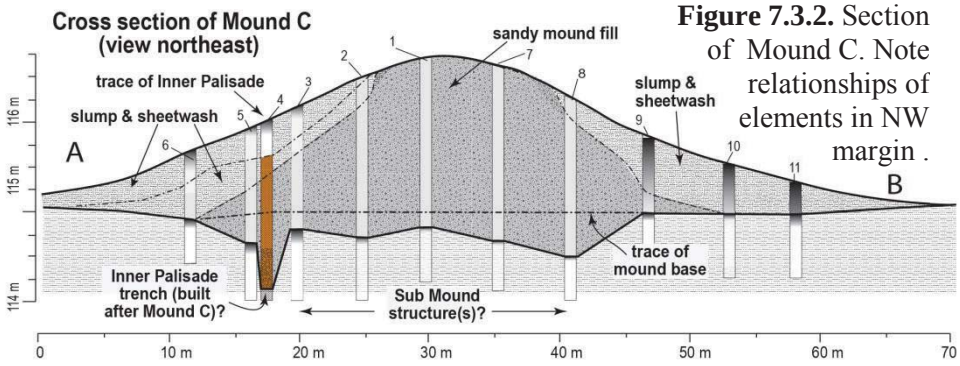

Figure 7.3.2. Section of Mound C. Note relationships of elements in NW margin .

defined lineations along the east edge of the mound may represent additional submound structures or features.

The Mound H image shows a complex pattern of magnetic anomalies within a discrete area. On the N and E sides of Mound H these anomalies likely are the mound edge (Fig. 7.3.4). The magnetic-high bands in the NE probably correspond with organic and fine-grained debris within an erosional channel. Because this area is topographically so low, the diffuse boundary between magnetically active and quieter areas S and W of the mound may reflect erosion and/or deposits related to Ohio River floods.

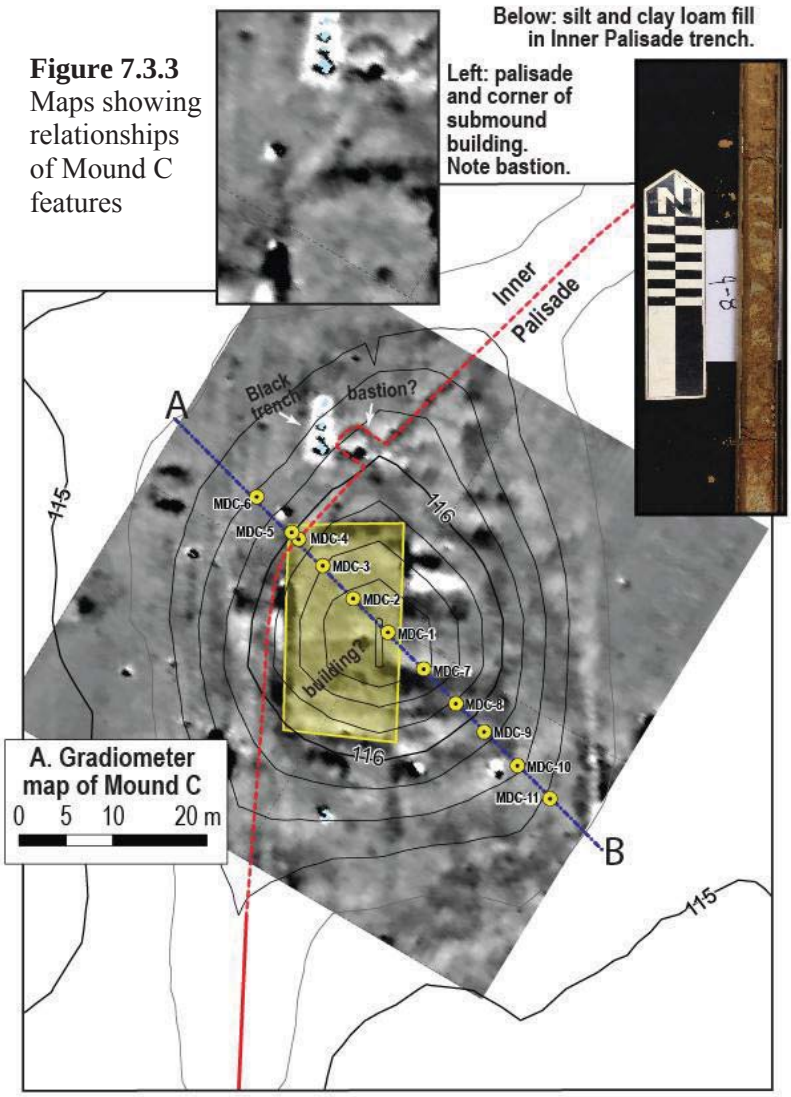

Figure 7.3.3 Maps showing relationships of Mound C features

Coring and cross sections of Mound C and H

A NW-SE transect of 11 cores was collected at ~5-m spacing at Mound C (Fig. 7.3.2). These cores consisted mainly of sandy loam and minor loamy sand deposits grouped into ~10- to 20-cm-thick fill (basket load?). The base of the cores was marked by a sharp contact with silt to clay loam, the top of which sometimes was marked by an Ab soil horizon. The trace of the large public building in the gradiometer image was noted by, at the base of the mound, a rough surface with minor dark (10YR3/3-3/4) disturbed Ab horizons. No mound-use surfaces or other depositional hiatus were noted within the mound fill sequence, which suggests rapid construction. The inner palisade trench cuts through Mound C fill and (apparently) a submound building.

A NW-SE cross section of Mound H was created but is based on two cores consisting of silt loam and minor sandy and clay loam (Fig. 7.3.5). This forms 10- to 20-cm-thick fills (basket load?) and extend 1 to 1.5 m deep. The base of cores graded into silt to clay loam, the top of which was marked by an Ab soil horizon that included charcoal. Above and grading into the Ab horizon is another dark (10YR3/2) Ab-like horizon that marks basal mound deposits and may represent the floor of a large public structure similar to those found in Mounds F and C. This horizon included charcoal, a piece of which dated to 875 ± 15 BP (2-σ cal AD 1154–1216 [94%]).

Chronology and significance

The relationships of features noted above suggest that Mound C (and H?) was constructed upon a large (public?) building, suggesting the public space probably predates the actual construction of mounds (Fig. 7.3.6). The inner palisade, whose construction was ~AD 1400 (Krus, 2012), was built into Mound C, which suggests that Mound C and the submound building were built before AD 1400, but their maximum

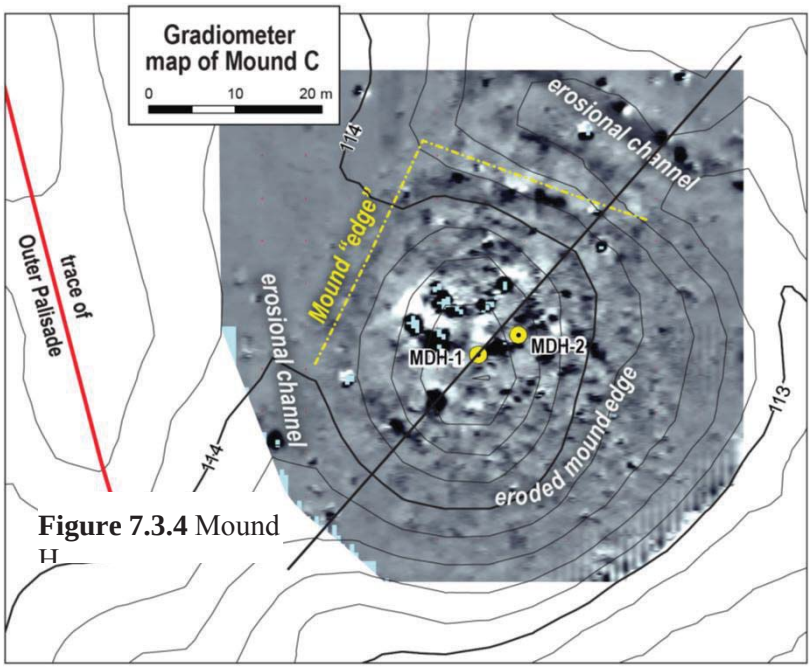

Figure 7.3.4 Mound H

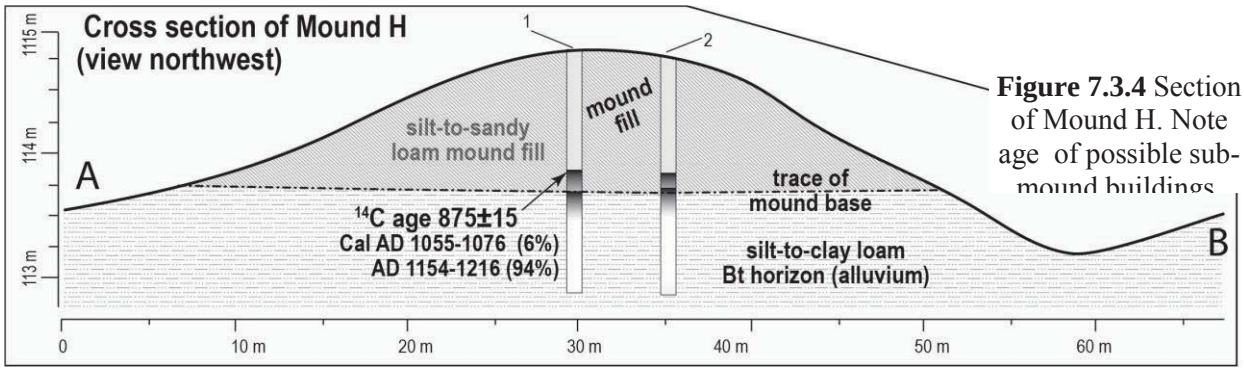

Figure 7.3.4 Section of Mound H. Note age of possible sub-mound buildings

ages are unknown. The radiocarbon age at the base of Mound H indicates that it was constructed soon after AD 1150–1200, which is more in line with AD 1100 age for the upper platform at Mound A and probably significantly earlier than Mound C. The different fill characteristics sandy Mound C and silty-clayey Mound H may related the different ages for their construction. Sandy fills may have been used late to build mound after AD 1200–1300 or to cap them after AD 1400.

Population and demography trends in eastern North America: a perspective from Angel Mounds

Population estimates in North America just prior to European contact range from 1.6 to >15 million. They are typically based on backward projections of village counts from European explorers, site distributions, or theoretical models of population density and environmental carrying capacities. Based mainly on historical records and compilations, Ubelaker (2006) suggested that ~2.5 million people lived across North America at AD 1500. Milner and Chapman (2012) used spatial statistics of archaeological sites and estimated that eastern North America had about 1.6 million inhabitants when Europeans arrived ca. AD 1500.

An order of magnitude difference in population estimates of North America indicates that some data or assumptions are better than others, but which are best is unclear. Prehistoric population estimates, similarly difficult to quantify and variable varied through time, were probably significantly greater than estimated at AD 1500. Cobb and Butler (1993) and Williams et al. (1994) suggested that Mississippian

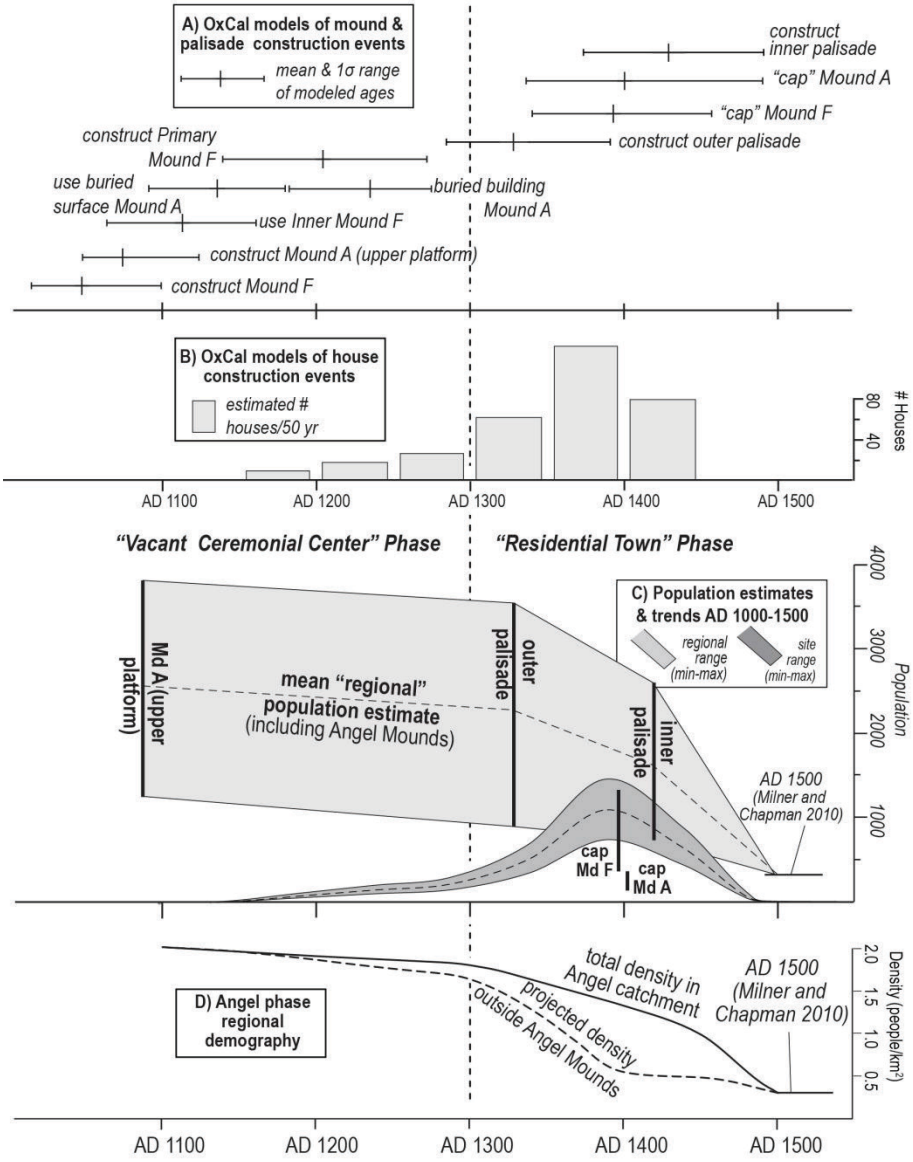

Figure 7.3.5 Population estimates and demographic trends for Angel Mound and surrounding area (ca 25km radis) s based on construction energetics and the chronology of structures at the site.

population was much larger ca. AD 1200 but collapsed throughout the lower Ohio valley before AD 1500. These data imply that region was more densely populated than the <0.3 people/km^2 projected by Milner and Chapman (2010). Although population collapse can be seen in the archaeological record, it can seldom be tracked on a fine scale. Site data is rarely sufficiently complete or chronologically discriminating enough to measure population dynamics on a finer than multiple century-scale.

Summary of the chronology of mounds, palisades, and structures

Research suggests that Angel Mounds was established prior to AD 1100, grew in prominence, and was abandoned by AD 1450. The site has been investigated since 1937, including extensive excavations of earthworks, habitation areas, and sitewide geophysical surveys and core sampling. As a result of this com-

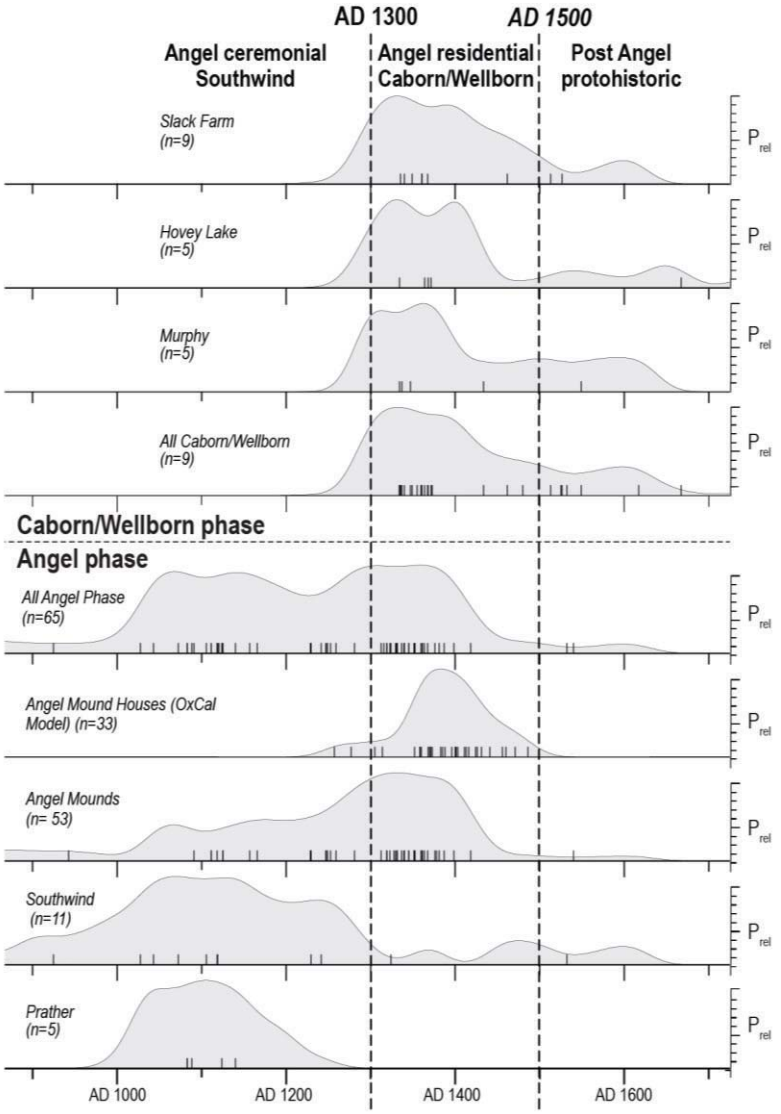

Figure 7.3.6 Probability Density Distribution of ^{14}C ages from Caborn- Welborn and Mississippian sites in the lower Ohio valley showing shifting demographic trends and probable depopulation near the mouth of the Wabash River.

bined research: 1) the locations of most building and the traces of most palisade walls have been mapped, 2) the internal structure and construction sequences of Mounds A and F are known, and 3) the stratigraphy and order of houses construction and palisade walls are constrained by several large block excavations, and their crosscutting or stratigraphic interrelationships, have been identified and placed within Bayesian framework and modeled through OxCal. The chronology of Angel Mounds is well controlled by more than 70 radiocarbon ages from key cultural contexts (Fig. 7.3.6).

Earlier research suggests that mound building began before AD 1100 when Mounds A and F built (Monaghan and Peebles, 2010; Monaghan et al., 2013). New ages based on very good contexts from Mounds A and F were obtained as part of the NSF-REU in 2013 and indicate that previous chronologies may need some revision, although the major outline is still valid.

The construction of Mound A at ~AD 1100 is consistent with the new data, the age of a submound

Table 1: Regional population estimate within 20 km of Angel Mounds based on mound construction.

Mound[1] stage (age constructed)	*stage volume (m^3)*	*m^3/day/ worker[7]*	*total worker days[8]*	*population estimate from support ratio (people/km^2) 2:1*	*4:1*
Md A[2] (AD 1080)	48,341	1.5	32,227	**1,209 (0.92)**	2,014 (1.53)
		0.79	61,191	2,295 (1.75)	**3,824 (2.91)**
Md F[3] (AD 1070)	144	1.5	96	**7 (0.01)**	12 (0.01)
		0.79	182	14 (0.01)	**23 (0.02)**
Md F[4] (AD 1250)	1,367	1.5	911	**68 (0.05)**	114 (0.09)
		0.79	1,730	130 (0.10)	**216 (0.16)**
Md F[5] (AD 1400)	8,524	1.5	5,683	**426 (0.32)**	710 (0.54)
		0.79	10,790	809 (0.62)	**1,349 (1.03)**
Md A[6] (AD 1400)	2,034	1.5	1,356	**102 (0.08)**	170 (0.13)
		0.79	2,575	193 (0.15)	**322 (0.25)**

[1]upper platform, 2 yrs to construct; [2]inner mound, 1 yr to construct; [3]primary mound, 1 yr to construct ; [4]secondary mound ("final cap"),1 yr to construct ; [5]"final cap", 1 yr to construct ; [6]1.5 m^3/day assumes a 5 hr work day and quarry 100 m from mound, 0.79 m^3/day assumes a 5 hr work day and quarry 200 m from mound (after Erasmus 1965); [7]workers contributed 40 days/year.

Table 2: Regional population estimate within 20 km of Angel Mounds based on palisade construction.

palisade segment (age constructed)	*# posts/ (length)*	*total worker days[5]*	*days to construct segment*	*population based on support ratio (people/km^2) 2:1*	*4:1*
Outer palisade[1] AD 1300	8600[3] (2100 m)	18000	30	1,800 (2.4)	**3,600 (4.9)**
			60	**900 (1.2)**	1,800 (2.4)
Inner palisade[2] AD 1400	6200[3] (1500 m)	13200	30	1,300 (1.8)	**2,600 (3.5)**
			60	**700 (0.9)**	1,300 (1.8)

1) maximum length of outer palisade wall; includes bastions; 2) maximum length of inner palisade --assumes rebuild of outer palisade on east side of site, includes bastions. 3) 5 post/m (Milner1998; 5) assumes 8 hour work day, includes post cutting and transporting; after Milner (1998)and Krus 2011).

Table 3: Resident population estimate at Angel Mounds based on house ages and sizes.

Age	*calculated houses[1]*	*mean m^2 of living area[2]*	*minimum population[3]*	*minimum population[3]*
1100-1150	0	0	0	0
1150-1200	6	240	42	60
1200-1250	12	480	84	120
1250-1300	18	703	123	176
1300-1350	26	1054	184	264
1350-1400	97	3865	676	966
1400-1450	105	4216	738	1054
1450-1500	61	2459	430	615
1500-1550	0	0	0	0

[1]estimated from distribution of 14C ages for structure (Figure 2), based on total number of 325 structures at Angel Mounds; [2]based on average size of 40±13 m^2 per structure (after Black 1967; Peebles and Peterson 2009; Peterson 2010)

building from Mound F and new ages for the Inner Mound F surface, indicate that Mound F was actually constructed after AD 1200. The new ages for Mound A, lower platform, are also consistent with previous work on the upper platform that showed it was constructed ~AD 1100, probably in one episode. A building was built and used on the upper platform ~AD 1200–1400. A series of radiocarbon ages from the lower platform indicate that it was built ~AD 1200–1250, with a few episodes of rebuilding/repair, until ~AD 1400. A lag between the upper and lower platform construction is suggested by major slumping and sheet-wash erosion; lower platform fills are built directly on these slumps and not on upper platform fills.

Fine-scale population changes can be tracked at archaeological sites by carefully sampling the constructed elements of the human landscape, determining their absolute age and crosscutting or stratigraphic

relationships, and then temporally interrelating them by statistically modeling those relationships. When rank ordering and interrelationships of features and their radiocarbon ages across the site are modeled within a Bayesian framework, the age uncertainty of events can be greatly reduced. The detailed chronology of a major constructional event at Angel Mounds can serve as surrogates that trace regional and local trends in populations from AD 1000–1500 in the lower Ohio valley, at least near its junction with the Wabash River (Fig. 7.3.5).

More than 60 radiocarbon ages from key cultural contexts and their crosscutting or stratigraphic interrelationships have been identified and placed within a Bayesian framework to model using OxCal software. The well-controlled chronology and developmental history for Angel Mounds derived from these data show that the site actually went through two different developmental phases. The first occurred AD 1070–1250 and was an unfortified ceremonial center focused around Mounds A, E, and F with few permanent residents. The second was a fortified village whose palisades and most structures were built after AD 1250–1300. Regional (e.g., within the catchment of the site) populations were estimated based on energetics and person-hours needed to construct these earthworks and palisades. Local (e.g., resident at the site) population was estimated based on the typical number of people living in an average-sized house at the site (Tables 1, 2, 3).

The number of people required to construct the outer Palisade and parts of Mound A and F erected before AD 1200 probably mainly reflects regional participates in the Angel Mounds ceremonial community (e.g., 1- to 2-day walk to site; 15–20 km radius). This population was estimated from earthwork and palisade construction energetics, which requires assumptions about how long it took to build, the labor require to obtain material (posts, fill/daub material, etc.), amount of labor that individual workers contributed, and ratio of support persons to workers (Tables 1, 2), and were based on experimental and ethnographic data. The resident population living at Angel Mounds was based on OxCal chronological models of dated houses, which were grouped by their frequency through time and based on estimates of how long structures probably lasted. Resident population was estimated by distributing the total number of houses at the site (determined by excavation and geophysical survey) through time, based on the frequency distribution of dated houses. Population was estimated by assuming the number of square meters required per person and the average size of houses (Table 3).

What Angel Mounds demography may tell us about regional population and settlement

1) From AD 1100–1300, few people lived at Angel Mounds. Most within a 20 km^2 radius lived in small hamlets or farmsteads and used Angel Mounds as a ceremonial center (Fig. 7.3.5).

2) The regional population (20 km radius from Angel) before AD 1300 was considerably greater than after AD 1500 and generally stable. Our estimates indicate that mean populations were 2,500 (~3.5 people/km^2) at AD 1100, and 1,800 (~2.4 people/km^2) at AD 1300 (Fig. 7.3.5).

3) Milner and Chapman's (2010) estimate of <0.3 people/km^2 indicates a regional population of ~375 people at AD 1500. This represents at least a 500 percent decline of the regional population within 200 years, which means that population declined by half each generation.

4) The residential population at Angel Mounds greatly increased after AD 1300 to a maximum of ~1,050 people by AD 1400. Angel Mounds essentially was abandoned by AD 1500 (Fig. 7.3.5).

5) The coincidence of Palisade construction at AD 1300 and increased residential population at Angel Mounds suggests that the regional population increasingly moved to the site permanently between AD 1300–1400. The reason for this is most likely related to growing regional violence after AD 1300.

6) The residential population at Angel Mounds peaked at ~AD 1400 and coincided with the inner palisade construction, which suggests a need for a more dense population within a more defensible town (Fig. 7.3.5).

7) Mounds A and F were capped and essentially abandoned soon after AD 1400, which may reflect the sociopolitical disintegration of Angel Mounds as a ceremonially important place.

8) Probability density distributions of Angel site that show all radiocarbon ages at the site compare well with the results of OxCal chronology models of houses, suggesting that the numbers of radiocarbon dates roughly corresponds with site use intensity (Fig. 7.3.6).

9) Probability density distributions of Angel Mounds and the Southwind site, which has no mounds, show opposite trends, suggesting either that Southwind was abandoned when regional warfare peaked or that its population moved to Angel Mounds (or other unidentified villages) after AD 1300. Estimates of palisade construction at Southwind correspond approximately with the initial Angel Mounds palisade, but not with the last episode of palisade construction.

10) Probability density distributions of Caborn-Welborn sites peak AD 1300–1400 and greatly decline before AD 1500, which generally corresponds to the Angel residential phase (Fig. 7.3.66). These relationships suggest that:

    10) Caborn-Welborn sites are part of the same demographic trends as Angel: population concentration into fortified town because of regional violence, or,

    10) other Mississippian people may have also migrated into the region.

    10) These others likely contributed to the population and environmental stresses that were the root causes of regional conflict in the lower Ohio Valley.

11) Probability density distribution data suggest that greater attention should be paid to the meaning, utility, or even reality of archaeological cultures. Analyzing sites by their ecology, developmental history, and regional chronological relationships may be a more productive way to understanding a region and associated changes in socioeconomic and political systems.

12) Depending on agricultural production (field or garden beds), these demographic patterns have important implications for sustainable production and cultural ecology of land use.

References Cited

Aitken, M. J., 1985, Thermoluminescence dating: New York, Academic Press, 359 p.

Alexander, C. S., 1974, Some observations on the late Pleistocene and Holocene history of the Lower Ohio Valley: University of Illinois, Occasional Publications of the Department of Geography, no. 7.

Alexander, C. S., and Nelson, R. N., 1972, Channel stability on the Lower Ohio River: Annals of the Association of American Geographers, v. 62, no. 3, p. 411-417.

Alexander, C. S., and Prior, J. C., 1971, Holocene sedimentation rates in overbank deposits in the Black Bottom of the lower Ohio River, southern Illinois: American Journal of Science, v. 270, no. 5, p. 361-372.

Black, G. A., 1967, The Angel Site–an historical, archaeological and ethological study (two vols.): Indianapolis, Indiana Historical Society.

Blum, M. D., 2008, Large river systems and climate change, *in* Gupta, A., ed., Large rivers–geomorphology and management: Chichester, UK, John Wiley & Sons, Ltd., p. 627-659.

Bodziak, R. M., 1999, High resolution seismic reflection and ground penetrating radar studies across the Maunie Fault in the Wabash Valley Seismic Zone: M.S. thesis, 175 p.

Booth, R. K., Jackson, S. T., Forman, S. L., Kutzbach, J. E., Bettis, E. A., Kreigs, J., and Wright, D. K., 2005, A severe centennial-scale drought in midcontinental North America 4200 years ago and apparent global linkages: The Holocene, v. 15, no. 3, p. 321-328.

Bronk Ramsey, C., 1995, Radiocarbon calibration and analysis of stratigraphy–the OxCal program: Radiocarbon, v. 37, no. 2, p. 425-430.

Bronk Ramsey, C., 2008, Deposition models for chronological records: Quaternary Science Reviews, v. 27, no. 1–2, p. 42-60.

Buikstra, J. E, Charles, D. K., and Rakita, G., 1998, Staging ritual–Hopewell ceremonialism at the Mound house site, Greene County, Illinois: Kampsville, Ill., Center for American Archeology, Kampsville Studies in Archeology and History 1.

Bull, W. B., 1991, Geomorphic responses to climatic change: New York, Oxford University Press, 326 p.

Bush, L. L. (n.d.), Report on file at the Glenn A. Black Laboratory for Archaeology, Indiana University (received 2007).

Clark, P. U., Clague, J. J., Curry, B. B., Dreimanis, A., Hicock, S. R., Miller, G. H., Berger, G. W., Eyles, N., Lamothe, M., Miller, B. B., Mott, R. J., Oldale, R. N., Stea, R. R., Szabo, J. P., Thorleifson, L. H., and Vincent, J. S., 1993, Initiation and development of the Laurentide and Cordilleran Ice Sheets following the last interglaciation: Quaternary Science Reviews, v. 12, no. 2, p. 79-114.

Clay, R. B., 1997, The Mississippian Succession on the Lower Ohio: Southeastern Archaeology, v/ 16, p. 16-32.

Cobb, C. R., and Butler, B. M., 2002, The vacant quarter revisited–Late Mississippian abandonment of the Lower Ohio Valley: American Antiquity, v. 67, p. 625-641.

Counts, R. C., 2008, Luminescence and radiocarbon chronology of loess-paleosol sequences in the lower Ohio River valley, *in* Proceedings of the Geological Society of America, Abstracts with Programs, v. 40, p. 3.

Crittenden, M. D., and Hose, R. K., 1965, Geology of the Rome quadrangle in Kentucky: U.S. Geological Survey Geologic Quadrangle Map GQ 362.

Dalan, R. A., Holley, G. R., Woods, W. I., Watters, H. W., Jr., and Koepke, J. A., 2003, Envisioning Cahokia–a landscape perspective: DeKalb, Northern Illinois University Press, p. 241.

Dean, W. E., Ahlbrandt, T. S., Anderson, R. Y., and Platt Bradbury, J., 1996, Regional aridity in North America during the middle Holocene: The Holocene, v. 6, no. 2, p. 145-155.

Dorale, J. A., Edwards, R. L., Ito, E., and González, L. A., 1998, Climate and vegetation history of the midcontinent from 75 to 25 ka–a speleothem record from Crevice Cave, Missouri, USA: Science, v. 282, no. 5395, p. 1,871-1,874.

Driese, S. G., Li, Z.-H., and Horn, S. P., 2005, Late Pleistocene and Holocene climate and geomorphic histories as interpreted from a 23,000 14C yr B.P. paleosol and floodplain soils, southeastern West Virginia, USA: Quaternary Research, v. 63, no. 2, p. 136-149.

Driese, S. G., Li, Z.-H., and McKay, L. D., 2008, Evidence for multiple, episodic, mid-Holocene Hypsithermal recorded in two soil profiles along an alluvial floodplain catena, southeastern Tennessee, USA: Quaternary Research, v. 69, no. 2, p. 276-291.

Duller, G. A. T., 1996, Recent developments in luminescence dating of Quaternary sediments: Progress in Physical Geography, v. 20, no. 2, p. 127-145.

Evans, A., 2007, Engineering earthen monuments: Midwest Archaeological Conference 2007 Annual Meeting, October 4 –6, 2007, Notre Dame, Indiana University of Notre Dame,.

Fenneman, N. M., 1928, Physiographic divisions of the United States: Annals of the Association of American Geographers, v. 18, no. 4, p. 261-353.

Forman, S. L., Oglesby, R., and Webb, R. S., 2001, Temporal and spatial patterns of Holocene dune activity on the Great Plains of North America: megadroughts and climate links: Global and Planetary Change, v. 29, no. 1–2, p. 1-29.

Foster, D. R., Oswald, W. W., Faison, E. K., Doughty, E. D., and Hansen, B. C. S., 2006, A climatic driver for abrupt mid-Holocene vegetation dynamics and the Hemlock decline in New England: Ecology, v. 87, no. 12, p. 2,959-2,966.

Fowler, M. L., 1989, The Cahokia atlas–a historical atlas of Cahokia archaeology: Springfield, Illinois, Illinois Historic Preservation Agency, Studies in Illinois Archaeology 6.

Fraser, G. S., 1986, Origin of mid-channel Islands in the Ohio River near Evansville, Indiana: Indiana Geological Survey Special Report 38, 15 p.

Fraser, G. S., 1994, Sequences and sequence boundaries in glacial sluiceways beyond glacial margins, *in* Dalrymple R. W., Boyd, R., and Zaitlin B. A., eds., Incised-valley systems; origin and sedimentary sequences: Society for Sedimentary Geology Special Publication 57, p. 337-351.

Fraser, G. S., and Fishbaugh, D. A., 1986, Alluviation of the Ohio River Valley near Evansville, Indiana and its effect on the distribution of sand and gravel in the area: Indiana Geological Survey Special Report 36, 26 p.

Frye, J. C., Leonard, A., Willman, H., and Glass, H., 1972, Geology and paleontology of Late Pleistocene Lake Saline, southeastern Illinois: Illinois State Geological Survey Circular 471, 44 p.

Fuller, M. L., and Ashley, G. H., 1902, Description of the Ditney quadrangle, Indiana: U.S. Geological Survey Geologic Atlas, Folio 84, 8 p.

Fuller, M. L., and Clapp, F. G., 1904, Description of the Patoka quadrangle: U.S. Geological Survey Geologic Atlas, Folio 105, 12 p.

Gibbons, A. B., 1972, Geologic map of parts of the Burlington and Addyston quadrangles, Boone County, Kentucky: U.S. Geological Survey Geologic Quadrangle Map 1025, scale 1:24,000.

Granger, D. E., Fabel, D., and Palmer, A. N., 2001, Pliocene-Pleistocene incision of the Green River, Kentucky, determined from radioactive decay of cosmogenic (super 26) Al and (super 10) Be in Mammoth Cave sediments: Geological Society of America Bulletin, v. 113, no. 7, p. 825-836.

Green, T. J., and Munson, C. A., 1978, Mississippian settlement patterns in southwestern Indiana, *in* Smith, B. D., ed., Mississippian settlement patterns: New York, Academic Press, p. 293-330.

Grover, N. C., ed., 1938, Floods of Ohio and Mississippi rivers, January-February 1937; with a section on flood deposits of the Ohio River January-February 1937 by G. R. Mansfield: U.S. Geological Survey Water Supply Paper 838, 746 p.

Grün, R., 1991, Age calculation software for Riso Laboratories.

Hayward, R. K., and Lowell, T. V., 1993, Variations in loess accumulation rates in the mid-continent, United States, as reflected by magnetic susceptibility: Geology, v. 21, no. 9, p. 821-824.

Hilgeman, S. L., 2000, Pottery and chronology at Angel: Tuscaloosa, University of Alabama Press.

Hughen, K. A., and others, 2004, Marine04 Marine radiocarbon age calibration, 0-26 ka BP: Radiocarbon, v. 46, p. 1,059-1,086.

Jackson, S. T., Overpeck, J. T., Webb, T., III, Keattch, S. E., and Anderson, K. H., 1997, Mapped plant-macrofossil and pollen records of late quaternary vegetation change in Eastern North America: Quaternary Science Reviews, v. 16, no. 1, p. 1-70.

Jackson, S. T., Webb, R. S., Anderson, K. H., Overpeck, J. T., Webb, T., III, Williams, J. W., and Hansen, B. C. S., 2000, Vegetation and environment in Eastern North America during the Last Glacial Maximum: Quaternary Science Reviews, v. 19, no. 6, p. 489-508.

Jain, M., and Singhvi, A. K., 2001, Limits to depletion of blue-green light stimulated luminescence in feldspars–implications for quartz dating: Radiation Measurements, v. 33, no. 6, p. 883-892.

Johnson, and Schwalb, 2010, Geology and structure of the Rough Creek area, western Kentucky, Kentucky Geological Survey Bulletin 1, University of Kentucy.

Johnson, G. H., 1965, The stratigraphy, paleontology, and paleoecology of the Peoria loess (Upper Pleistocene) of southwestern Indiana: Indiana University, Department of Geosciences, Ph.D. thesis.

Johnson, W. D., 1973, Geologic map of part of the Wilson quadrangle, Henderson County, Kentucky: U.S. Geological Survey Geologic Quadrangle Map GQ-1136, scale 1:24,000.

Johnson, W. D., and Norris, R. L., 1974, Geologic map of the Smith Mills quadrangle, Henderson and Union counties, Kentucky: U.S. Geological Survey Open-File Report 74-245.

Johnson, W. D., 1973, Geologic map of part of the Henderson quadrangle, Henderson County, Kentucky: U.S. Geological Survey Geologic Quadrangle Map GQ-1074, scale 1:24,000.

Kepferle, R. C., 1974, Geologic map of parts of the Louisville West and Lanesville quadrangles, Jefferson County, Kentucky: U.S. Geological Survey Open-File Report 74-18.

Kottek, M., Grieser, J., Beck, C., Rudolf, B., and Rubel, F., 2006, World map of the Koppen-Geiger climate classification updated: Meteorologische Zeitschrift, v. 15, no. 3, p. 259-263.

Kvale, E., and Archer, A., 2007, Paleovalley fills–trunk vs. tributary: AAPG Bulletin, v. 91, no. 6, p. 809.

Leidy, J., 1856, Notice of some fossil bones discovered by Mr. Francis A. Lincke, in the banks of the Ohio River, Indiana: Proceedings of the Academy of Natural sciences of Philadelphia, Filadélfia, v. 7, p. 199-201.

Leopold, L. B., Wolman, M. G., and Miller, J. P., 1964, Fluvial processes in Geomorphology: San Francisco and London, W. H. Freeman and Company, 535 p.

Leverett, F., 1902, Glacial formations and drainage features of the Erie and Ohio basins: U.S. Geological Survey Monograph 41, 801 p.

Lowell, T. V., Savage, K. M., Scott Brockman, C., and Stuckenrath, R., 1990, Radiocarbon analyses from Cincinnati, Ohio, and their implications for glacial stratigraphic interpretations: Quaternary Research, v. 34, no. 1, p. 1-11.

Luft, S. J., 1971, Geologic map of part of the Covington quadrangle, Northern Kentucky: U.S. Geological Survey Geologic Quadrangle Map GQ 955, scale 1:24,000.

Maddy, D., Bridgland, D. R., and Green, C. P., 2000, Crustal uplift in southern England–evidence from the river terrace records: Geomorphology, v. 33, no. 3–4, p. 167-181.

Maddy, D., Bridgland, D., and Westaway, R., 2001, Uplift-driven valley incision and climate-controlled river terrace development in the Thames Valley, UK: Quaternary International, v. 79, no. 1, p. 23-36.

Markewich, H. W., Wysocki, D. A., Pavich, M. J., Rutledge, E. M., Millard, H. T., Rich, F. J., Maat, P. B., Rubin, M., and McGeehin, J. P., 1998, Paleopedology plus TL, ^{10}Be, and ^{14}C dating as tools in stratigraphic and paleoclimatic investigations, Mississippi River Valley, U.S.A: Quaternary International, v. 51-52, p. 143-167.

Maxwell, B. W., and Devaul, R. W., 1962, Reconnaissance of ground-water resources in the Western Coal Field region, Kentucky: U.S. Geological Survey Water Supply Paper 1599, 34 p.

Mayewski, P. A., Rohling, E. E., Curt Stager, J., Karlén, W., Maasch, K. A., David Meeker, L., Meyerson, E. A., Gasse, F., van Kreveld, S., Holmgren, K., Lee-Thorp, J., Rosqvist, G., Rack, F., Staubwasser, M., Schneider, R. R., and Steig, E. J., 2004, Holocene climate variability: Quaternary Research, v. 62, no. 3, p. 243-255.

McDowell, R. C., ed., 1986, The geology of Kentucky–a text to accompany the geologic map of Kentucky: U.S. Geological Survey Professional Paper 1151-H, 76 p.

Melhorn, W. N., and Kempton, J. P., 1991, Geology and hydrogeology of the Teays-Mahomet bedrock valley systems: Geological Society of America Special Paper 258, 128 p.

Miao, X., Mason, J. A., Johnson, W. C., and Wang, H., 2007, High-resolution proxy record of Holocene climate from a loess section in Southwestern Nebraska, USA: Palaeogeography, Palaeoclimatology, Palaeoecology, v. 245, no. 3-4, p. 368-381.

Milner, G. R., 1998, The Cahokia chiefdom–the archaeology of a Mississippian society: Washington, D.C., Smithsonian Institution Press.

Moore, D. W., Newell, W. L., Counts, R. C., Fraser, G. S., Fishbaugh, D. A., and Brandt, T. R., 2007, Surficial geologic map of the West Franklin quadrangle, Vanderburgh and Posey Counties, Indiana, and Henderson County, Kentucky: U.S. Geological Survey Scientific Investigations Map 2967, scale 1:24,000.

Moore, D. W., Lundstrom, S. C., Counts, R. C., Martin, S. L., Andrews, W., Newell, W. L., Murphy, M. L., Thompson, M. F., Taylor, E. M., and Kvale, E. P., 2009, Surficial Geologic Map of the Evansville, Indiana, and Henderson, Kentucky area: U.S. Geological Survey Scientific Investigations Map 3069, scale 1:50000.

Muller, J., 1986, Archaeology of the lower Ohio River Valley: Orlando, Florida, Academic Press.

Murray, A. S., and Wintle, A. G., 2000, Luminescence dating of quartz using an improved single-aliquot regenerative-dose protocol: Radiation Measurements, v. 32, no. 1, p. 57-73.

Nelson, J. W., 1991, Structural styles of the Illinois Basin, *in* Leighton, M. W., Kolata, D.R., Oltz, D. F., and Eidel, J. J, ed., Interior cratonic basins, v. 1: American Association of Petroleum Geologists Memoir 51, p. 209-243.

Nuttli, O. W., 1979, Seismicity of the central United States, *in* Hatheway, A. W., and McClure, C. R., Jr., eds., Geology in the siting of nuclear power plants: Geological Society of America Reviews in Engineering Geology, v. 14, p. 67-93.

Obermeier, S. F., Bleuer, N. R., Munson, C. A., Munson, P. J., Martin, W. S., McWilliams, K. M., Tabaczynski, D. A., Odum, J. K., Rubin, M., and Eggert, D. L., 1991, Evidence of strong earthquake shaking in the Lower Wabash Valley from prehistoric liquefaction features: Science, v. 251, no. 4997, p. 1,061-1,063.

Owen, D. D., 1861, Fourth report of the geological survey in Kentucky, made during the years 1858 and 1859: Frankfort, Kentucky, Yeoman Office.

Owen, D. D., 1859, Report of a geological reconnaissance of the State of Indiana, made in the year 1837 [-1838], in conformity to an order of the Legislature, Indianapolis: John C. Walker, state printer.

Pollack, D., 2004, Caborn-Welborn–constructing a new society after the Angel chiefdom collapse: Tuscaloosa, University of Alabama Press.

Porat, N., 2006, Use of magnetic separation for purifying quartz for luminescence dating: Ancient TL, v. 24, p. 33-36.

Prescott, J. R., and Hutton, J. T., 1994, Cosmic ray contributions to dose rates for luminescence and ESR dating–large depths and long-term time variations: Radiation Measurements, v. 23, p. 497-500.

Ray, L. L., 1957, Two significant new exposures of Pleistocene deposits along the Ohio River Valley in Kentucky: Journal of Geology, v. 65, no. 5, p. 542-545.

Ray, L. L., 1963, Quaternary events along the unglaciated lower Ohio River valley, *in* Geological Survey Research 1963: U. S. Geological Survey Professional Paper 475-B, p. B125-B128.

Ray, L. L., 1974, Geomorphology and Quaternary geology of the glaciated Ohio River valley–a reconnaissance study: U.S. Geological Survey Professional Paper 826, 77 p.

Ray, L. L., 1965, Geomorphology and Quaternary geology of the Owensboro Quadrangle, Indiana and Kentucky: U.S. Geological Survey Professional Paper 488, 72 p.

Redmond, B. G., 1990, The Yankeetown phase–emergent Mississippian cultural adaptation in the lower Ohio River Valley: Indiana University, Bloomington, Department of Anthropology, Ph.D. thesis.

Rice, C. L., 1979, The Mississippian and Pennsylvanian (Carboniferous) Systems in the United States, Kentucky–historical review and summary of areal, stratigraphic, structural, and economic geology of Mississippian and Pennsylvanian rocks in Kentucky: U.S. Geological Survey Professional Paper 1110-A-L.

Rodbell, D. T., Forman, S. L., Pierson, J., and Lynn, W. C., 1997, Stratigraphy and chronology of Mississippi Valley loess in western Tennessee: Geological Society of America Bulletin, v. 109, no. 9, p. 1,134-1,148.

Ruhe, R. V., and Olson, C. G., 1980, Clay-mineral indicators of glacial and nonglacial sources of Wisconsinan loesses in Southern Indiana, U.S.A: Geoderma, v. 24, no. 4, p. 283-297.

Ruhe, R. V., Hall, R. D., and Canepa, A. P., 1974, Sangamon paleosols of southwestern Indiana, U.S.A: Geoderma, v. 12, no. 3, p. 191-200.

Ruhe, R. V., and Olson, C. G., 1978, Loess stratigraphy and paleosols in southwest Indiana: Guidebook, 25th Field Conference, Midwest Friends of the Pleistocene, May 19–21, 1978.

Rutledge, F. A., 2004, High resolution geophysical investigation of late quaternary deformation in the lower Wabash valley fault system, M.S. Thesis, University of Kentucky, Lexington, KY.

Sambrook Smith, G. H., Ashworth, P. J., Best, J. L., Woodward, J., and Simpson, C. J., 2006, The sedimentology and alluvial architecture of the sandy braided South Saskatchewan River, Canada: Sedimentology, v. 53, no. 2, p. 413-434.

Schumm, S. A., 1977, The fluvial system: New York, Wiley, 338 p.

Schumm, S. A., Mosley, M., and Weaver, W., 1987, Experimental fluvial geomorphology: New York, Wiley, 413 p.

Shaw, E. W., 1915, On the origin of loess in southwestern Indiana: Science, v. 41, no. 1046, p. 104-108.

Shaw, E. W., 1911, Preliminary statement concerning a new system of Quaternary lakes in the Mississippi Basin: The Journal of Geology, v. 19, no. 6, p. 481-491.

Sherwood, S.A., 2006, The geoarchaeological study of Mound A, Shiloh Indian Mounds National Historic Landmark, Hardin County, Tennessee: Geological Society of

America Abstracts with Programs, v. 38, p. 391.

Smith, M., III, 2007, A geological and geophysical study of the Maunie fault: M.S. thesis, Southern Illinois University at Carbondale, 158 p.

Snyder, S. L., and Duval, J. S., 2003, Design and construction of a gamma-ray spectrometer system for determining natural radioelement concentrations in geological samples at the U.S. Geological Survey in Reston, Virginia: U.S. Geological Survey Open File Report 03-029.

Steig, E. J., 1999, Mid-Holocene climate change: Science, v. 286, no. 5444, p. 1,485-1,487.

Stokes, S., 1999, Luminescence dating applications in geomorphological research: Geomorphology, v. 29, no. 1–2, p. 153-171.

Straw, W. T., 1968, The upper alluvial terrace along the Ohio River Valley in south-central Indiana: Proceedings of the Indiana Academy of Science, v. 77, p. 231-235.

Stuiver, M., Reimer, P. J., Bard, E., Beck, J. W., Burr, C., Hughen, K. A., Kromer, B., McCormac, G., Plicht, J., and Spurk, M., 1998, ARTICLES-INTCAL98 Radiocarbon Age Calibration, 24,000-0 cal BP: Radiocarbon, v. 40, no. 3, p. 1,041-1,084.

Swadley, W. C., 1976, Geologic map of part of the Carrollton quadrangle, Carroll and Trimble counties, Kentucky: U.S. Geological Survey Geologic Quadrangle Map 1281, scale 1:24,000.

Swadley, W. C., 1969, Geologic map of parts of the Patriot and Florence quadrangles, north-central Kentucky: U.S. Geological Survey Geologic Quadrangle Map 846, scale 1:24,000.

Swadley, W. C., 1978, Tentative dating of pre-Pleistocene deposits along the Kentucky River of central Kentucky: U.S. Geological Survey Professional Paper .

Szabo, J. P., Angle, M. P., and Eddy, A. M., 2011, Pleistocene glaciation of Ohio, USA, *in* Jürgen Ehlers, P. L. G., and Philip, D. H., eds., Quaternary glaciations–extent and chronology, v. 15–A closer look: Amsterdam, The Netherlands, Elsevier, p. 513-520.

Talma, A. S., and Vogel, J. C., 1993, A simplified approach to calibrating C14 dates: Radiocarbon, v. 35, p. 317-322.

Tankersley, K. B., Munson, C. A., and Smith, D., 1987, Recognition of bituminous coal contaminants in radiocarbon samples: American Antiquity, v. 52, p. 318-330.

Tankersley, K.B., and Munson, C. A., 1992, Comments on the Meadowcroft Rockshelter radiocarbon chronology and the recognition of coal contaminants: American Antiquity, v. 57, p. 321-326.

Theis, C. V., 1929, Geology of Henderson County, Kentucky: Ph.D. dissertation, University of Cincinnati.

Van Nest, J., Charles, D. K., Buikstra, J. E., Asch, D. L., 2001, Sod blocks in Illinois Hopewell mounds: American Antiquity, v. 66, p. 633-650.

Walker, E. H., 1957, The deep channel and alluvial deposits of the Ohio Valley in Kentucky: U. S. Geological Survey Water-Supply Paper W1411, 25 p.

Wallinga, J., 2002, Optically stimulated luminescence dating of fluvial deposits–a review: Boreas, v. 31, no. 4, p. 303-322.

Wang, H., Hughes, R. E., Steele, J. D., Lepley, S. W., and Tian, J., 2003, Correlation of climate cycles in middle Mississippi Valley loess and Greenland ice: Geology, v. 31, p. 179-182.

Wang, H., Lundstrom, C. C., Zhang, Z., Grimley, D. A., and Balsam, W. L., 2009, A mid-late Quaternary loess-paleosol record in Simmons Farm in southern Illinois, USA: Quaternary Science Reviews, v. 28, no. 1-2, p. 93-106.

Wanner, H., Beer, J., Bütikofer, J., Crowley, T. J., Cubasch, U., Flückiger, J., Goosse, H., Grosjean, M., Joos, F., Kaplan, J. O., Küttel, M., Müller, S. A., Prentice, I. C., Solomina, O., Stocker, T. F., Tarasov, P., Wagner, M., and Widmann, M., 2008, Mid- to Late Holocene climate change: an overview: Quaternary Science Reviews, v. 27, no. 19–20, p. 1,791-1,828.

Wayne, W., 1952, Pleistocene evolution of the Ohio and Wabash Valleys: The Journal of Geology, v. 60, no. 6, p. 575-585.

Wilkins,G.R., Delcourt, P., Delcourt, H. R., Harrison, F. W., and Turner, M. R., 1991, Paleoecology of central Kentucky since the last glacial maximum: Quaternary Research, v. 36, no. 2, p. 224-239.

Williams, J. W., 2003, Variations in tree cover in North America since the last glacial maximum: Global and Planetary Change, v. 35, no. 1–2, p. 1-23.

Wintle, A. G., 2008, Luminescence dating–where it has been and where it is going: Boreas, v. 37, no. 4, p. 471-482.

Wintle, A. G., and Murray, A. S., 2006, A review of quartz optically stimulated luminescence characteristics and their relevance in

single-aliquot regeneration dating protocols: Radiation Measurements, v. 41, no. 4, p. 369-391.

Witten, A. J., 2006, Handbook of Geophysics and Archaeology: Oakville, Connecticut, David Brown Book Co., 329 p.

Wood, J. R., Forman, S. L., Everton, D., Pierson, J., and Gomez, J., 2010, Lacustrine sediments in Porter Cave, Central Indiana, USA and possible relation to Laurentide ice sheet marginal positions in the middle and late Wisconsinan: Palaeogeography, Palaeoclimatology, Palaeoecology, v. 298, no. 3–4, p. 421-431.

Woodfield, M. C., 1998, Wabash and Ohio River megasequences–Little Pigeon Creek Basin, Evansville, Indiana: Indiana University Bloomington, master's thesis, 73 p.

Woods, A., Omernik, J., Brockman, C., Gerber, T., Hosteter, W., and Azevedo, S., 1998, Ecoregions of Indiana and Ohio: U.S. Geological Survey, scale 1:500,000.

Woolery, E. W., 2005, Geophysical and geological evidence of neotectonic deformation along the Hovey Lake Fault, Lower Wabash Valley Fault System, central United States: Bulletin of the Seismological Society of America, v. 95, no. 3, p. 1,193-1,201.